ÉCOLE DE TECHNOLOGIE SUPÉRIEURE
UNIVERSITÉ DU QUÉBEC

THESIS PRESENTED TO
ÉCOLE DE TECHNOLOGIE SUPÉRIEURE

IN PARTIAL FULFILLEMENT OF THE REQUIREMENTS FOR
THE DEGREE OF DOCTOR OF PHILOSOPHY
Ph.D.

BY
Yan ZHAO

INVESTIGATION OF UNCERTAINTIES IN ASSESSING CLIMATE CHANGE IMPACTS ON THE HYDROLOGY OF A CANADIAN RIVER WATERSHED

MONTREAL, JULY 21 2015

BOARD OF EXAMINERS

THIS THESIS HAS BEEN EVALUATED

BY THE FOLLOWING BOARD OF EXAMINERS

Mr. Robert Leconte, Thesis Supervisor
Department of Civil Engineering, Université de Sherbrooke

Mr. Robert Benoit, President of the Board of Examiners
Department of Mechanical Engineering, École de technologie supérieure

Mr. François Brissette, Member of the jury
Department of Construction Engineering, École de technologie supérieure

Mrs. Annie Poulin, Member of the jury
Department of Construction Engineering, École de technologie supérieure

Mr. Alain N. Rousseau, External Evaluator
Institut national de la recherche scientifique, Centre Eau, Terre et Environnement

THIS THESIS WAS PRESENTED AND DEFENDED

IN THE PRESENCE OF A BOARD OF EXAMINERS AND PUBLIC

ON JUNE 16 2015

AT ÉCOLE DE TECHNOLOGIE SUPÉRIEURE

FOREWORD

This PhD research started in May 2008 at the École de technologie supérieure, Université du Québec, under the supervision of Professor Robert Leconte, now at the Université de Sherbrooke. This thesis is part of the project entitled “Impact of climate change in Canadian River Basins and adaptation strategies for the hydropower industry”, which was supported by the Natural Science and Engineering Research Council of Canada (NSERC), Hydro-Québec, Manitoba Hydro and the Ouranos Consortium on Regional Climatology and Adaptation Climate Change.

ACKNOWLEDGMENT

Upon writing this thesis, many emotions came to me. Throughout these years of my life, I have encountered many dilemmas and also received many help. I am very grateful for all the people who supported me, encouraged me and provided me with advice and suggestions in the course of my research. Without them, I cannot imagine how I could have made this achievement.

First of all, I would like to express my particularly appreciation and thanks to my supervisor, Prof. Robert LECONTE. Since I came to Canada, I have received countless help and support from you. Even after you moved to the University of Sherbrooke, you continued supervising my research work. Your serious and responsible attitude in scientific research greatly impressed me. And your modesty and optimism in daily communications also deeply touched me. When I felt trapped in my research, you helped me to find solutions; when I was homesick, your words gave me great comfort; when I felt tired and frustrated in dealing with technical problems, you were a good advisor who gave me much encouragement and cheered me up. During these years of PhD research, you were not only a research supervisor to me, but also a close friend and a reliable mentor. Your powerful support encouraged me to complete my PhD study. I very much appreciated your years of guidance and help.

Secondly, I would like to thank another important advisor in ÉTS, Prof. François P. BRISSETTE. You possess a wealth of knowledge and also a rigorous working attitude. You have vast interests and can easily entertain a pleasant conversation. You helped me discovering uncertain points and gave me sound advice in my research. Since my supervisor left ÉTS, you were always concerned about my studies, providing help when needed. I appreciate what you have done for me. I am also very grateful to Prof. Annie POULIN who gave me great assistance in applying the hydrological model HYDROTEL in my research and provided me with numerous helpful ideas. You are a very nice and intelligent professor. Thank you.

I am extremely grateful to all the members of the jury who evaluated my thesis. Your comments were very important to me to enhance this work.

This PhD research was also supported by scientists at Hydro-Québec and at the Ouranos Consortium: Marie Minville, Blaise Gauvin St-Denis and Diane Chaumont. Thank you all for giving me valuable expertise and providing me important technical information. Your sensible suggestions prompted me to find a way out. Heartily thank you.

I would like to thank the following persons with whom I had the privilege of working alongside, or interacted with, during these years I was doing my PhD study: postdoctoral colleague Jie CHEN (École de technologie supérieure, Canada), postdoctoral colleague Zhi LI (North West Agriculture and Forestry University, China), postdoctoral colleague Mélanie TRUDEL (Université de Sherbrooke, Canada), postdoctoral colleague Didier HAGUMA (Université de Sherbrooke, Canada), PhD student Richard ARSENAULT (École de technologie supérieure, Canada), Master student Jean-Luc MARTEL (École de technologie supérieure, Canada), as well as students who graduated including Johnathan ROY, Chloé ALASSIMONE, Josée BEAUCHAMP, Anne-Sophie PRUVOST, Pascal CÔTÉ, Jean Stéphane MALO, Antonin COLADON and Sébastien TILMANT. Thanks to you, my PhD study was anything but humdrum and painful. It was so pleasing to work with these joyful peoples. Special thanks to Didier HAGUMA who helped me working with the hydrological model SWAT, provided the NLWIS data and the geographical information of the Manicouagan River Basin. I sincerely thank these enthusiastic colleagues. They gave me many valuable comments and suggestions. My research is inseparable from the cooperation and assistance of this group.

Thanks to the secretaries and librarians at the École de technologie supérieure, for helping me in many different ways. Thank you to Lise DAIGNEAULT and Dominique CHARRON at the Décanat des études for explaining academic issues. Thank you, Mathieu DULUDE, for helping me to resolve the computer-related technical problems.

I would also like to express my appreciation to my dear friends: Master student Yingying DONG (École de technologie supérieure, Canada), PhD student Jing LI (McGill University, Canada), MBA student Wei XUE (Concordia University, Canada), Dr. Xing CHEN (Hohai University, China) and Dr. Qin XU (Nanjing Hydraulic Research Institute, China). When I was homesick and sad, you gave me encouragement, straightened me out and helped me to overcome difficulties and concentrate on my study. You were my spiritual support.

Most importantly, I am deeply indebted to my family for all their help. Especially, thanks to my parents, my older brother, my sister-in-law and my niece. Since I left home to pursue my study in France in 2006, I spent very limited time to see them. They always comforted me to focus on my study. When I worried about my parents, my brother and sister-in-law appeased while taking good care of them. I am grateful that my family understands me, supports me and loves me unconditionally. Their encouragement inspired me to persevere in my objective for so long. Especially, I would like to thank an important person in my life, Yaochi ZHANG. It is him who encouraged me to come to Canada to do my PhD research. He always shared my worries; let me feel at ease when we were separated on different continents. I found serenity because he is always besides me at any time.

Great thanks to the organizations for providing financial support for this project: the Natural Science and Engineering Research Council of Canada (NSERC), Hydro-Québec, Manitoba Hydro and the Ouranos Consortium.

Finally, I want to express endless thanks to all the people who made this thesis possible, those who are mentioned above and those who are not. This thesis owes to your support. Thank you very much!

INVESTIGATION OF UNCERTAINTIES IN ASSESSING CLIMATE CHANGE IMPACTS ON THE HYDROLOGY OF A CANADIAN RIVER WATERSHED

Yan ZHAO

ABSTRACT

It is known that climate change will affect water resources. The impact of climate change on river regimes attracted the attention of hydropower companies over the recent years. Although general trends in future river flows can be reasonably well assessed using climate and hydrological models, their overall uncertainty is much more difficult to evaluate. An improved evaluation of uncertainty in the hydrological response of watersheds to climate change would help designing hydropower projects as well as adapting existing systems to better cope with the anticipated changes in flow regimes.

The uncertainty in assessing the potential hydrological impacts of a changing climate is of high interest for the scientific community. A framework for evaluating the uncertainty of climate change impacts on watershed hydrology is developed in this thesis. The sources of uncertainty studied comprise the global climate model (GCM) structure, climate sensitivity, natural variability and, to a lesser extent, hydrological model structure. Climate sensitivity is the global mean climatological temperature change due to a doubling of atmospheric CO_2 concentration. Natural variability refers to the uncertainties resulting from the inherent randomness or unpredictability in the natural world. Climate projections under IPCC A2 scenario for the 2080 horizon were downscaled to regional scale using the change factor method and developed into long time series with WeaGETS, a stochastic weather generator developed at the École de technologie supérieure. The predicted future climate scenarios were forced into four hydrological models to simulate future flows in the Manicouagan River Basin, located in the province of Quebec, Canada. The Monte Carlo sampling method was implemented as a probabilistic approach to trace out the magnitude of uncertainty in accordance with the weighting schemes attributed to the different sources of uncertainty. In particular, equal and unequal weights were attributed to the GCMs to see whether this would have a significant impact on the resulting flow return periods. This experiment was motivated by the fact that GCM structure is usually the most significant contribution to the overall uncertainty in projected flows. Experiments using equal and unequal weights on climate sensitivities were also performed.

Modelling results indicate that the future hydrological cycle will intensify as precipitation and temperature will increase in the future for all GCMs projections. The spring peak flow will occur earlier by a few weeks for all GCMs investigated and will increase for a majority of them.

The uncertainty related to GCM structure, climate sensitivity, natural variability and to hydrological model structure were assessed separately. Uncertainty due to the GCM structure

was found to be significant and to vary seasonally and monthly especially during the month of April. Variations in climate sensitivity and natural variability introduced moderate changes in the hydrological regime when compared with the uncertainty due to GCM structure. The choice of hydrological model will also result in a non-negligible uncertainty in climate change studies.

At last, the magnitude of uncertainty under various weighting schemes attributed to GCMs and climate sensitivities was evaluated. Weight scheme experiments indicate that assigning equal or unequal weights to the GCM structure had a marginal to small effect on the return periods calculated for the hydrological variables studied, i.e. monthly discharge and spring runoff volume. However, for climate sensitivity, the weights assignment notably influenced the probability of occurrence of large hydrological events. The choice of the hydrological model also had a significant impact on return periods of large hydrological events. It should be given due attention in selecting hydrological models and assigning weights on climate sensitivities in uncertainty assessment of climate change impacts in designing water resources systems.

Keywords: climate change, uncertainty, impact, hydrology, climate sensitivity, Monte Carlo method

ÉTUDE DES INCERTITUDES ASSOCIÉES À L'ÉVALUATION DE L'IMPACT DES CHANGEMENTS CLIMATIQUES SUR L'HYDROLOGIE D'UN BASSIN VERSANT CANADIEN

Yan ZHAO

SUMMARY

Il est connu que le changement climatique aura une incidence sur les ressources en eau. L'impact du changement climatique sur les régimes hydriques a attiré l'attention des entreprises hydroélectriques au cours des dernières années. Bien que les tendances générales dans les débits en rivière puissent être raisonnablement bien évaluées à l'aide des modèles climatiques et hydrologiques, leur incertitude globale est beaucoup plus difficile à quantifier. Une meilleure évaluation de l'incertitude de la réponse hydrologique des bassins versants aux changements climatiques permettrait la conception de projets hydroélectriques ainsi que l'adaptation des systèmes existants afin de mieux faire face aux changements prévus dans les régimes d'écoulement.

L'incertitude dans l'évaluation des impacts hydrologiques potentiels du changement climatique est d'un grand intérêt pour la communauté scientifique. Une méthodologie pour l'évaluation de l'incertitude des impacts du changement climatique sur l'hydrologie des bassins versants est développée dans cette thèse. Les sources d'incertitudes étudiées comprennent la structure des modèles de climat global (MCG), la sensibilité du climat, la variabilité naturelle du climat et, dans une moindre mesure, la structure du modèle hydrologique. La sensibilité du climat est le changement de la température climatologique moyenne mondiale en raison d'un doublement de la concentration de CO_2 dans l'atmosphère. La variabilité naturelle réfère aux incertitudes résultant de l'aléa inhérent ou imprévisibilité dans le monde naturel. Les projections climatiques dans le scénario A2 du GIEC pour l'horizon 2080 ont été réduites à l'échelle régionale par une méthode du facteur de changement et développées en longues séries chronologiques avec le générateur météorologique WeaGETS conçu à l'École de technologie supérieure. Les scénarios climatiques futurs ont été forcés dans quatre modèles hydrologiques pour simuler les débits futurs sur le bassin de la rivière Manicouagan, situé dans la province de Québec, Canada. La méthode d'échantillonnage de Monte Carlo a été mise en œuvre comme approche probabiliste pour établir l'ampleur de l'incertitude en conformité avec les schémas de pondération attribués aux différentes sources d'incertitude. En particulier, des poids égaux et inégaux ont été attribués aux MCG pour voir si cela avait un impact significatif sur les périodes de retour des débits simulés. Cette expérience a été motivée par le fait que la structure des MCG est habituellement la plus importante contribution à l'incertitude globale des débits projetés. Des expériences utilisant des poids égaux et inégaux sur la sensibilité du climat ont également été réalisées.

Les résultats de la modélisation indiquent que le cycle hydrologique futur s'intensifiera à mesure que les précipitations et la température vont augmenter dans l'avenir pour toutes les

projections des MCG. Le débit de pointe du printemps aura lieu plus tôt de quelques semaines pour tous les MCG analysés et va augmenter pour une majorité d'entre eux.

L'incertitude liée à la structure des MCG, à la sensibilité du climat, à la variabilité naturelle et à la structure du modèle hydrologique ont été évalués séparément. L'incertitude due à la structure du MCG a été jugée importante et varie mensuellement, en particulier durant le mois d'avril. Les variations de la sensibilité du climat et de la variabilité naturelle introduisent des changements modérés dans le régime hydrologique, par rapport à l'incertitude due à la structure des MCG. Le choix du modèle hydrologique se traduit également par une incertitude non négligeable dans les études sur le changement climatique.

Enfin, l'ampleur de l'incertitude pour différents systèmes de pondération attribués aux MCG et à la sensibilité du climat a été évaluée. Les résultats indiquent que l'attribution de pondérations égales ou inégales à la structure du MCG a un effet marginal à faible sur les périodes de retour calculées pour les variables hydrologiques étudiées, soient le débit mensuel et le volume de ruissellement printanier. Cependant, pour la sensibilité du climat, le schéma de pondération a notamment influencé la probabilité d'occurrence de grands événements hydrologiques. Le choix du modèle hydrologique a également eu un impact significatif sur les périodes de retour de grands événements hydrologiques. Une attention particulière devra donc être accordée quant au choix des modèles hydrologiques et dans l'attribution de pondérations sur la sensibilité du climat, pour l'évaluation de l'incertitude des impacts du changement climatique sur les régimes hydriques.

Mots-clés: changement climatique, incertitude, impact, hydrologie, sensibilité du climat, méthode de Monte Carlo

TABLE OF CONTENTS

Page

LIST OF TABLES

LIST OF FIGURES

LIST OF ABREVIATIONS

ANN	Artificial neural network
AOGCM	Atmosphere-ocean global climate model
AR4	IPCC's Fourth Assessment Report: Climate Change 2007
AR5	IPCC's Fifth Assessment Report: Climate Change 2013
BC	Bias correction
BCCR-BCM2.0	General circulation model of Bjerknes Centre for Climate Research, Norway, version 2
CDED	Canadian Digital Elevation Data
CEHQ	Centre d'expertise hydrique du Québec
CF	Change factor
CGCM3.1	General circulation model of Canadian Centre for Climate Modelling and Analysis, version 3.1
CH_4	Methane
CMIP3	Coupled Model Intercomparison Project Phase 3
CMIP5	Coupled Model Intercomparison Project Phase 5
CNRM-CM3	General circulation model of the Centre national de recherches météorologiques, Météo France, version 3
CO_2	Carbon dioxide
CPI	Climate prediction index
CSIRO-MK3.0	General circulation model of the Australian Commonwealth Scientific and Research Organization
CTI	Centre for Topographic Information
CV	Coefficient of variation
DASR	Discriminant analysis coupled with step-wise regression method

DDM	Dynamic downscaling method
DEM	Digital elevation model
GCM	Global climate model or General circulation model
GDB	Geospatial Data Base
GFDL-CM2.0	General circulation model of Geophysical Fluid Dynamics Laboratory, United States, version 2.0
GGES	Greenhouse gas emission scenario
GHG	Greenhouse gas
GLUE	Generalised Likelihood Uncertainty Estimation
HBV	A semi-distributed conceptual hydrological model developed by the Swedish Meteorological and Hydrological Institute
HMETS	Hydrological model of the École de technologie supérieure
HSAMI	A lumped conceptual rainfall-runoff model developed by Hydro-Québec
HYDROTEL	A spatially-distributed and physicially-based hydrological model developed by the Institut National de la Recherche Scientifique in Québec City, Canada
INM-CM3.0	General circulation model of the Institute of Numerical Mathematics, Russian Academy of Science, version 3.0
INRS-ETE	Institut national de la recherche scientifique - Eau Terre Environnement
IPCC	Intergovernmental Panel on Climate Change
IPSL-CM4	General circulation model of L'institut Pierre-Simon Laplace, France, version 4
IRCPI	Impact relevant climate prediction index
ISO	International Organization for Standardization
LARS-WG	Long Ashton Research Station weather generator

LHS	Latin hypercube sampling
LR	Linear regression
MAGICC/SCENGEN	Model for the Assessment of Greenhouse-gas Induced Climate Change/ a Regional Climate SCENario GENerator
MEM	maximum entropy method
MIROC3.2(medres)	General Circulation Model of Interdisciplinary Research on Climate, Japan, version 3.2
MPI-ECHAM5	General Circulation Model of Max Planck Institute for Meteorology, Germany, version 5
MRB	Manicouagan River Basin
MSII	Model structure indicating index
NARCCAP	The North American Regional Climate Change Assessment Program
NCAR-PCM1	General circulation model of the National Center for Atmospheric Research, United States
NLWIS	National Land and Water Information Service
N_2O	Nitrous oxide
NTDB	National Topographic Data Base
PDF	Probability density function
PDM	Probability distributed model
PE	Potential evaporation
PPT	Precipitation
PET	Potential evapotranspiration
RCM	Regional climate model
REA	Reliability ensemble averaging
RHHU	Relatively homogeneous hydrological units

RMSE	Root mean square error
RMSEMM	Root mean square error minimization method
RS	Remote sensing
SCE-UA	Shuffled Complex Evolution-University of Arizona
SDM	Statistical downscaling method
SDSM	Statistical Downscaling Model
SMEAM	Simple multi-model ensemble average method
SMHI	Swedish Meteorological and Hydrological Institute
SRES	Special Report on Emission Scenarios
SVM	Support vector machine
TGCM	Thermospheric general circulation model
TIE-GCM	Thermospheric-Ionosphere-Electrodynamics general circulation model
Tmax	Maximum air temperature
Tmin	Minimum air temperature
WeaGETS	Weather generator of the École de technologie supérieure
WG	Weather generator
WEC	World Energy Council

LIST OF SYMBOLS AND UNITS OF MEASUREMENT

UNITS OF GEOMETRY

Length

m	meter
mm	millimeter

Area

km^2	square kilometer (= 1 000 000 m^2)

UNITS OF TIME

Discharge

m^3/s	cubic meter per second

Power

kWh	kilowatt hour
MW	megawatt

THERMAL UNITS

°C	degree Celsius

INTRODUCTION

What is climate? Climate is generally defined as “average weather”, which is described as the mean and variability of temperature, precipitation and wind over a period of time that may range from months to millions of years (IPCC, 2007). The change of climate is commonly described by the statistics of change as average weather over time. The weather condition is mostly expressed by the state of air temperature, precipitation, wind and humidity, etc. (Wilby et al., 1998). Information on average weather is particularly important for the study of change in the climate system and for predicting future environmental conditions.

It is recognized that the world is undergoing global climate change (IPCC, 2013). Over the last decades, the global average surface air temperature rose up sharply (Henson, 2008). The Intergovernmental Panel on Climate Change (IPCC, 2013) has reported in its Fifth Assessment Report (AR5) that, over the last 60 years (1951-2012), the linear warming trend of 0.12°C per decade was nearly twice that of the last 100 years. Indeed, over the 1880-2012 period, global average surface temperature has increased by 0.85°C (IPCC, 2013). The temperature increase is greater in the winter season in northern high latitude regions (IPCC, 2007). Meanwhile the global average sea level had risen up at an average rate of 3.1 mm/year between 1993 and 2003 and the mean annual snow cover area in the northern hemisphere shrank from 24.4 million km^2 between 1967 and 1987 to 23.1 million km^2 between 1988 and 2006. In the last 100 years, precipitation increased significantly, mostly in the northern regions of the continental interior, but declined in some southern areas (IPCC, 2007). With global warming, winter seasons are becoming less harsh, icebergs are melting at an increasing rate, drinking water is getting more valuable and extreme events are more likely to happen (Gates et al., 1992). The IPCC summarized in its Fourth Assessment Report (AR4) in 2007 that an unequivocal warming of the climate system is manifest, based on the observations made, on all continents, of many natural climate indicators over the last decades. These observations were confirmed in the AR5. Significant trends of higher winter flows, early spring flood and diminished summer flows have been observed in several

regions of Canada (Whitfield and Cannon, 2000; Hernández-Henríquez et al, 2010). This observational evidence has made people recognize the fact that the natural systems are being affected in many ways by climate change and this worldwide warming trend will influence the future of mankind significantly.

Regional climate change, for example, changes in the frequency and amount of rainfall, could lead to distinct effects in river flows, especially at higher latitudes (Whitfield and Cannon, 2000, Ferrari, 2008). Changes in watershed hydrological regime could subsequently impact the normal operations and management of local water systems, as changes in river flows may alter the operation of reservoir systems and hydropower generation. Therefore, the assessment of regional hydrological impacts of a changing climate, especially with respect to extreme climatic events, is a cause for concern in the environmental and socio-economic sectors, including the hydropower industry.

As a primary source of renewable energy, hydropower makes a significant contribution to the world energy production (WEC, 2010). Hydroelectricity is a necessary source of energy at a time when the world is faced with dwindling natural resources, since its production only requires access to a sustainable source of flowing water, as influenced by topography and climate. Canada has a century long history of adopting hydroelectric energy. Today Canada is the world's third largest producer of hydroelectricity after China and Brazil, generating 348.1 billion kWh in 2010. This accounts for 60% of the electricity it produces (Canadian Energy Overview, 2010). Most of the energy produced in Quebec is hydroelectricity. Owing to its abundant water resources, 94% of the province's electricity is drawn from hydropower installations (Hydro-Quebec, 2010). Hydropower plays an important role in the modern economy, especially in this province. Global climate change impacts local and regional water resources and therefore has hydrological implications that are of concern for hydropower management. Credible analyses of future climate change impacts are required by water regulatory authorities, watershed planning agencies and governmental decision makers to establish long-term strategic plans for the regional management and rational use of water resources. The evaluation of such future uncertainty is becoming increasingly important for

assessing the hydrological impacts of a changing climate and analysing the risks for water resource systems.

Given this context, this research work aims to provide a framework for assessing the uncertainties related to the hydrological impacts of climate change on a river basin in the province of Quebec (Canada). Such an assessment is essential to evaluate response strategies that would enable water systems to better cope with future climate and hydrological conditions. This study was conducted on the Manicouagan River Basin (MRB), where hydropower facilities are owned and operated by Hydro-Québec.

This thesis is made up of six major sections: Research-related issues, Literature review, Methodology, Studied watershed and data, Results and discussion, and finally Conclusions and recommendations.

Chapter 1 describes the research issues, including the incentives and objectives of this research. It also explains the background of the impact study of the effects of climate change on water resources, the usual strategies used to assess the hydrological impacts of a changing climate and the problem of evaluating sources of uncertainty during the modeling process. It examines arguments for or against assigning weights to different sources of uncertainty. Finally, it states the objectives and contributions of this research.

Chapter 2 is devoted to the literature review. It presents the theoretical foundational work and approaches that have been published on how uncertainty is assessed for the purpose of evaluating the impact of climate change on river flow regimes. It describes the frameworks that have been developed to model various sources of water system uncertainty in the context of climate change. It highlights the advantages and limitations of the described approaches. Finally, it presents the techniques used to estimate specific sources of uncertainty in recent studies.

Chapter 3 describes the methodology followed in this research. It introduces the climate simulation tools used for producing future climate change projections and the downscaling method proposed to bring the global climate models projections at the watershed scale. Four hydrological models were used in this study to assess the effect of model structure on the overall uncertainty in future hydrological regimes. These models are then described. The Monte-Carlo sampling method used for uncertainty assessment is also described, along with the approaches used to assign weights to the climate model structure and climate sensitivity.

Chapter 4 describes the watershed that is the subject of the study. First, the main characteristics of the Manicouagan River Basin are presented and the hydro-climatic context is summarized. This is followed by a description of the water resource system and the characteristics of sub-watersheds. Finally, the climatological and river flow data used in this research are briefly described.

Chapter 5 presents the results of study, followed by a discussion of these results. Both results and the discussion are divided in two subsections: the quantification of major sources of uncertainty and the Monte Carlo experiments performed to quantify these sources of uncertainty in a probabilistic framework. Various sources of uncertainty related to climate change impacts on the hydrological regime of the Manicouagan River Basin are analyzed. The magnitude of this uncertainty is identified individually for each source. An integrated assessment of all sources of uncertainty is conducted by using Monte Carlo experiments in which different weighting schemes are implemented. The experiments highlight the influence, or lack of, that applying diverse weighting schemes can have on the probabilistic distribution of selected hydrological variables that characterize the watershed hydrological regime.

Finally, the Conclusion summarises the major outcomes of this research and makes some recommendations for future research.

CHAPITRE 1

RESEARCH STATEMENT

This chapter covers the scientific issues that are raised and outlines the objectives of the research project. First, the usual procedure of simulating the climate change impacts on water systems is presented. Secondly, the problems found in recent researches are exposed. A key issue in studying the hydrological impacts of climate change is the difficulty that the inclusion and quantification of various sources of uncertainty poses. Thirdly, the topic of applying weighting schemes to the sources of uncertainty is addressed. Finally, the project's objectives are described.

1.1 Background

In the early 19th century, the scientific investigation of climate change started with the discovery of natural changes in paleoclimate. Later in this century, human emissions of greenhouse gas were identified as a possible factor that could change the climate (IPCC, 2013; Knutti and Hegerl, 2008; Prudhomme et al., 2003). Two centuries later, the trend toward global warming has become much more evident with increasing global mean temperatures, which have been especially noticeable in recent years (IPCC, 2007). Higher temperatures result in more snow melting, increased droughts and the shrinking of polar ice (Alekseev et al., 2009). It is clear that water is among the resources that will be most severely affected by climate change (Minville et al., 2008). Many studies have been conducted to assess the effects of climate change and its impacts on regional hydrology. These are described in recently published articles (e.g. Katz, 2002; Wilby, 2005; Ludwig et al., 2009; Prudhomme and Davies, 2009 a, b; Johnson and Weaver, 2009) and show that approaches used to measure the impact have improved and the theories of climate change have progressed.

The methodology employed to evaluate the hydrological impacts of climate change usually follows a top-down modelling scheme (Vicuna et al., 2007; Minville et al., 2008; Poulin et al., 2011). Firstly, future greenhouse gas (GHG) emissions projections are produced. Then Global Climate (or General Circulation) Models (GCMs) are implemented to generate future climate projections at the global scale, according to predicted greenhouse gas emission scenarios. Because these climate models are too coarse for regional or local scale watersheds impact studies, downscaling methods must be applied to adjust the GCM projections (usually precipitations and temperatures) at the desired scale. The downscaling approaches fall into two categories: dynamic and statistical (Schmidli et al., 2007; Prudhomme and Davies, 2007; Fowler et al., 2007). Dynamic downscaling employs Regional Climate Models (RCMs) that are nested into the coarse GCMs to produce high resolution climate change simulations. A number of studies, such as the North American Regional Climate Change Assessment Program (NARCCAP), applied RCM projections to investigate uncertainties in regional scale climate projections. As the RCMs are resolved at a regional spatial resolution, typically a ~0.5° latitude and longitude scale, using dynamic downscaling is computationally expensive (Solman and Nunez, 1999, Fowler et al., 2007). Owing to high computational costs, dynamic downscaling was not used in this study. Statistical downscaling establishes a statistical relationship between a GCM predictor and a local scale predictand. Their application implies that the statistical relationships are independent of climate change and that these relationships are assumed to be consistent in the future, which is yet to be proven (Baguis et al., 2008). Statistical downscaling approaches are more numerically efficient than dynamical approaches, but must rely on observations to be applicable. A simple statistical downscaling method, the change factor (CF), is applied in this study. The last step consists in converting the climate projection into streamflow. This is done by forcing climate change projections into hydrological models to estimate the watershed hydrological response.

1.2 Research statement

As explained above, the entire simulation process to assess the impacts of climate change on watershed hydrological regimes requires a suite of models, including climate and

hydrological models (Prudhomme et al., 2002). Quantifying the magnitude of uncertainty in this modeling process becomes difficult since the sources of uncertainties are numerous.

Sources of uncertainty in climate change impact studies include: (1) GCM structure; (2) Greenhouse Gas Emissions Scenarios (GGES); (3) natural variability; (4) climate sensitivity; (5) downscaling methods; (6) hydrological model structure; (7) hydrological model parameters. Most studies focused on one or a few sources of uncertainties. For instance, Bergström et al. (2002) and Benke et al. (2008) studied the parameter uncertainty in hydrological models; Chiang et al. (2007) focused on the uncertainty of hydrological model's structure; Kay and Davies (2008) and Blenkinsop and Fowler (2007) presented an investigation of uncertainty due to climate model structure; Salathé (2003), Khan et al. (2006) and Fowler et al. (2007) studied the uncertainty derived from downscaling methods; Murphy et al., (2004) described the uncertainty due to the variation of climate model parameters. Chen et al. (2011a) present what is probably one of the few studies that investigated all major sources of uncertainty in a hydrological impact study. However, the combined effect of various sources of uncertainties was only partly addressed. Although some studies (New and Hulme, 2000; Wilby and Harris, 2006; Prudhomme and Davies, 2009 a, b; etc.) have proposed frameworks that embrace major sources of uncertainty, there is still a long way to go before an integrated method can be developed to evaluate all the sources of uncertainty in hydrological impact studies of climate change.

When compared to other sources of uncertainty, according to several studies (e.g. Prudhomme et al., 2003; Wilby and Harris, 2006; Minville et al., 2008; Kay et al., 2009, Chen et al., 2011a), the uncertainty associated with GCM structure is the most significant. It is therefore studied in this thesis. Climate sensitivity describes how much the doubling of atmospheric CO_2 concentration in air will impact the global mean surface temperature (Prudhomme et al., 2002) for a given GCM. This source of uncertainty is seldom explicitly considered, but it plays a significant role in long-term temperature projections (Rogelj et al., 2012). It is investigated in this study. The uncertainty due to natural variability, stemming from the inherent randomness of long-term climatic data series, is also studied in this thesis,

as it is an essential element in producing future climate scenarios (Prudhomme and Davies, 2009b). To simulate hydrologic processes based on the predicted climate, hydrological models are used. The uncertainty of hydrological model structure, which can be assessed by running independent individual hydrological models, has been investigated in recent studies (e.g. Chen et al., 2011a, Poulin et al., 2011, Vansteenkiste et al., 2014). The comparison of hydrological outputs using different hydrological models is also addressed in this study. Among the remaining sources of uncertainty, downscaling uncertainty is shown to be a critical factor in the climate change impact study presented by Chen et al. (2011b). However, as individual downscaling techniques have their own distinctive behavior in downscaling climate output compared to other downscaling methods, it is difficult to make a direct comparison of downscaling methods to identify the most appropriate method for a given situation (Chen et al., 2011a). Even simple downscaling methods seem to perform as well as more sophisticated methods in reproducing climate characteristics (Fowler et al., 2007). The investigation of downscaling methods is not among the objectives of this thesis. Lastly, the uncertainties related to GGES and hydrological model parameterization are described in Chen et al. (2011a) as being the least significant among the major sources of uncertainty. Owing to the lack of any firm evidence of their crucial impacts in the rainfall-runoff processes, these uncertainties are not examined in this study.

Approaches to determine the magnitude of different sources of uncertainty in the hydrological impact of climate change have been developed in recent research (e.g. Murphy et al., 2004; Khan et al., 2006; Laurent and Cai, 2007; Christensen et al., 2010; Ghosh and Katkar, 2012). Some models or approaches may perform differently under certain conditions, such as a specific season or a given climate, or within certain study area (e.g. Arora and Boer, 2001; Fowler and Kilsby, 2007; Maurer, 2007). Furthermore, there is still a disagreement on how to assign weights to selected climate models depending on their performance, on combining the models to analyze the uncertainty of climate change impact, or even on the need to assign weights (e.g. Morgan and Henrion, 1990; Stainforth et al., 2007; New and Hulme, 2000; Wilby and Harris, 2006). The following section explores this issue in more details.

1.3 Weight assignment

Scientific arguments were proposed about whether climate and/or hydrological models that offer good performance in producing more accurate simulations of observations should be assigned stronger weights as compared to models that lack accuracy in re-establishing the observations of climate change impact assessments. Scholze, et al. (2006) considered that climate models are equally good based on their performance and assigned equal weights to each model. Stainforth et al. (2007) claimed that any attempt to assign weights is futile as all current climate models are far from being adequate. In their study, they argued, that relative to the real world, all models have effectively zero weight, which indicates that they are all equally good (or bad). Weigel et al. (2010) stressed the fact that so far there is no consensus on what is the best method of combining the output of several climate models, and that it is not clear that appropriate weights can be obtained from all existing data and methods. Furthermore, the IPCC (2007) refused to assign any explicit probability to climate projection and regarded all model applications as equally important. Above all, as Morgan and Henrion (1990. p. 68) argued: "Every model is definitely false. Although we may be able to say that one model is better than another, in the sense that it produces more accurate predictions, we cannot say it is more probable. Therefore, it is inappropriate to try to assign probabilities to models."

On the other hand, recent studies were conducted to explore the weighting schemes in assessment of uncertainty. New and Hulme (2000) demonstrated a methodology for quantifying various uncertainties through the use of Bayesian Monte-Carlo simulation to define posterior probability distributions for climate change. Butts et al. (2004) noticed large variations in climate model performance amongst the model structures used and suggested that the implementation of an ensemble of models, based on model performance, could improve the overall accuracy of the simulations. Murphy et al. (2004) attempted to assign weights to climate sensitivity in order to construct ensembles to sample structural uncertainties. Wilby and Harris (2006) presented a probabilistic framework for addressing the systematic weights on various sources of uncertainty, including GCMs, hydrological

model and model parameters, in climate change impact studies. Fowler and Ekström (2009) described the application of a regional multi-model ensemble by developing a model specific weighting scheme. Their results revealed that the overall effect of using the weighting scheme could tighten the regional distributions compared with an unweighted distribution. Christensen et al. (2010) applied performance indices to assign weights on a large ensemble of climate model simulations. Although results of their study indicated that the use of model weights did not show a compelling sensitivity, when compared to the use of equal weights, it did indicate that the use of a weighting scheme on other sources of uncertainty should be given more attention. These attempts at assigning weights to different sources of uncertainty, and in particular to climate models and climate sensitivity, is drawing attention on their use for the investigation of the magnitude of uncertainty in climate change impact studies. Different impacts on hydrological output can be discovered through the use of weighting schemes in the simulation process.

1.4 Objectives

There is a general consensus that future climate variability and change will pose increasing challenges to water resources managers. The objective of this research is to develop a framework based on a probabilistic approach to assess the magnitude of different sources of uncertainty in the hydrological response to future climate change of a watershed, the Manicouagan River Basin, in the province of Quebec, Canada. This watershed was selected as the study site because it is an important hydropower source for the province of Quebec. More specifically, this study will address the sources of uncertainty due to GCM structure, climate sensitivity, natural variability and hydrological model structure. These sources of uncertainty were included in the study because GCM structure is associated with significant uncertainty, climate sensitivity plays a critical role in the production of long-term temperature projections, and natural variability is an essential characteristic of the climate data series and hydrological models are required to simulate watershed hydrologic regimes. A secondary objective of the study is investigating the feasibility of quantifying uncertainty by applying various weighting schemes to selected sources of uncertainty. A Monte Carlo

simulation approach is used to investigate the relative contribution of various sources of uncertainty by sampling simulation results with probabilistic weights assigned to uncertainty components. This technique is conducive to the application of risk analysis to calculate, for example, the return periods of hydrologic events and how they are affected by the weights applied to the various sources of uncertainty.

It is expected that this will improve the existing assessment methods for quantifying the effects of sources of uncertainty in climate change studies on watersheds hydrological response. A better quantification of the uncertainty in projected flows and other hydrological variables is essential to establishing efficient response strategies to limit adverse impacts or to capitalize on positive outcomes of climate change on water resources.

This study is part of a larger project funded by Natural Sciences and Engineering Research Council of Canada, the Ouranos Consortium on Regional Climatology and Adaptation to Climate Change, Manitoba Hydro and Hydro-Québec, which aims to contribute to a better understanding of climate change impacts on river runoff in areas of interest to Hydro-Quebec and Manitoba Hydro.

In this thesis, ten GCMs, five climate sensitivities and fifty series of natural variability were used to produce an array of climate change scenarios (i.e. $10\times5\times50=2500$ climate scenarios). Four hydrological models were used to simulate future hydrological regimes of the Manicouagan River Basin, a northern watershed, based on these climate scenarios. Finally a probabilistic approach was used to conduct random samplings of the hydrological simulations produced by each individual hydrological model for the purpose of analyzing the uncertainty in selected hydrological variables. The main contribution of this study consists in the application of weighting schemes to evaluate various sources of uncertainty in the entire modeling process. In particular, the uncertainty due to climate sensitivity was explicitly investigated by assigning to it equal and unequal weights. No study to date has evaluated the major sources of uncertainty, from climate projections to hydrological modeling, by using weighting schemes. A few studies (e.g. Minville et al., 2008; Chen, 2011b) assessed various

sources of uncertainty on hydrological regimes, however they did not explore the effects of unequal weighting schemes on the hydrological response. In rare cases, studies estimated different sources of uncertainty through weighting experiments. However these were performed on a single hydrological variable such as, for example, low flows (e.g. Wilby and Harris, 2006). On the basis of existing researches, this thesis refines existing frameworks for evaluating the main sources of uncertainty in the simulated hydrological regimes of climate change studies. In particular, it makes innovative progress in evaluating the impacts due to GCM and climate sensitivity. The thesis also explores how assigning different weighting schemes to sources of uncertainty affects the return period of extreme hydrological events, which is a relevant aspect of the design of hydrological systems in the context of a changing climate.

CHAPITRE 2

LITERATURE REVIEW

This chapter provides general information about uncertainty and the empirical techniques and frameworks that appear in the scientific literature and that are used to evaluate the uncertainty in climate change impact assessments of watersheds hydrological response. First, the definition of uncertainty is discussed, with regard to the current understanding of natural world. Next, the major sources of uncertainty in climate change study are classified and briefly stated. General techniques used in recent research to estimate various sources of uncertainty in climate change projections and in the hydrological modeling process are also described. Finally, the advantages and limitations of the various approaches used are highlighted.

2.1 Definition of uncertainty

What is “uncertainty”? Why it always exists. How it propagates and how to reduce it.

Over the millennia, humans have struggled to increase their understanding and knowledge of the natural world. In doing so, they discovered ‘laws’ that helped them understand how things and events in the universe come into being. According to Dr. Sheldon Gottlieb (Gottlieb, 1997) “Science is an intellectual activity carried on by humans that is designed to discover information about the natural world in which humans live and to discover the ways in which this information can be organized into meaningful patterns. A primary aim of science is to collect facts (data). An ultimate purpose of science is to discern the order that exists between and amongst the various facts.”

Although science can quantitatively describe phenomena or forecast events, in a way that is very close to ‘reality’, the processes that are studied are more often than not incompletely known through a lack of understanding or information. This means that our representation of ‘reality’ is imperfect. Scientifically speaking, the gap between ‘reality’ and our description of

it is described as “uncertainty”. Uncertainty is often used to describe the state of being unsure, for example, in making some predictions of future events. Two published definitions of uncertainty are presented in this study:

a) A parameter associated with the result of a measurement that characterises the dispersion of the values that could reasonably be attributed to the measurand (ISO, 1993);
b) The lack of certainty, a state of having limited knowledge where it is impossible to exactly describe an existing state or a future outcome (Hubbard, 2010).

The first definition states the theoretical concept of uncertainty. The second is more relevant in explaining uncertainty in the context of climate change assessment studies.

The common and practical way of solving a wide range of biological, environmental and engineering problems is to build models (e.g. hydrological, transport/transformation, and biological models) to simulate natural processes. Uncertainty occurs and propagates in these models because of a number of factors, such as the randomness (variability) inherent to natural processes, errors due to imperfect human knowledge in developing the models, imprecise calibration of the parameters used to ‘fit’ the models to observations (Isukapalli, 1999), differences in temporal or spatial resolution between reality and simulation, and so on. The main sources of uncertainty in the modeling process are identified and classified in the next section.

Uncertainty exists therefore throughout the modelling process because the natural phenomena that are being represented are complex and the scientific knowledge is always incomplete. People must confront uncertainty, which is inevitable, in order to make better use of it.

Two general categories of uncertainty exist: random, or aleatory, and epistemic (Kiureghian and Ditlevsen, 2009). Aleatory uncertainty is used to describe the inherent variation

associated with the physical system or the environment under consideration (Oberkampf et al., 2004). Epistemic uncertainty, which is related to the human ability to understand and to describe nature, stems from a level of ignorance of the system or the environment. It is caused by a lack of knowledge or information in the modeling process. The common way to reduce epistemic uncertainty is to gather more data or to refine the models. Reducing aleatory uncertainty cannot be achieved as it is intrinsic to nature (Kiureghian and Ditlevsen, 2009).

2.2 Classification of uncertainty

Sources of uncertainty can be broadly classified as natural uncertainty, model uncertainty, parameter uncertainty and behavioral uncertainty (Isukapalli, 1999).

2.2.1 Natural uncertainty

It is a recognized fact that unavoidable unpredictability or "randomness" contributes to the inherently stochastic characteristic of natural systems and which is generally defined as natural uncertainty. Synonyms to natural uncertainty are aleatory uncertainty, random variability, stochastic uncertainty, objective uncertainty, inherent variability and basic randomness (Merz et al., 2005). If one admits that natural randomness exists, then observable phenomena cannot be precisely measured. But trends can be discovered via mean values. For example, according to the weather forecast, there will be rain tomorrow, but the exact time it will rain and the exact amount of rainfall cannot be forecasted, even though the 'perfect' model is available. Due to air movement, cloud formation, etc., it is virtually impossible to predict all information about a rainfall as such processes are random by nature. Broadly speaking though, natural uncertainty can be characterized by using ensemble averages, but the stochasticity inherent to natural processes makes the accurate estimation of system properties impossible (Isukapalli, 1999).

2.2.2 Model uncertainty

Mathematical models are commonly used to represent natural phenomena. However, the modeling process has inevitable consequences which are directly linked to the uncertainty in the choice of the model, known as "model uncertainty" (Cont, 2006). Model uncertainty is defined as the uncertainty of the model output and is related to the model's inability to perfectly reproduce the dynamics of a natural system (Montanari, 2011). Model uncertainty may include mathematical errors, programming errors, statistical uncertainty (Farhangmehr and Tumer, 2009) and model structure uncertainty.

There are two types of mathematical errors: approximation errors and numerical errors. Approximation errors are errors due to approximate relationships used in models. Numerical errors stem from the selection of the computational method or technique (Thunnissen, 2003), for example, finite difference methods to solve differential equations. Other examples of mathematical errors in model results stem from the spatial or temporal resolution of the models. Programming errors refer to errors produced by computers and application programs (Hatton, 1997), such as bugs in hardware/software, errors in programming codes, inaccurate applied algorithms in simulation, etc. Statistical uncertainty arises from the process of extrapolating results of a statistical model, for example to generate extreme estimates (Bedford and Cooke, 2001). Finally, uncertainty in model structure is often acknowledged to be one of the principal sources of uncertainty (New and Hulme, 2000; Wilby and Harris, 2006; Christensen et al., 2010), arising from the incompleteness of a model and its inability to actually represent the difference between the real causal structure in the studied system and the perceived causal structure of the model. Therefore, choosing an inappropriate model in an ensemble of models to make simulations of interest may result in increased model uncertainty.

2.2.3 Parameter uncertainty

Parameter uncertainty has attracted researchers' attention in recent literature (e.g., Wilby, 2005; Gitau and Chaubey, 2010; Jung et al, 2012). Parameter uncertainty is caused by the

lack of an adequate high quality database or by the inefficiency of the optimization algorithm used to obtain parameter values (Montanari, 2011). Generally speaking, parameter uncertainty stems from a set of parameters that is selected to run the mathematical model. Hydrological models incorporate many parameters that require sound estimations in order to produce reasonable results (Benke et al., 2008). However, due to the wide-range of applications and various degrees of complexity of hydrological models, it is not easy to quantify parameter uncertainty (Bergström et al., 2002; Blenkinsop and Fowler, 2007).

Hydrological model performance (and environmental models in general) is affected by parameter uncertainty (Wilby, 2005). In models, the true value of parameters is unknown because the data and the methods used to calibrate the models also have uncertainty. The usual way to quantify parameter uncertainty is to vary the parameter's value and compare the model's outputs (Benke et al., 2008). Probabilistic approaches, such as the Generalised Likelihood Uncertainty Estimation (GLUE) of Beven and Binley (1992) or the Markov Chain Monte Carlo (MCMC) of Hasting (1970), have been developed to address uncertainty, with respect to the specific aim of calibration and parameter estimation (Benke et al., 2008). However, it is not an easy task to identify a "true" set of parameters due to the parameterization equifinality, which is primarily caused by the dependence of the parameters (Beven, 2006). The concept of equifinality in hydrology suggests that different sets of parameters could result in same or similar predictions (Montanari, 2011). In other words, there is not a unique set of parameters for a hydrological modeling system, even with the same model structure, climate forcing and initial conditions (Tang and Zhuang, 2008). Thus, choosing an efficient optimization algorithm for estimating an "appropriate" set of parameters for the purpose of narrowing the range of parameter uncertainty becomes a crucial objective in the hydrologic community (Muttil and Jayawardena, 2008; Moradkhani and Sorooshian, 2009, Arsenault et al., 2013).

As more and more hydrological models were developed and applied in various studies, efforts were made to look for an effective optimization algorithm to calibrate hydrological models. For example, Singh et al., (2012) compared three different optimization algorithms,

Shuffled Complex Evolution (SCE-UA) developed by Duan et al. (1992), parameter estimation (PEST) developed by Goegebeur and Pauwels (2007) and robust parameter estimation (ROPE) developed by Bardossy and Singh (2008), that were used in the calibration of the physically-based hydrological model WaSiM-ETH of the Rem catchment in Germany. The calibration of the hydrological model was based on critical events selected by the Identification of Critical Events (ICE) algorithm. Results showed that the SCE-UA and ROPE algorithms could be used for multivariable calibration. PEST was inferior when the relationships between the variables and the observations were highly nonlinear.

2.2.4 Behavioral uncertainty

Behavioral uncertainty is a subjective source of uncertainty, which is associated with the human behaviour of individuals in decision-making groups or organizations (Ullma, 2006). Behavioral uncertainty mostly depends on the deciders. The human factor plays an important role in making a right strategic policy. This type of uncertainty is derived from four main sources: human error, decision uncertainty, volitional uncertainty and dynamic uncertainty (Ullma, 2006, Stump et al., 2004). Human error uncertainty refers to uncertainty that stems from the decision-makers' subjective knowledge. It is normally the result of the individuals' viewpoint. Decision uncertainty refers to uncertainty in the choice of one or more appropriate decision from a series of possible options. This choice usually depends on the decision makers' understanding and judgment. Volitional uncertainty pertains to the unpredictable decisions that people make on a topic. Nobody has the capability of making the perfect decision and controlling all possibilities. It is acknowledged that accidents exist as a reality. Finally, dynamic uncertainty refers to changes in the decision-making process that are caused by the organization or the individuals' variables, or alterations in the initially determined decisions that are influenced by certain unexpected events. Furthermore, dynamic uncertainty is affected by the degree of confidence in the selected decision and in the subjective judgment (Ullma, 2006).

2.2.5 Summary

The combination of the various sources of uncertainty can be very complex (De Rocquigny et al., 2008). Numerous classifications of existing uncertainties have already been produced in the literature (Prudhomme et al., 2003; Stainforth et al., 2007; Kay et al., 2009). However, a perfect and comprehensive classification scheme cannot be established. Different types of uncertainty often appear to overlap. For instance, uncertainty in downscaling methods can be classified as part of model uncertainty, which is associated with selected mathematical methods, but it also can be categorized as parameter uncertainty, as it depends on the data that needs to be downscaled (Khan et al., 2006).

Due to difficulties in quantifying natural uncertainty, which is inherently stochastic, and behavioural uncertainty, which is influenced by subjective factors, scientists are often more concerned with model uncertainty and parametric/data uncertainty that can be assessed and controlled by comparing models or model ensembles and by model calibration and validation. In general, in climate change impact studies, research work on uncertainty has mainly focused on the following sources of uncertainty: GCM structure, GCM parameters, greenhouse gas emission scenarios, climate sensitivity, natural variability, downscaling methods, hydrological model structure, and hydrological model parameters (e.g., New and Hulme, 2000; Prudhomme et al., 2003; Wilby and Harris, 2006; Kay et al., 2009; Chen et al., 2011a, b; Poulin et al., 2011). Recent research on uncertainty assessment in climate change impact on hydrology is described in the next section.

2.3 Uncertainty assessment in climate change impacts on hydrological regimes

As the global climate changes, it is becoming increasingly important to understand, quantify and reduce uncertainties in the assessments of climate change impacts, in a hydrologic perspective, to ensure the development of adaptive water resources management plans (Ghosh and Katkar, 2012). Climate change will have a significant direct impact on the strategic planning of hydroelectric industry, in terms of both hydroelectric production and demand (Ouranos, 2010). Figure 2.1, which is taken from the 2006-2010 strategic plan of

Hydro-Québec, presents the dominant risk, as assessed by the company in its projected net income for 2008. The net income would be principally influenced by watershed runoff conditions and could vary between +645 and -635 million dollars because of the inherent randomness of inflows into Hydro-Québec's hydroelectric systems. Thus, the analysis of future hydrological regimes plays an important role in the strategic planning of hydroelectric production.

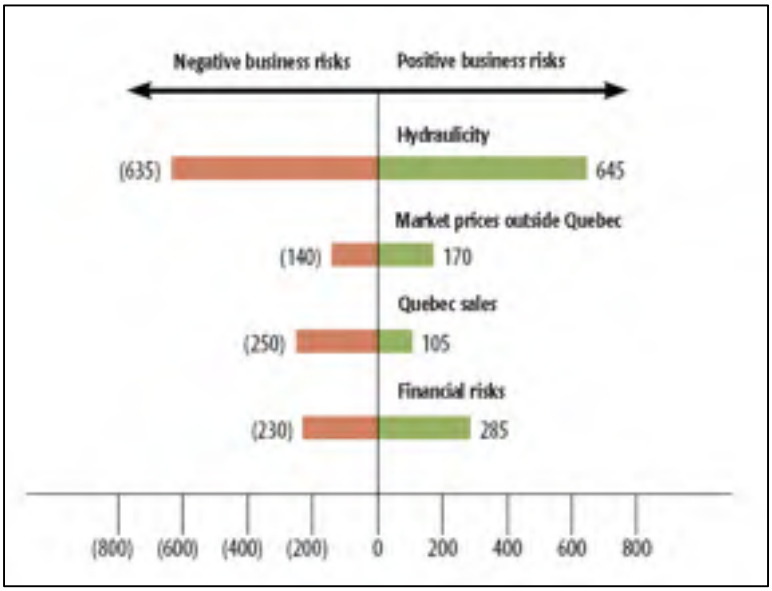

Figure 2.1 Analysis of net earnings sensitivity to various risks for 2008 (in millions of dollars) Taken from Hydro-Québec (2006, p. 52)

The efficient use of techniques and models to assess uncertainties has been encouraged by scientists. Such tools have improved the accuracy and simulation ability of models, and improved the precision of meteorological data (e.g. Jones et al., 2006; Kay and Davies, 2008). Along with a wide range of simulated output from different climate models associated with unquantified uncertainties in the modeling process (Murphy, et al., 2004), credible computation results are more than ever required by decision-makers, such as watershed managers, in order to establish regional strategic plans that have less uncertainty. So far, most of the research has focussed on quantifying the uncertainty arising from one specific source in the hydrological response to climate change (e.g. Bergström et al., 2002; Kay and

Davies, 2008, Poulin et al., 2011) and few examples of combining sources of uncertainty have been reported (e.g. New and Hulme, 2000; Prudhomme et al., 2003; Wilby and Harris, 2006; Kay et al., 2009; Chen et al., 2011a; Jung et al., 2012).

2.3.1 Uncertainty in climate models

Global Climate Models (GCMs), sometimes referred as General Circulation Models, are a class of computer-driven models which are used to simulate climate, forecast weather and project climate change. They attempt to represent physical processes in the atmosphere, ocean and cryosphere, as well as on land, and have been improved for the simulation of many aspects of climate (Prudhomme et al., 2003). Initially used for numerical weather predictions, they have been adapted for the physical characterization of atmosphere and ocean dynamics (Stute et al., 2001). The spatial resolution of GCMs is typically a few degrees of latitude and longitude, or about 200 to 500 km horizontal resolution. The atmosphere is discretized in 3D cells or grid boxes. The time steps for the atmospheric dynamics and radiation calculations may be minutes to hours (IPCC, 2007). Each grid-box at the land/ocean surface has appropriate fractions of land and ocean. Land topography is also taken into account in solving the climate models' equations (Hansen et al., 1983). Figure 2.2 schematically represents the GCM's general structure in an individual land/ocean-atmospheric column comprised of superimposed grid-boxes. Different climate models may apply different equations to represent the atmospheric/land/ocean processes (including subgrid modelling) and use different computational approaches, such as the computational grid and time step, numerical method, etc. (Edwards, 2010), and these differences will contribute to the GCMs structure uncertainty.

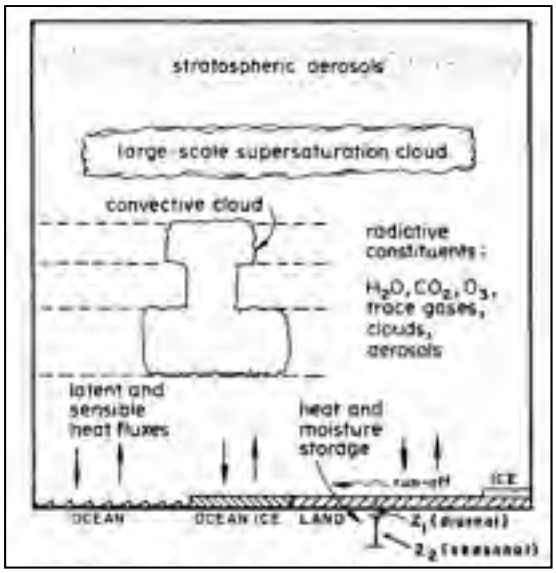

Figure 2.2 Schematic illustration of the GCM structure of an individual land/ocean-atmospheric column
Taken from Hansen, J., et al. (1983, p. 611)

Many climate models have been developed over the last four decades in an attempt to provide feasible and credible climate projections that vary from simple models, which are easy to apply and save computing time because fewer parameters are required (e.g. MAGICC/SCENGEN) (Wigley et al., 2000), to more comprehensive three-dimensional GCMs (e.g. TGCM, TIE GCM) (IPCC, 2007), which include more elaborate representations of energy, water and biochemical cycles. Although GCMs use fundamental physics' based equations to represent the climate system, they differ in the way various processes, such as precipitation, are parameterized and in the spatial resolution used to represent atmospheric, earth and ocean, and energy and water exchanges and processes (Randall et al., 2007).

Researchers (e.g. New and Hulme, 2000; Prudhomme et al., 2003; Wilby and Harris, 2006; Kay and Davies, 2008) have evaluated differences in current/projected climates due to GCM structure. Uncertainty in climate models is recognized as an important source of uncertainty in climate change impact studies (e.g. Wilby and Harris, 2006; Chen et al., 2011a).

Murphy et al. (2004) presented a systematic attempt that involved using multi-ensemble experiments with one GCM to determine the range of climate change responses that are consistent with modelling uncertainties. This is one of the few studies dealing with uncertainties due to GCM parameters. A 53-member ensemble of model versions was constructed by varying the set of GCM parameters. The investigation revealed that the structural choices made in building the GCMs, the choice of climate model parameters and the assumed distributions of parameter values can impact the result of the ensemble experiment. The ensemble with perturbed parameters can produce a wider range of regional changes than those shown by traditional methods that scale the output of an individual simulation. This study was based on the assumption that individual perturbations will combine linearly, something which is unlikely to be valid at the regional scale. They proposed more experiments of using multiple parameter perturbations for creating GCM ensembles to further investigate structural uncertainties.

Many studies looked at the uncertainty stemming from the climate model structure. For instance, Blenkinsop and Fowler (2007) studied mean and extreme precipitation in the British Isles by using six RCMs, driven by four different GCMs, and quantified the range of uncertainty in current and future climates. They concluded that the choice of RCM and the driving GCM are an important factor that contributes to the overall uncertainty in both current and future climate projections. In particular, they found that the uncertainty in future climate projections stemming from the choice of GCM or RCM varies with the variable being investigated, e.g. precipitation, as well as the time of the year and the spatial resolution. In this study, the models failed to properly simulate persistent low precipitation, particularly during summers. This suggested a deficiency in the RCMs ability to simulate longer and more severe events, such as droughts. The authors also reported that running RCMs requires expensive computations, which made these models unusable for uncertainty assessment.

Kay and Davies (2008) compared the performance of two potential evaporation (PE) formulae used on a set of climate model outputs (five GCMs and eight RCMs) to investigate the effects on the hydrological impact of climate change. One is a simple but more empirical,

temperature-based PE formula, and the other is the well-established and more physically based Penman-Monteith PE formula, which is data-intensive, needing temperature, humidity, radiation and wind speed data. The delta-change downscaling approach (Hay et al., 2000; Diaz-Nieto and Wilby, 2005) was used to downscale the GCM output to the watershed scale. The probability distribution model (PDM) (Moore, 2007) was used to calculate the current and future hydrological response (high and low flows) of three catchments situated in Britain by means of two different forms of PE. Results showed that the simple temperature-based method generally got a better fit than that using the Penman-Monteith formula for the 1961-1990 period. In the case of the future 2071-2100 period (used in the A2 emission scenario (IPCC, 2007)), the two methods had different effects on the hydrological impact of climate change. For example, when using the Penman-Monteith formula, the impact on seasonal changes of low flows was found to be more significant, than with the simple temperature-based method, in regions of South and East Britain. For high flows, the effects would differ because the simple temperature-based PE produced larger increase in winter and spring flows than the Penman-Monteith PE for the catchment in South Britain. This paper also found that the impact of uncertainty in hydrology due to PE formulae was negligible compared to GCM structure or RCM structure. Other studies dealing with climate model structure include Minville et al. (2008), Horton et al. (2006), Serrat-Capdevila et al. (2007).

The studies above consider the GCMs to be equally ‘good’ at representing present and future climates. Other studies specifically addressed the issues of climate model structure possibly being given unequal weights in climate change assessment studies. Fordham et al. (2012) noted that different climate model structures do not perform equally well in their ability to hindcast the key dynamics of climatic system. Some efforts were made to evaluate the importance of individual climate model among ensembles, such as the studies of Wilby and Harris (2006) who introduced an ‘impact relevant climate prediction index’, based on precipitation minus potential evapotranspiration, to evaluate the impact of climate change on low flows. A maximum entropy method (MEM) was adopted by Laurent and Cai (2007) in an experiment to optimally use Atmosphere-Ocean Global Climate Models (AOGCMs) to assess climate change impact. They developed the MEM to assess the probability-weighted

multi-model ensemble average of a particular climate variable such as temperature or precipitation. Two other methods, the root mean squared error minimization method (RMSEMM) and the simple multi-model ensemble average method (SMEAM), were compared with MEM via a performance criteria calculated by error bounds on precipitation or on temperature. The entropy of a probability distribution, as introduced by Shannon (1948), was used to measure how close a given probability distribution is to the uniform distribution, i.e. the entropy reaches the maximum when the distribution is uniform. It was reported that MEM provided helpful results in analyzing the uncertainty and that this method performed better than the SMEAM and RMSEMM in combining AOGCMs to compute the climate projections. This research only focused on the average monthly precipitation and temperature. They also found that the regional variability due to model uncertainty in their study area was more significant for precipitation than for temperature. The implementation of MEM proved useful in combining a set of AOGCMs for climate change assessment.

A European integrated project, the ENSEMBLES project (ENSEMBLES, 2009), identified six metrics to produce the RCM-specific weights, based on their ability to simulate the present climate. These six metrics were (1) large scale circulation based on a weather regime classification; (2) meso-scale signal based on seasonal temperature and precipitation analysis; (3) probability density distribution match of daily and monthly temperature and precipitation analysis; (4) extremes in terms of re-occurrence periods for temperature and precipitation; (5) trend analysis of temperature; (6) representation of the annual cycle in temperature and precipitation. This investigation assumed that a good performing model was expected to have relatively high weights in all metrics. Déqué and Somot (2010) used the probability density distribution of daily temperature and precipitation ENSEMBLE metrics to weight RCMs. Chistensen et al. (2010) also presented an aggregated model weight by compounding the ENSEMBLES six weights. Another study on quantifying RCMs, presented by Fowler and Ekström (2009), applied an averaged weight to each RCM combined with the UK-wide spatial-similarity weights and region-specific magnitude-discrepancy weights.

Tebaldi et al. (2004) proposed a Bayesian statistical model to derive probability distributions of precipitation change for a set of GCMs with the purpose of determining weights. They made another attempt in 2005 to evaluate the GCMs, based on the probability distribution of temperature change. Their Bayesian statistical method was inspired by an earlier study by Giorgi and Mearns (2002), who used the Reliability Ensemble Averaging (REA) method to estimate GCM weights or reliability factors, according to individual model performance, in other words, models having a small bias and offering good convergence (i.e. for which the response is close to a majority of the other models analyzed) would be rewarded. This was seen as an innovative step in the combination of ensemble projections (Tebaldi et al., 2005). Sperna-Weiland et al. (2012) investigated four weighting methods, including the original REA method, two extensions of the REA method and a performance-based GCM selection method that were compared with the equal weight method. They found that the original REA method and the extensions of this method produced smaller uncertainty ranges when compared to the equal weight method. The REA method has been used in many studies around the world, such as Huisman et al. (2009), Torres and Marengo (2013) and Sun et al. (2014).

2.3.2 Uncertainty in climate sensitivity

New and Hulme (2000) defined climate sensitivity as an increase in the equilibrium of the global-mean surface air temperature caused by a doubling of atmospheric CO_2 concentration. Climate sensitivity has been reported to be in the range of 1.5-4.5°C of the equilibrium global temperature increase with a most likely value of about 3.0°C (Gates et al., 1992; IPCC, 2013). The uncertainty related to climate sensitivity is wide because atmosphere/land/ocean feedbacks are still not well understood. Through its effect on global-mean temperature, climate sensitivity plays a primary role as a determinant of overall climate change (Fordham et al., 2012) and remains a notable source of uncertainty in long term temperature projections (Rogelj et al., 2012). In a recent research, it was reported that the uncertainty in climate sensitivity could be reduced by a well-designed program for climate model evaluation and

improvement, and also by reducing the uncertainties related to other sources of radiative forcing such as aerosols. (Caldeira et al, 2003).

Since climate sensitivity in GCMs is estimated according to climate model simulations which are inherently linked to model structure, uncertainty assessment in climate change studies has seldom addressed GCM structure and climate sensitivity separately (Brekke et al., 2008; Kay et al., 2009; Jung et al., 2012). Uncertainty due to climate sensitivity was investigated in the following studies.

Schwartz (2008) studied the key reasons for the currently large uncertainty related to climate sensitivity and examined approaches to reduce it. He indicated that climate sensitivity is of fundamental importance for the development of mitigation scenarios but that its uncertainty is difficult to accurately quantify. In his paper, he concluded that the key limit in evaluating uncertainty in climate sensitivity is the small fractional changes in temperature and in radiative fluxes. Another restriction is the complexity of cloud processes and the difficulty of representing them in climate models. The treatment of clouds leads to model-to-model differences in climate sensitivity. Finally, the limited understanding of the processes that control the radiative influences of atmospheric aerosols also hinders the investigation of climate sensitivity.

Caldeira et al. (2003) did a study on CO_2-induced climate change to show how uncertainty in allowable carbon emissions caused uncertainty in climate sensitivity. By developing scenarios with stabilized atmospheric CO_2 contents, they concluded that climate sensitivity uncertainty produced much greater uncertainty in allowable CO_2 emissions than did carbon cycle uncertainty. Uncertainty in climate sensitivity is only one factor that affects uncertainty in allowable CO_2 emissions.

Knutti and Hegerl (2008) reviewed recent estimates of the equilibrium climate sensitivity and indicated that climate sensitivity is one of the largest sources of uncertainty in projections of climate change. As climate sensitivity is not a directly tunable quantity in climate models, the

sensitivity in models was investigated by perturbing parameters related mainly to atmospheric processes, such as clouds, precipitation, convection, radiation, land surface, etc. They concluded that climate models generally perform well when climate sensitivity is in the range 1.5-4.5°C with a most likely value of about 3.0°C. However an upper limit of climate sensitivity was difficult to determine because strong aerosol forcing or large ocean heat uptakes might hide an intense greenhouse warming.

2.3.3 Uncertainty in emission scenarios

The IPCC Special Report on Emission Scenarios (SRES) team developed four main greenhouse gases emission scenarios, A1, B1, A2 and B2, which predicted a range of conceivable change in population and economic activity over the 21st century. These became the basis for recent climatological studies (IPCC, 2007). Each emission scenario reflects independent assumptions about future possible demographic, technological and socio-economic story lines. These scenarios were developed to evaluate the impacts of global atmospheric concentrations of CO_2, CH_4 and N_2O due to human activities, such as in the historical experiment 20c3m conducted by the Coupled Model Intercomparison Project Phase 5 (CMIP5) (Taylor, et al., 2012). CMIP5 is a project based on a set of coordinated climate model experiments performed by the WCRP's Working Group on Coupled Modelling (http://www.wcrp-climate.org/index.php/wgcm-overview).

Prudhomme et al. (2003) evaluated the output of GCMs by using the four SRES emission scenarios on five catchments in Great Britain. Their results showed little uncertainty among the four scenario groups. Kay et al. (2009) studied a range of emission scenarios derived from the four SRES storylines applied to two catchments in England and showed that uncertainty of emission scenario was very low for the larger and flatter catchment, but was more important for the smaller and steeper catchment. Chen et al. (2011a) also studied the uncertainty of two SRES emission scenarios, A2 and B1, compared with other sources of uncertainty. Results showed that the future discharges predicted by the A2 scenario were consistently greater than by those predicted by the B1 scenario and that the uncertainty due to

the emission scenarios is less than that of GCM structure, downscaling method and GCM initial conditions.

2.3.4 Uncertainty in downscaling methods

GCMs are used to represent various climate states and are not specifically designed for assessing hydrological responses to climate change. Although results vary considerably between models, GCM runoff predictions are over-simplified relative to the output of hydrological models. For example, GCMs lack lateral transfers of water within the land system between grid cells (Fowler et al., 2007). A hydrological model constitutes a better way of simulating watershed flow regimes. However, due to the mismatch between outputs generated from global climate models and the input to hydrological models, GCMs precipitation and temperature output need to be spatially downscaled and their inherent bias removed or diminished before these projections can be used into hydrological models.

Downscaling is a hot issue in climate change impact studies (Prudhomme et al., 2003). The relative performance of different downscaling methods for hydrological impact assessment has been assessed in an increasing number of studies (e.g. Hay and Clark, 2003; Diaz-nieto and Wilby, 2005; Wilby and Harris, 2006; Prudhomme and Davies, 2009a, Chen et al., 2011a, b) and revealed that the choice of a downscaling method is critical owing to the distinct structure and algorithm (Chen et al., 2011b).

Downscaling methodologies are classified as dynamic or statistical. The dynamic downscaling method (DDM) employs regional climate models (RCMs) that are applied to a limited area in which boundary conditions come from GCM output (Serrat-Capdevila et al, 2007). DDM is capable of producing a finer resolution output which is typically resolved at the $\sim 0.5^{o}$ latitude and longitude scale by embedding high-resolution models within a GCM (Fowler et al., 2007). However, DDM is computationally expensive and is strongly dependent on GCM boundary forcing (Fowler et al., 2007). Statistical downscaling methods (SDM) apply statistical equations to establish empirical relationships between large scale

climate features (e.g. circulation patterns) and local scale climate variables (Wilby et al., 1998). The simplest statistical method is the change factor method, also referred to as the delta change approach (Fowler et al., 2007). The other SDMs are classified into the following groups: regression models, weather typing schemes and weather generators (Fowler et al., 2007). SDM directly incorporates observed information in the downscaling process. Compared to DDM, this method is computationally efficient (Fowler et al., 2007). However, the basic assumption of SDM is that the statistical relationships between large scale climate features and local scale climate variables are time invariant, i.e. they remain identical in a future climate as compared to the current climate (Ghosh and Katkar, 2012), a shortcoming not found in DDM. A number of research projects investigated the uncertainty related to different downscaling methods (e.g. Hay and Clark, 2003; Prudhomme and Davies, 2009a; Chen, et al., 2011a).

Prudhomme and Davies (2009a) studied the uncertainty in downscaling techniques. The regional climate model HadRM3, from the Hadley Centre (http://www.metoffice.gov.uk/), and the Statistical Downscaling Model (SDSM) developed by Wilby et al. (2002) were used in assessing uncertainty in a climate change impact study. Results showed that HadRM3 overestimated early spring flow, while SDSM underestimated early spring flows and late autumn flows. A similar modeling experiment is found in the study of Hay and Clark (2003) that used one statistically downscaled atmospheric model and the RegCM2 regional climate model (Giorgi et al., 1988). Because of the fundamental mathematical treatment of downscaled climate variables, these two downscaling techniques were assumed to perform equally well. Up till now, no acknowledged approach has been able to establish their relative performance because of their very different structure (Ghosh and Katkar, 2012).

Chen, et al. (2011b) applied six downscaling techniques to downscale GCM output to the watershed scale in order to quantify the climate change impact on a Canadian river basin (Quebec province). These techniques included RCM data without any bias correction (BC) but with a specific hydrologic model calibration, RCM data with bias correction method, the change factor (CF) method, a stochastic weather generator (WG), the SDSM of Wilby et al.

(2002) and a discriminant analysis coupled with step-wise regression method (DASR). Overall, the methods produced hydrographs similar to those simulated by using observed precipitation and temperature data, with the RCM data with bias correction and the SDSM having the best fit to the observations. The analysis of climate change scenarios showed a large uncertainty during the snowmelt season that is related to downscaling techniques. The uncertainty envelope of the simulated hydrological variables due to the downscaling methods was slightly less than the uncertainty envelope associated to the combination of GCM structure and GGES. The main conclusion of this study was that the results of climate change impact studies that use only one downscaling method should be interpreted with caution.

Khan, et al. (2006) compared the performance of three statistical downscaling methods by conducting an uncertainty analysis of the downscaled results of daily precipitation, daily maximum and minimum temperature. They investigated the following approaches: SDSM, the Long Ashton Research Station Weather Generator (LARS-WG) model (Semenov and Barrow, 1997, 2002) and an Artificial Neural Network (ANN) model (Coulibaly et al., 2005). Regarding the performance of these models, they concluded that SDSM was the best statistical downscaling method of the three studied and that it was capable of reproducing almost all statistical characteristics of the observed data with a 95% confidence level. LARS ranked second and ANN was last. This study also stated that the performance of these three downscaling models would remain the same under future climate forcing scenario because the uncertainty of the results would be mostly dominated by the uncertainty of GCMs.

2.3.5 Uncertainty in natural variability

Climate varies in a range of scales, from intra-annual, to decadal, to very long time scales. Long-term climatic data series enable researchers to study of natural variability. Natural variability is difficult to assess based on the short-term observations that are commonly used to predict future climate conditions. Natural variability is defined as the uncertainties stemming from the inherent randomness or unpredictability found in the natural world (Willows et al., 2003) and can usually be subdivided into low-frequency variability and high-

frequency variability according to their timescales (IPCC, 2007). Only by using climatic data series that span long time periods one can properly assess the entire spectrum of frequency variability. Because observed climatic time series seldom exceeds a few hundred years, researchers must construct series that will enable them to define the magnitude and characteristics of natural variability and extremes.

Several approaches have been developed to assess the magnitude of natural variability. For instance, Prudhomme and Davies (2009a) described a method involving block resampling to create multiple series from a limited period of observation. Observations were divided into seasonal blocks and classified into four sub-series (winter, spring, summer and autumn). The blocks were randomly and independently selected from each of the four seasonal sub-series, in the normal annual sequence (i.e. a spring block was selected after a winter block), to construct long-term series.

Another approach is to use a stochastic weather generator (Chen et al., 2009; Chen et al., 2012) to produce long climatic time series. For example, Minville et al. (2008) used a stochastic weather generator to produce daily time series of precipitation and temperature in order to evaluate the range of simulated hydrological regimes in a northern basin under current and future climates. However, both the block resampling and the stochastic weather generator approaches will underestimate long term climate variability because they are based on generating climatic information derived from a limited time series of observed climate.

2.3.6 Uncertainty in hydrological modeling

Hydrologic models result from an integration of mathematical descriptions of conceptualized hydrologic processes at the watershed scale and serve a specific purpose in water resources engineering and in understanding the dynamic interactions between climate and land-surface hydrology (Chiang, et al., 2007). Such models are based on mathematical and statistical concepts and are used to represent the hydrologic cycle and provide a wide range of structures, from lumped conceptual models to semi-distributed and distributed physics-based

models (Liu and Gupta, 2007). Over the last decades, watershed hydrologic models have played an increasing role in water resources planning, development and management (Singh and Woolhiser, 2002; Benke et al., 2008). The sources of uncertainty in hydrological models are mainly related to model structure and parameters (Liu and Gupta, 2007). The uncertainty of hydrological model structure stems from the inability of a hydrological model to accurately represent hydrological processes (Liu and Gupta, 2007). This uncertainty is related to components of a hydrological model, such as the equations used to describe the hydrological processes, the numerical methods used, etc. (Butts et al., 2004). The usual way to evaluate the uncertainty of hydrological model structure is to compare the performance of different hydrological models in representing watershed hydrological regimes. The parameter uncertainty in hydrological models refers to the uncertainty of the parameter estimates. Parameter uncertainty is caused by an over-parameterization of the model and/or results from the optimization algorithm used to estimate parameter values (Montanari, 2011). As it is less significant than other sources of uncertainty (Kay et al., 2009; Chen et al., 2011a), it is not examined in this study.

Poulin et al. (2011) investigated the uncertainty related to the hydrological model structure and model parameters of a snow-dominated watershed in province of Quebec, Canada. One lumped conceptual model, HSAMI (Fortin, 2000), and one spatially-distributed physically-based model, HYDROTEL (Fortin et al., 2001), were used in this study to illustrate the uncertainty of the model structure. Parameter uncertainty was estimated by performing multiple automatic calibrations. The results revealed that the uncertainty of the hydrological model structure is more significant than the uncertainty of model parameters. They concluded that the use of hydrological models with different levels of complexity should be included in studies of the global uncertainty associated to hydrological impact assessments.

Butts, et al. (2004) developed a hydrological framework that can be used to explore different hydrological model structures within the same modeling tool in both the rainfall-runoff and channel routing components of hydrological models. Their framework enables the assessment of a variety of alternative distributed hydrological models (model structure),

including both conceptual and physically-based process descriptions, for the purpose of generating multi-model ensembles. An analysis was conducted with this framework to evaluate the performance of ten different model structures, for example, lumped vs Muskingum-Cunge vs fully dynamic routing, and determine the impact of varying model structure on the uncertainty of hydrological simulations for a particular basin in Oklahoma. The impact of uncertainty in the rainfall input data and uncertainty in the hydrological model parameters were also described. This study showed multi-model simulations to be a superior alternative to current single-model simulations and found that the model structure was the main source of hydrological modeling uncertainty. The challenge in this study was to devise a strategy for selecting appropriate model structures for particular applications. It was proposed that different sources of uncertainty should be systematically evaluated for not only hydrological simulation but also hydrological forecasting.

The hydrological model's sensitivity to climate change was explored by Jones, et al. (2006), who applied a large number of scenarios in various hydrological models to a variety of catchments. Sensitivity analyses were performed using three hydrological models, two lumped conceptual daily rainfall-runoff models and one simple top-down two parameter model, on 22 Australian catchments covering a range of climates, from cool temperate to tropical, and from moist to arid. The results showed that model sensitivity to climate change is influenced by model structure, potential errors in climate inputs and model parameters like soil moisture storage and physiographic properties, such as vegetation cover.

Chiang, et al. (2007) developed a methodology for identifying the uncertainty in river-flow prediction through the quantification of the different sources of uncertainty in hydrologic models used for comparing model performance. Different sources of uncertainty, including system uncertainty, entire uncertainty and inherent uncertainty, were evaluated through the observation of the hydrological model's behaviour under increasing input uncertainty levels, based on an index, called the Model Structure Indicating Index (MSII), that originated from the Nash-Sutcliffe efficiency. In this study, system uncertainty refers to the discrepancies between observed data and model outcome obtained with the best-fitted parameter set. Entire

uncertainty represents the discrepancies between observed data and model outcome by using parameter sets in the calibrated parameter space. Inherent uncertainty is the discrepancy between model outcome obtained with the best-fit parameter set and with parameter values within the parameter space. The results demonstrated that the index can be used to compare and rank hydrological models, and to help the selection of the best model for the intended application.

Among the other hydrological studies that address the issue of hydrological model structure and parameter uncertainty are those of Liu and Gupta (2007) and Staudinger et al. (2011).

2.3.7 Multi-source uncertainty assessment and risk analyses

Risk analyses are required to evaluate systems performance under extreme operating conditions. In hydrological studies, one might be interested, for example, in evaluating the risk of flooding or the risk of failure of a dam. In climate change impact studies, these assessments are more complex to conduct because of the various uncertainties that plague the estimation of future flows. As many sources of uncertainty are present, this poses the problem of adequately combining these sources of uncertainty. A common approach to the combination of various sources of uncertainty is the Monte Carlo sampling method. This method requires establishing weighting schemes for each source of uncertainty, i.e. a probability distribution. For example, climate sensitivity is usually assigned a triangular probability distribution (New and Hulme, 2000, Prudhomme et al., 2003), while uncertainty due to a GHG emission scenario is usually assigned a uniform distribution, as each scenario is assumed to occur equally (Prudhomme et al., 2003; Kay et al., 2009). Approaches developed for assigning weights to GCM models were presented in section 2.3.1, while the method developed by Chiang et al. (2007), described in section 2.3.6, can be used to assign weights to hydrological models based on their performance.

A number of studies investigated the combination of different sources of uncertainties and their cascading effects on the hydrological regime of watersheds. While some of them

assumed that each source of uncertainty had an equal weight in the overall hydrological response, other studies assumed unequal weight strategies. The next paragraphs present some of the more salient studies that deal with the uniform and unequal weighting strategies used to assess climate change impact in the water resources sector.

2.3.7.1 Uniform weighting strategies

The following studies evaluated multi-source uncertainties in climate change impact studies. They assessed independent sources of uncertainty throughout the modeling process with no attempt of giving unequal weights and then quantified the significant source among those studied.

Kay et al. (2009) investigated six sources of uncertainty, involving future GHG emissions, GCM structure, downscaling techniques, hydrological model structure, hydrological model parameters and the internal variability of the climate system (with different GCM initial conditions) in the impact of climate change on flood frequency. The study was conducted on two catchments in England that had very different characteristics in terms of area, rainfall regime and topography. Five GCM structures, four SRES scenarios, two downscaling methods (delta change method and direct use of RCM data), two hydrological model structures, a number of different calibrated parameter sets for hydrological models and two ways of assessing the effect of climate variability were explored. The results showed that for both catchments, the GCM structure uncertainty was the largest source of uncertainty, while the hydrological model parameter uncertainty presented a very small effect.

Chen, et al. (2011a) evaluated the global uncertainty of hydrological variables such as annual discharge, winter discharge, time to peak, etc., in a watershed located in Quebec, Canada, using an ensemble of six GCMs, two GGES, five GCM initial conditions, four downscaling techniques, three hydrological model structures and ten sets of hydrological model parameters. Based on the relative change of each hydrological variable, it was concluded that the GCMs were the most important source of uncertainty, followed by the downscaling methods. GCM initial conditions, GGES and hydrological model structure were ranked third,

fourth and fifth respectively. The least important source of uncertainty was found to be the hydrological model calibration parameters. This study outlined the overall uncertainty of a range of sources by using only equal-weighting schemes. However, the use of unequal-weighting schemes was recommended for future research.

Other studies in which equal weights were given to various sources of uncertainty in climate change impact studies include Minville et al. (2008), Prudhomme and Davies (2007), Déqué et al. (2007) and Jung et al. (2012), etc. These studies concluded that climate model structure carries the largest uncertainty when compared to other sources.

2.3.7.2 Unequal-weight assigning strategies

In the past decade, some researchers began to undertake unequal-weight experiments in order to assess multi-source uncertainties in hydrological studies. Each independent source of uncertainty was given a probability distribution that was either based on accredited knowledge (e.g. for climate sensitivity, see New and Hulmes, 2000) or on quantitative approaches (e.g. for GCM structure, see Wilby and Harris, 2006).

New and Hulme (2000) described a methodology for quantifying uncertainties inherent to the production of future climate change information in climate impact assessments. Their study combined, by means of a Bayesian Monte-Carlo simulation, the following sources of uncertainty: GHG emissions scenarios, climate sensitivity and GCM structure using pre-defined prior probability distributions. The simulation results produced by the seven different GCMs were given equal prior probabilities. The four emission scenarios used in their study were assumed to be all equally likely to occur. Four frequency distributions, among them a simple triangular probability distribution and a skewed distribution, were adopted for climate sensitivity. Different climate change signals in mean temperature and precipitation were compared in order to extract the probability distributions of outputs linked to the GCMs. This research mostly focused on the uncertainty in climate change scenarios, and assumed GCM performance to be equal and made no assumptions about uncertainty due to hydrological model structure. Its major conclusion was that the posterior probability distribution of the

simulated changes in temperature and precipitation of climatic simulations indicated that significant uncertainty arises from GCM structure and that the triangular prior distribution to climate sensitivity produced a more elongated posterior distribution of temperature and precipitation than the other distributions used in the study.

Similarly to New and Hulme (2000), Prudhomme et al. (2003) explored a methodology for quantifying sources of uncertainty, including GCM structure, GGES and climate sensitivity, in the hydrological response of a set of five river catchments located in Great Britain. The uncertainty due to downscaling techniques was excluded. They adopted a Monte Carlo simulation approach to sample the sources of uncertainty according to prescribed weights. Equal weights were assigned to individual GCM and emission scenarios. Different weights were given to climate sensitivity values, based on an approach presented by New and Hulme (2000). Natural variability was included as a source of uncertainty by a bootstrapping method. The study demonstrated that uncertainty in GCM structure generally appears to be the largest single source of uncertainty. The uncertainty due to emission scenarios and climate sensitivity was less significant in the total uncertainty assessment.

Wilby and Harris (2006) developed a probabilistic framework for combining information from an ensemble of 2 GGES, 4 GCMs, 2 downscaling methods and two sets of hydrologic model parameters, as well as a lumped conceptual hydrological model, to evaluate different components of uncertainty affecting the hydrological response of a river basin located in England. A Monte Carlo approach was applied to explore components of uncertainty. Emission scenarios, downscaling methods and hydrological model parameters were given equal probabilities. Weights were assigned to the GCMs according to their performance in simulating current effective rainfall by using an ‘impact relevant climate prediction index’ (precipitation minus potential evapotranspiration) adapted from a climate prediction index approach introduced by Murphy et al. (2004). This study highlighted that low-flows were most sensitive to uncertainty in GCM structure, and then to the uncertainty in downscaling method and lastly, to the effect of hydrologic model parameter and emission scenario uncertainties. Although it was one of the most comprehensive uncertainty analyses to date,

the study only explored uncertainty in future low flows in a watershed dominated by rainfall. The choice of the weighting scheme, which was based on effective rainfall, was dictated by the hydrological process analysed, i.e. low flows.

Christensen, et al. (2010) suggested that model weighting brings certain effects to the generation of ensemble-based climate projections. They explored the applicability of combining 6 performance indices into a weighting scheme and applying them to a large ensemble of RCM simulations. The indices were (1) large-scale circulation based on a weather regime classification; (2) meso-scale signal based on seasonal mean temperature and precipitation; (3) probability density distributions of daily and monthly temperature and precipitation; (4) extremes in terms of re-occurrence periods for temperature and precipitation; (5) long-term trends in temperature; (6) annual cycle in temperature and precipitation. By combining these independent indices, relative weights for each model were generated. This use of model weights, which was sensitive to the aggregation procedure, resulted in different sensitivities to the selected metrics. For instance, different models would emerge as best performers if different weighting schemes were applied. The authors suggested that the uncertainty of using weighting schemes should be explored by considering multiple metrics and aggregation procedures, since the weighing itself was also regarded as a source of uncertainty.

Other unequal-weight assigning studies that incorporate multiple sources of uncertainties in climate change assessment include those of Tebaldi et al. (2004, 2005), Knutti et al. (2010) and Sansom et al. (2013).

The abovementioned studies all involved multi-sources uncertainty assessments, as well as weight-assigning experiments that reflect the scientific attempts made so far at applying various weighting schemes to the sources of uncertainty. These studies have acknowledged that the uncertainty due to GCM structure will be quite significant when compared to other sources of uncertainty (e.g. Prudhomme et al., 2003; Wilby and Harris, 2006; Minville et al., 2008; Kay et al., 2009, Chen et al., 2011a). None of them presented a comprehensive

framework that could be used to evaluate all sources of uncertainty, starting from climate projection all the way to hydrological modeling using equal/unequal weighting schemes. This thesis is intended to be a step toward the achievement of such comprehensive uncertainty assessments. It aims to establish a framework for the quantification of the main sources of uncertainty, including GCM's structure, climate sensitivity, natural variability and, to a lesser extent, hydrological model's structure, that are associated to climate change impacts on hydrology. Finally, it also aims to assess the respective effect of these sources of uncertainty on GCM and climate sensitivity through the use of weighting schemes.

CHAPITRE 3

METHODOLOGY

To evaluate hydrological uncertainties in climate change impact assessments, three main steps were carried out in this research. First, regional climate projections were established for a range of GCMs and climate sensitivities. Then, hydrological simulations were performed to evaluate the impact of climate change on the hydrological regime of the study watershed, the Manicouagan River Basin (MRB), which is described in Chapter 4. To that end, regional climate projections were statistically downscaled from coarse GCM scale to regional scale. Finally, Monte Carlo experiments were carried out to quantify various sources of uncertainty and to evaluate the effect of assigning different weights to the climate projections according to GCM structure and model sensitivity. The entire process therefore required a suite of models (climate and hydrological) and methods to generate the hydrological response to climate change. Among the possible sources of uncertainty which are found in simulated hydrological regimes, the following were considered: (1) GCM structure, (2) climate sensitivity, (3) natural variability and (4) hydrological model structure.

This chapter describes the methodology that was employed in this study. Four hydrological models were used to evaluate the impact of different model structures on the overall hydrological response to climate change. A schematic flow chart of the methodology is presented in Figure 3.1. It is applicable to each hydrological model. Climate projections used to force the hydrological models were produced using ten GCMs and five climate sensitivities. Each climate projection covers a span of 33 years, which is commensurate with the length of the control period (1975-2007). A change factor (CF) approach was used as a downscaling tool to bring the GCM projections at the watershed scale, and a stochastic weather generator was applied to generate statistically similar precipitation and temperature time series that could be used to investigate uncertainty due to natural variability. The analysis was conducted with a future time horizon centered in 2080 (2065-2097). Finally, to

combine different uncertainty components of the hydrological response to climate change, a Monte Carlo approach was adopted.

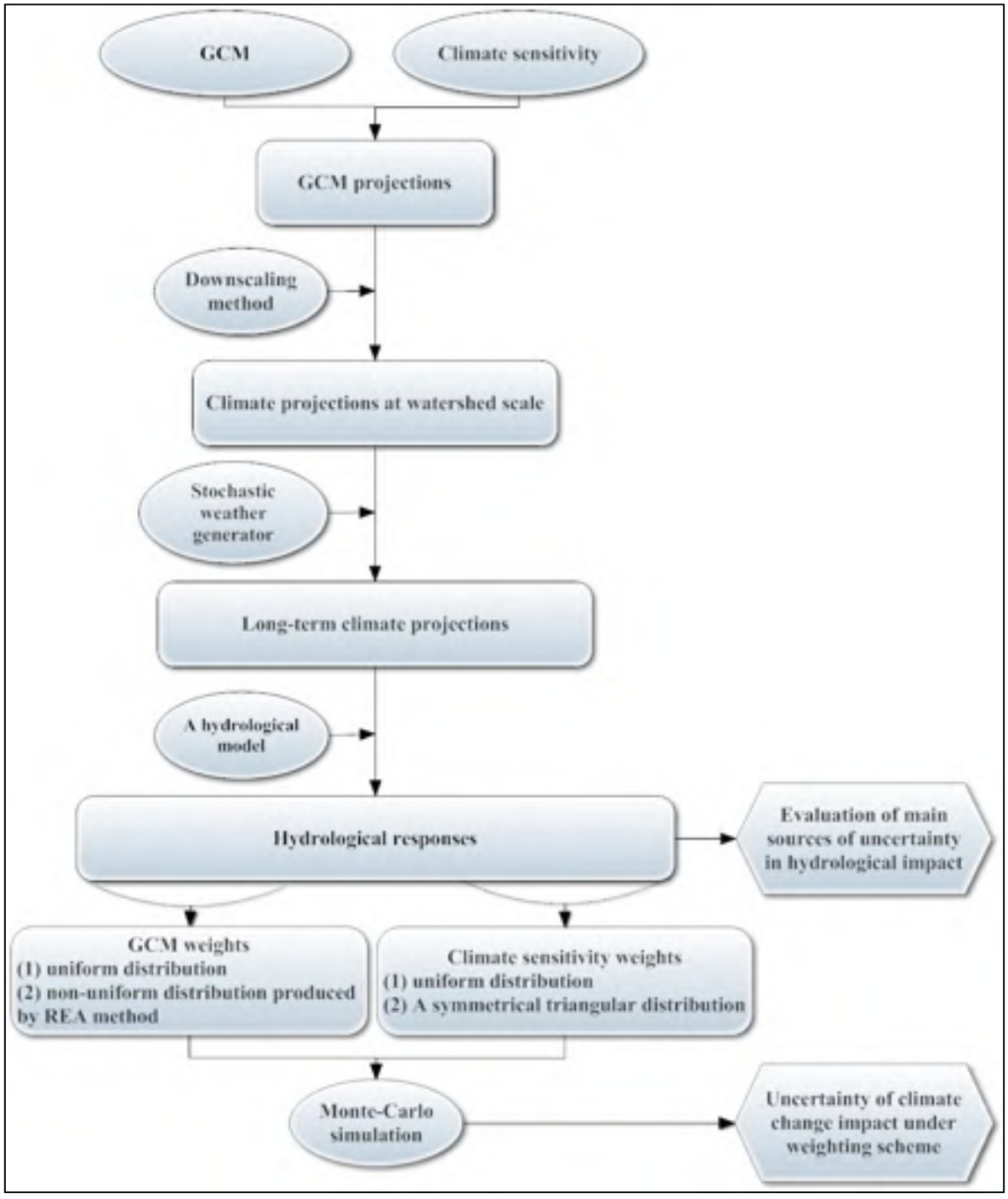

Figure 3.1 Flow chart of the methodology. The flow chart applies to each of the four hydrological models employed in this study

3.1 Research assumptions

The research assumptions on which the proposed methodology is based are presented below:

(1) The four main sources of uncertainty, which are mentioned above, were investigated in this study. Other sources of uncertainty, such as GHG emission scenarios, downscaling methods and hydrological model parameters, were not addressed, although recent research suggests that some may be important sources of uncertainty in hydrological impact studies (see, for example, Chen et al., 2011a). Emphasis here was more on combining sources of uncertainty with different weighting scenarios, rather than on covering all sources of uncertainty.

(2) The MAGICC/SCENGEN software applied to produce the climate projections with specific climate sensitivity is a simple climate model which could make the emulation of GCMs over a wide range of scenarios (Meinshausen et al., 2011a). The IPCC AR4 (2007) reported that MAGICC has a slight warm bias in global-mean temperature projections, but this is unfounded (Wigley et al., 2000). This is partly associated with forcing differences between the standard MAGICC forcing and those used in AR4 GCMs (Wigley et al., 2000). This forcing difference is not considered in this study. The estimations from MAGICC/SCENGEN were assumed to properly emulate the IPCC AR4 values.

(3) The stochastic weather generator used in this study to generate synthetic time series daily temperature and precipitation does not explicitly take into account low frequency climate variability. It therefore underestimates long term climate variability. Moreover, low frequency natural variability is further underestimated because the weather generator is calibrated with time series of rather short length (33 years) to fully capture the ‘true’ natural variability of the observed climate.

(4) The CF method used in this study, combined with the stochastic weather generator, produces time series of daily precipitation which neglects changes in the number of wet and dry days that are likely to occur in the future. Moreover, the methodology assumes that the probabilities of the occurrence of a wet day following a wet day, a dry day following a wet day, etc. as well as the bias, will remain unchanged in the future. Finally, the variability of precipitation remains unchanged in the future.

(5) The range of climate sensitivity covers 2.0 to 4.0°C, in accordance with the generally accepted range in the research community (Rogejl et al., 2012).

3.2 Climate projections

The first step of the methodology consists in producing the climate projections that will be used as input for the hydrological models. The climate projections were developed in order to encompass a range of GCM structures and climate sensitivities. To that end, monthly temperature and precipitation output fields from 10 GCMs were first retrieved from the study area. The outputs from each GCM selected reflect a global-mean temperature condition, which is described as climate sensitivity. There have been efforts to investigate the uncertainties of hydrological regimes that are related to alternative GCM structures by using different individual GCM projections in the environmental models (Bradley, 2010). These investigations demonstrated that climate projections varied from model to model but failed to properly account for inter-GCM differences in climate sensitivity (Fordham et al., 2012). By averaging GCM predictions based on models with different sensitivities, the results obtained showed a tendency to bias the average response towards models with high sensitivity (Fordham et al., 2012). It is therefore important to assess the two sources of uncertainty (GCM structure and climate sensitivity) separately. In order to separate the GCM structure from the climate sensitivity as two distinct sources of uncertainty, a modeling approach was used to generate, starting with each original GCM temperature and precipitation fields, monthly time series of temperature and precipitation that correspond to different climate sensitivities. This was done using the MAGICC/SCENGEN climate model (Wigley et al.,

2000, see Section 3.2.2 for a description of the model). In this work, only one GGES was utilised to produce the climate projections, i.e. SRES-A2.

To spatially and temporally downscale future GCM projections to the watershed scale, as well as to account for natural variability as a source of uncertainty, a change factor approach and a stochastic weather generator were combined to generate a suite of future daily temperature and precipitation time series. These time series then became the climate projections that were inputted into the hydrological models.

Each step of the climate projection process is now described.

3.2.1 Global climate models

As mentioned in Chapter 2 (section 2.3.1), the GCM structure is probably the most important source of uncertainty in the assessment of the hydrological impacts caused by climate change. In this study, the uncertainty of climate change impact due to GCM structure was investigated by using ten GCMs, namely: BCCR-BCM2.0, CGCM3.1, CNRM-CM3, CSIRO-MK3.0, GFDL-CM2.0, INM-CM3.0, IPSL-CM4, MIROC3.2 (medres), MPI-ECHAM5 and NCAR-PCM1 (IPCC, 2007). General information related to these GCMs is presented in Table 4.2. These GCMs were selected, from all currently existing GCMs, because they display a wide spectrum of predicted precipitation and temperature changes (IPCC, 2007).

3.2.2 Climate sensitivity

Climate sensitivity, which is defined as the global mean climatological temperature change due to a doubling of CO_2 content, is a primary determinant of overall climate change (Fordham et al., 2012). As a measure of the temperature response of the Earth to a change in radiative forcing (Loehle, 2014), climate sensitivity is neither a physical quantity that can be measured directly through observations nor a directly tunable quantity in GCMs, as it depends on many parameters that are primarily related to atmospheric processes (Knutti and

Hegerl, 2008; Knutti et al., 2010). Each GCM generates climate projections that are inherently linked to a given climate sensitivity, depending on the representation of the various feedback processes in the model, including, for example, clouds and water vapor. Some models (e.g. MPI) reflect higher sensitivities for higher forcing scenarios than for lower forcing scenarios (Meinschausen et al., 2011a).

The estimate of the climate sensitivity of a model will come from the model's outputs rather than be based on the model itself (Caldeira et al., 2003; Rogelj et al., 2012; Masters, 2013; Loehle, 2014). By perturbing parameters affecting clouds, precipitation, convection, radiation, land surface and other process used in producing GCMs projections, one can produce new climatic output and therefore obtain different climate sensitivities (Knutti and Hegerl, 2008). However, such simulations are usually not available, so that it is hardly possible to obtain, for a given GCM, a suite of climate projections that reflect a range of climate sensitivities. Therefore, uncertainty assessment in climate change studies has seldom tackled GCM structure and climate sensitivity separately (Brekke et al., 2008; Kay et al., 2009; Jung et al., 2012). New and Hulme (2000) presented an uncertainty study in climate sensitivity using the MAGICC/SCENGEN model. This reduced-complexity carbon-cycle and climate model allows the production of climatological time series that reflect the effects of climate sensitivities in a simple manner.

In this thesis, the MAGICC/SCENGEN (Model for the Assessment of Greenhouse-gas Induced Climate Change and the Global and Regional Climate Scenario Generator, v5.3 – Wigley et al., 2000) software is used to mimic GCMs climate projections with the prescribed climate sensitivities. This freely available software package for the Windows operating system has been (and continues to be) one of the essential tools used by the IPCC since 1990 to generate projections of future global mean temperature and sea level rise (Meehl et al., 2007; Meinshausen et al., 2011b). It is a climate model "emulator" that contains two modeling parts, MAGICC and SCENGEN (see Figure 3.2). MAGICC/SCENGEN enables users to generate multi-model ensemble of averaged forecasts of temperature, precipitation and mean sea level pressure for the full suite of GCMs used in the IPCC's fourth Assessment

Report (AR4) and for more than 50 SRES scenarios, and this, for any given year up to 2100. MAGICC is a coupled gas-cycle (representing the process of a gaseous fluid undergoing a series of thermodynamic states), climate and ocean model that creates global climate projections related to empirical atmospheric composition changes. A range of gas-cycle models are interactively coupled with the global-mean temperature and sea level model in MAGICC to produce climate projections of atmospheric carbon dioxide concentrations, based on anthropogenic emissions scenarios and climate system feedbacks (Fordham et al., 2012). Default values of the climate model parameters suggested by MAGICC were used in this study. A sensitivity analysis on the aerosol forcing parameter did not produce significantly different results. SCENGEN uses the global-mean climate information, in conjunction with a pattern scaling regionalization algorithm (Santer et al., 1990) and the Coupled Model Intercomparison Project 3 (CMIP3) archived GCM database (http://www-pcmdi.llnl.gov/ipcc/about_ipcc.php), to produce spatially detailed climate outputs on future changes in temperature, precipitation and mean sea level pressure in 5° by 5° grid boxes. The projections are generated first by running MAGICC with specified GGES and climate sensitivities. The MAGICC output is then passed to the SCENGEN component to produce spatial patterns of change in terms of studied GCMs by means of the regionalization algorithm. The entire procedure is easy to operate and takes only a few minutes to run on a personal computer.

A distinct feature of MAGICC/SCENGEN is that it can easily perform a factor separation analysis (i.e., to evaluate the effects of various choices of forcing assumptions, such as aerosols and carbon cycle climate feedbacks, or to separate the effects of climate or carbon cycle uncertainties from the forcing uncertainties) in order to produce individual GCM projections (Meinshausen et al., 2011a). By modifying a number of gas-cycle and climate model parameters (see Figure 3.3), MAGICC/SCENGEN users can produce climatological time series with specific forcing and climate sensitivities.

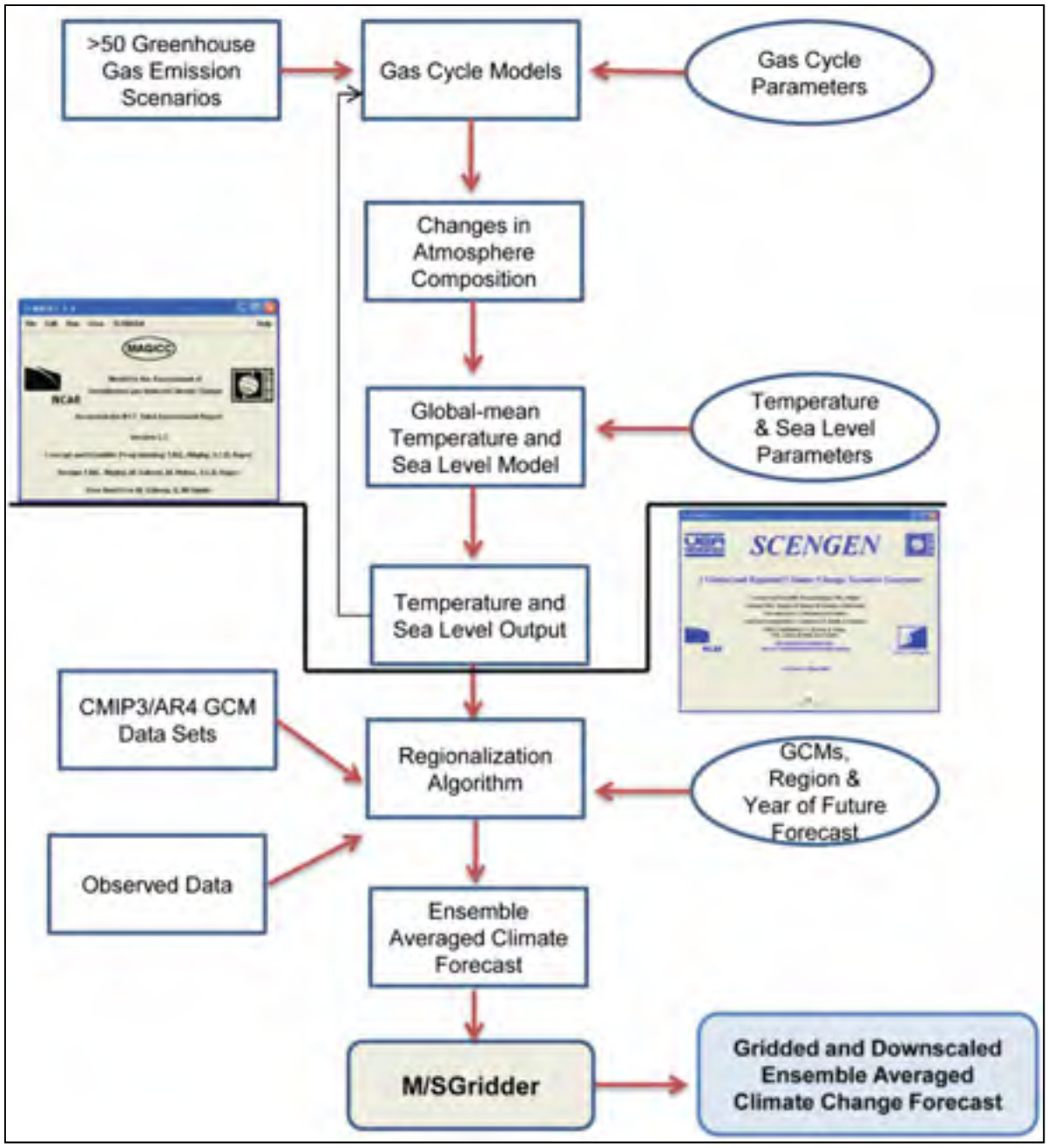

Figure 3.2 Schematic diagram of the structure and flow of the MAGICC/SCENGEN software. The user-defined parameters of the model are displayed in the elliptical shapes Taken from Fordham et al. (2012, p. 5)

Figure 3.3 Adjustable forcing controls and climate model parameters in the MAGICC model

It was therefore possible, in this study, to generate climate model outputs, such as temperature and precipitation, that covered a range of GCM structures and climate sensitivities.

To that end, a 'change factor' approach, described by equations (3.1) and (3.2), was employed to generate the climate projections for the prescribed climate sensitivities, based on 'original' climate sensitivity values estimated from the original GCMs output (as described in Section 4.2.1.2). Subscript $\Delta T(n)$ refers to the original climate sensitivity of each GCM (see Table 4.2), and subscript $\Delta T(m)$ refers to the climate sensitivities selected for the analysis. Subscript m|s refers to the MAGICC/SCENGEN model. The equations are:

$$T_{new,\Delta T(m)} = T_{gcm,\Delta T(n)} + \left(\overline{T}_{m|s,\Delta T(m)} - \overline{T}_{m|s,\Delta T(n)}\right) \tag{3.1}$$

$$P_{new,\Delta T(m)} = P_{gcm,\Delta T(n)} \times \frac{\overline{P}_{m|s,\Delta T(m)}}{\overline{P}_{m|s,\Delta T(n)}} \tag{3.2}$$

where $T_{new,\Delta T(m)}$ and $P_{new,\Delta T(m)}$ are the GCM-derived monthly temperature and precipitation for climate sensitivity $\Delta T(m)$, $T_{gcm,\Delta T(n)}$ and $P_{gcm,\Delta T(n)}$ are the original GCM

monthly temperature and precipitation over the study area for climate sensitivity $\Delta T(n)$. $\overline{T}_{m|s,\Delta T(n)}$ and $\overline{P}_{m|s,\Delta T(n)}$ refer to the spatially-averaged monthly temperature and precipitation in the study area as produced by MAGICC/SCENGEN using the original GCM climate sensitivity $\Delta T(n)$. The estimation of the original GCM climate sensitivity will be stated in section 4.2.1.2. $\overline{T}_{m|s,\Delta T(m)}$ and $\overline{P}_{m|s,\Delta T(m)}$ are similar to $\overline{T}_{m|s,\Delta T(n)}$ and $\overline{P}_{m|s,\Delta T(n)}$ but for climate sensitivity $\Delta T(m)$. Change factors are described by $(\overline{T}_{m|s,\Delta T(m)} - \overline{T}_{m|s,\Delta T(n)})$ and $\frac{\overline{P}_{m|s,\Delta T(m)}}{\overline{P}_{m|s,\Delta T(n)}}$.

3.3 Downscaling

The downscaling technique employed here combines both temporal disaggregating and spatial downscaling. The former converts monthly values of temperature and precipitation into daily values. The latter brings the temperature and precipitation fields from the GCM to the watershed scale. In this study, the change factor (CF) method (Diaz-Nieto and Wilby, 2005; Hay et al., 2000), which is also called the 'perturbation method' (Prudhomme et al., 2002) or the "delta-change method" (Fowler et al., 2007), was used as the downscaling procedure. According to Fowler et al. (2007), the CF method is the simplest downscaling technique that can be used to translate large-scale GCM output to a finer resolution. A major advantage of using this downscaling method is the ease with which alternative emissions scenarios or scenarios based on alternative GCMs can be synthesized (Kay et al., 2009). The equations are:

$$T_{cor,day} = T_{obs,day} + \left(\overline{T}_{fut,mon} - \overline{T}_{pre,mon}\right) \tag{3.3}$$

$$P_{cor,day} = P_{obs,day} \times \frac{\overline{P}_{fut,mon}}{\overline{P}_{pre,mon}} \tag{3.4}$$

Where $T_{cor,day}$ and $P_{cor,day}$ are the downscaled and bias corrected temperature and precipitation at the daily time step, $\overline{T}_{pre,mon}$ and $\overline{P}_{pre,mon}$ are the monthly mean simulated temperature and precipitation over the present period (1961-1990), as produced by the GCMs, $\overline{T}_{fut,mon}$ and

$\bar{P}_{fut,mon}$ are the monthly mean future temperature and precipitation produced by the GCMs with different climate sensitivities, obtained from equations 3.1 and 3.2. $T_{obs,day}$, and $P_{obs,day}$ are the observed temperature and precipitation at the daily time step, which is based on data from the National Land and Water Information Service database (NLWIS) of Agriculture and Agri-Food Canada (AAFC, http://www.agr.gc.ca/eng/?id=1343071073307) and covers the Canadian territory on a 10km grid. Information on NLWIS is presented in Chapter 4. ($\bar{T}_{fut,mon}$-$\bar{T}_{pre,mon}$) and $\frac{\bar{P}_{fut,mon}}{\bar{P}_{pre,mon}}$ are respectively the change factors for temperature and precipitation for various GCMs and climate sensitivities.

3.4 Natural variability

In this study, natural variability was investigated by using the stochastic weather generator of the École de Technologie Supérieure (WeaGETS) (Caron et al., 2008; Chen et al., 2012) to generate long times series of daily temperature and precipitation. WeaGETS is a Matlab-based software package which integrates several options of other weather generators that are used to produce daily meteorological series of unlimited length (Chen et al., 2012). WeaGETS enables users to perform impact studies on the rare occurrences of meteorological variables, which is not possible when using a block resampling approach. However, the original version of WeaGETS (Caron, 2008) used in this work underestimates interannual variability. More recently, WeaGETS was upgraded to explicitly account for interannual variability (Chen et al., 2012). The original version of WeaGETS was used in this study because the improved version was unavailable at the time the decision was made to use this method to investigate natural variability. This version was also used by Minville et al. (2008) to take into account natural variability in climate change impact studies.

In this work, 50 climate projections (minimum and maximum air temperature, precipitation) were produced by using equations (3.3) and (3.4) to combine 10 GCMs and 5 climate sensitivities. Each projection, covering 33 years of future climate (2065-2097), was inputted into WeaGETS to generate 50 time series of 33-year duration that were statistically similar to the original projection. Although the weather generator underestimated interannual

variability, it successfully retained the original features of the input data with a high-frequency natural variability (Chen et al., 2012). As a result, a total of 2500 time series (10 GCMs × 5 climate sensitivity × 50 natural variability) of future daily precipitation and temperature were generated for input into each of the four hydrological models used in this study. Figure 3.4 graphically shows the combination of GCM structure, climate sensitivity and natural variability that resulted in the 2500 time series used in the hydrological models.

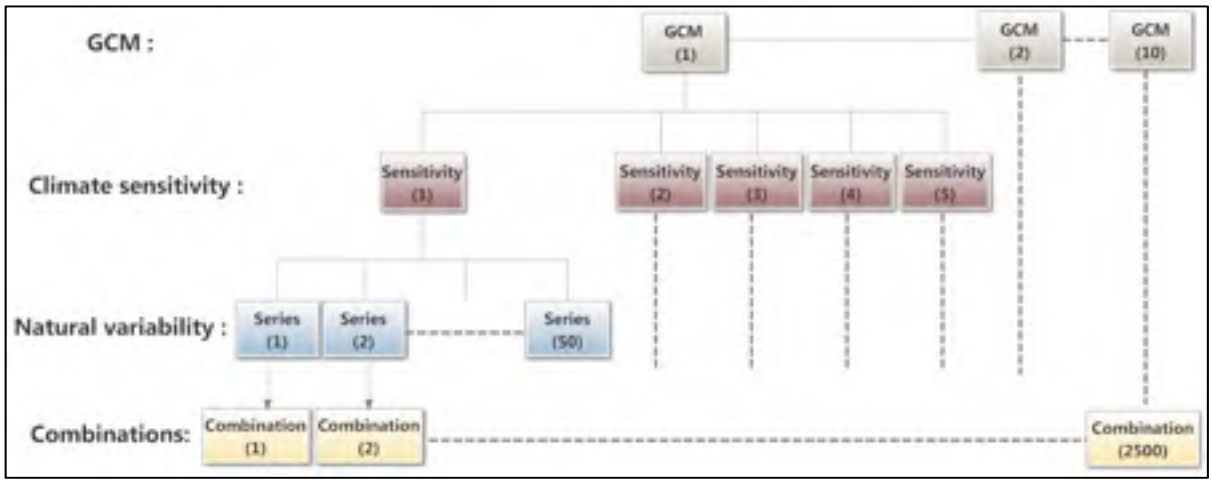

Figure 3.4 Flowchart showing the combination of GCM structure, climate sensitivity and natural variability that was used to produce the precipitation and temperature time series inputted into the hydrological models

Lastly, distinct time series were produced for each sub-watershed of the MRB (see Chapter 4 for a description of the sub-watersheds).

3.5 Hydrological modeling

Previous studies (Chen et al., 2011a; Poulin et al., 2011) have shown that the uncertainty linked to hydrological model parameters was small when compared to the uncertainty of hydrological model structure. Therefore, only the uncertainty associated to model structure was considered in this study.

3.5.1 Hydrological models

Four hydrological models were used, namely two lumped conceptual models (HSAMI and HMETS), one physically-based distributed model (HYDROTEL) and one semi-distributed conceptual model (HBV). These models are described below. The rationale for using four models displaying a range of model structures was that it would provide a clearer understanding of the importance of this particular factor in uncertainty assessment. Previous studies had generally considered a few number of hydrological models (e.g. Wilby and Harris, 2006; Kay et al., 2009; Poulin et al., 2011; Chen et al., 2011a). Table 3.1 outlines the general properties of the hydrological models used in this study.

Table 3.1 Main properties of the hydrological models
Taken from Bergström (1995, p. 446) Singh and Woolhiser (2002, p. 273)
Ludwig et al. (2009, p. 66) and Poulin et al. (2011, p. 629)

Model name	**HYDROTEL**	**HBV**	**HSAMI**	**HMETS**
Model structure	Physically-based	Conceptual	Conceptual	Conceptual
Spatial discretization	Distributed	Semi-distributed	Lumped	Lumped
Time step	Daily/sub-daily	Daily/hourly	Daily	Daily
Input data	Tmin, Tmax, P	Tmean, P	Tmin, Tmax, P	Tmin, Tmax, P
Physiographic info	Required	Required	No-required	No-required
Snowmelt routine	Yes	Yes	Yes	Yes
Automatic parameter calibration routine	Yes	No	Yes	Yes

3.5.1.1 HSAMI model

The HSAMI is described by Fortin (2000) as being a lumped conceptual rainfall-runoff model that was developed and used by Hydro-Québec. This hydrological model is used to simulate the daily and hourly natural stream flows at a watershed outlet. It can also simulate

the major processes of the hydrological cycle such as snowmelt, evapotranspiration, frozen ground, vertical flow and horizontal runoff. The basin-averaged minimum required daily input data for HSAMI are maximum and minimum temperatures, and liquid and solid precipitations (water equivalent) (Chen et al., 2011a). HSAMI contains 23 parameters. Two are used for evapotranspiration, six for snowmelt, ten for vertical water movement, and five for horizontal water movement (Chen et al., 2010). An empirical equation using the observed daily maximum and minimum temperature is applied to compute potential evapotranspiration. HSAMI computes five variables of the snow accumulation and melt process, including ground snow, melt, net ground snow, total melt and number of days since last snow. Snowmelt is simulated with a degree-day model. Vertical flows are simulated using four interconnected linear reservoirs, which correspond to unsaturated and saturated soil zones. Runoff components are filtered through two unit hydrographs and one linear reservoir (Chen et al., 2011a). Soil freezing/thawing is also taken into account in this model. Figure 3.5 illustrates the flow chart of the model.

3.5.1.2 HMETS model

HMETS, which was developed at the École de Technologie Supérieure (Brissette, 2010), is categorized as a lumped conceptual rainfall-runoff model. It operates in the MATLAB environment. Input data for HMETS consists of daily and averaged minimum air temperature, maximum air temperature, liquid precipitation and solid precipitation (water equivalent) or total precipitation in the basin. Twenty parameters are found in HMETS, ten are used for snowmelt, one for evapotranspiration, four for computing infiltration and five for upper and lower soil reservoirs (Chen et al., 2010). The modeling routines of HMETS include snow accumulation, snowmelt, soil freezing, soil thawing and evapotranspiration. HMETS offers a simple degree-day model that allows for the melting and refreezing processes within the snowpack. A simple empirical approach is adopted for the infiltration process, using two different formulations depending on whether the ground is frozen or not. Model calibration is performed by using the Shuffled Complex Evolution algorithm (SCE-UA) that was developed by Duan et al. (1992). The Nash-Sutcliffe criterion is selected to optimize model parameters.

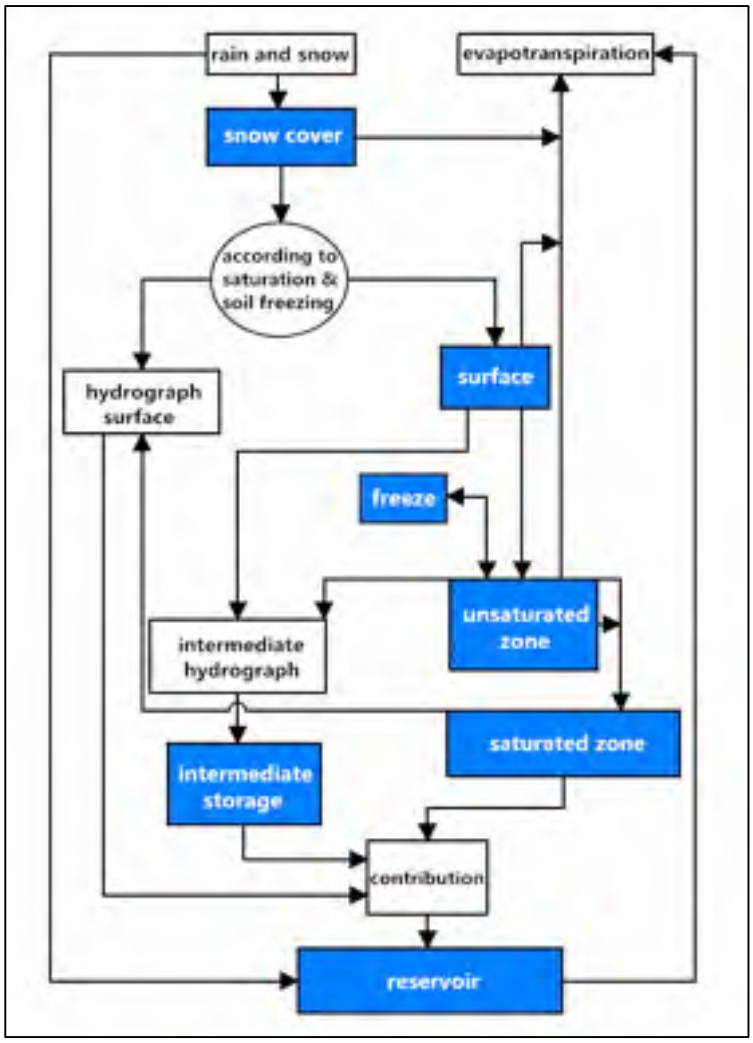

Figure 3.5 Flow chart of the lumped conceptual HSAMI model
Taken from Fortin (2000, p. 8)

3.5.1.3 HYDROTEL model

HYDROTEL, which is categorized by its authors as a spatially-distributed and physically-based hydrological model, was developed at the Institut National de la Recherche Scientifique - Eau Terre Environnement (INRS-ETE) (Fortin et al., 2001). It takes advantage of available remote sensing (RS) data and geographic information system (GIS) data to provide a picture of the spatial variation of watershed characteristics, such as soil type, land use and topography. Vertical water budgets are computed separately in simulation units (or elementary subwatersheds) that are called "relatively homogeneous hydrological units"

(RHHUs). These RHHUs are delineated based on high resolution digital elevation models (DEM). Land use, soil type, and other characteristics in each RHHU are obtained from high resolution RS data and various databases (pedology, etc.) (Fortin et al., 2007). Infiltration and percolation are based on soil hydraulic conductivity and saturation of the subsurface layer (Ludwig et al., 2009). HYDROTEL can run at daily or sub-daily time steps. The main routines in HYDROTEL are snowpack accumulation and melt; potential evapotranspitation (PET); vertical water budget, in which the soil column is subdivided into three zones; surface runoff on RHHUs and channel flow in watercourses (Chen et al., 2011a). The snow accumulation and melt process in HYDROTEL is based on a hybrid degree-day/energy balance approach. The formulation of the potential evapotranspitation of HYDROTEL used in this study is same as that of HSAMI.

HYDROTEL is used operationally by the Centre d'expertise hydrique du Québec (CEHQ) to do streamflow forecasting for several watersheds located in Southern Quebec (Canada). It has been also used for watersheds in Mexico, Côte d'Ivoire, France and Argentina (Fortin et al., 1995; Fortin et al., 2007).

3.5.1.4 HBV model

HBV is categorized by its authors as a semi-distributed conceptual model (Bergström, 1995). It was originally developed at the Swedish Meteorological and Hydrological Institute (SMHI) in the early 70's to assist hydropower operations and it became the standard tool for spillway design flood studies of hydropower systems in Sweden (Bergström et al., 1992). HBV uses the sub-basin as the primary hydrological unit, as well as an area-elevation distribution curve and a classification of land use within each sub-basin for calculation of runoff (Bergström, 1995). Operational or scientific applications of the HBV model have been reported in more than 30 countries around the world (Lindström et al., 1997). HBV requires daily values of mean temperature and total precipitation as meteorological data. The model includes subroutines for meteorological interpolation, snow accumulation and melt, vertical soil moisture movement, evapotranspiration, runoff response, and a simple routing procedure between sub-basins and through lakes (Lindström et al., 1997). HBV has 33 parameters,

including 17 parameters for precipitation, snow accumulation and melt processes, 7 for soil moisture, 5 for runoff response, 1 for routing, 2 for lake simulation and 1 for defining the time step. The snowmelt routine follows a simple degree-day approach, with a water holding capacity of snow which delays runoff. Soil moisture accounting is based on a modification of the linear reservoir theory, insofar as it assumes a statistical distribution of reservoir storage capacities in a basin. Moisture movement is conceptualized with one upper non-linear reservoir and one lower linear reservoir. The runoff generation process is modelled by a response function which transforms excess water from the soil moisture zone into runoff. HBV also take into account direct precipitation and evaporation on lakes, rivers and other wet areas. Figure 3.6 presents the schematic structure of the simulation done of one sub-basin with the HBV model. The left diagrams schematize the routines for snow (top), soil (middle) and runoff response (bottom) respectively. Version 6.0.1 of the model was used in this thesis.

3.5.2 Model calibration and validation

The optimal parameter sets in the hydrological models are selected by doing model calibration and validation. Parameter optimization is performed over a calibration period and model validation, over a different period. The commonly used criterion for model performance is the Nash-Sutcliffe coefficient, NS (Nash and Sutcliffe, 1970):

$$NS = 1 - \frac{\sum_{i=1}^{n}[Q_{com}(i) - Q_{rec}(i)]^2}{\sum_{i=1}^{n}[Q_{rec}(i) - \overline{Q_{rec}}]^2} \tag{3.5}$$

where Q_{com} and Q_{rec} indicate the computed and recorded flows respectively. The NS value ranges from -∞ to 1. As NS approaches 1, model performance improves to perfectly match the entire recorded flows. When NS equals 0, model predictions are as good as the mean of the recorded flows.

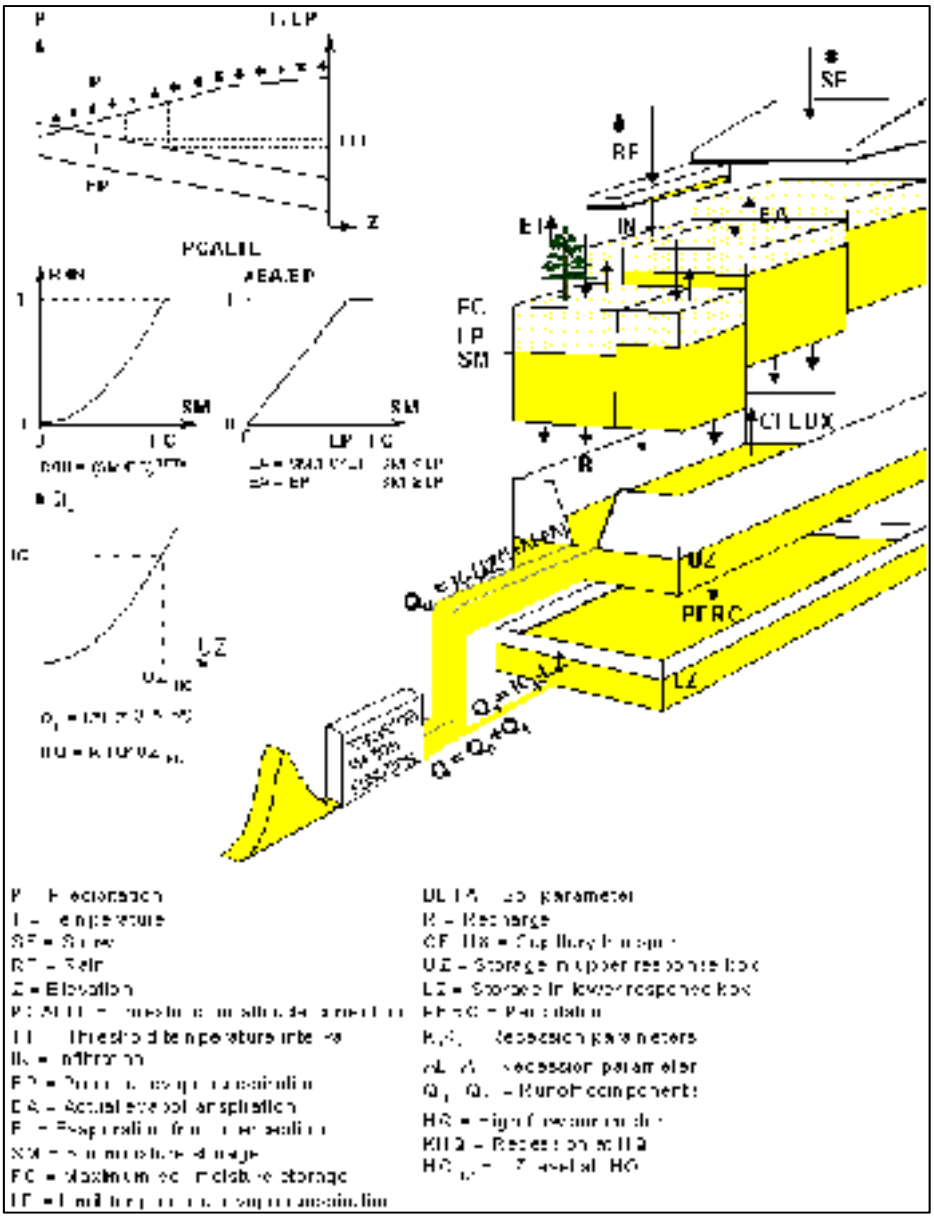

Figure 3.6 Schematic structure of one subbasin in the HBV model
Taken from Lindström et al. (1997, p. 280)

Model calibration for HSAMI, HMETS and HYDROTEL was performed automatically using the Shuffled Complex Evolution-University of Arizona (SCE-UA) algorithm (Duan et al., 1992; Duan, 2003; Arsenault et al., 2013). HBV was calibrated manually. Calibration was done at the daily time step, based on observed streamflow data. Optimal parameter sets were based on maximising the Nash-Sutcliffe coefficient (Poulin, et al., 2011). Calibration results are presented in Chapter 5 (section 5.2.1).

3.6 Uncertainty assessment

In the proposed modeling framework, the distribution of hydrological response for future climate conditions was estimated by using a Monte Carlo approach in which equal and unequal weighting schemes were applied to sources of uncertainty, including GCM structure and climate sensitivity. In Monte Carlo simulations, the pivotal step is providing the probability distribution functions, from which weights are computed that describe the relative importance of different modeling components. Uniform and a triangular distribution functions were applied to climate sensitivity, as justified in the next section. The Reliability Ensemble Averaging (REA) method (Giorgi and Mearns, 2002; Giorgi and Mearns, 2003) was used to evaluate GCMs weights. Both Monte Carlo and REA methods are described in the following paragraphs.

3.6.1 Monte Carlo simulation

To perform uncertainty assessments, probabilistic approaches were used to treat the independent sources of uncertainty as "random variables" used to analyze the range and distribution of uncertainty in the results. A Monte Carlo simulation was chosen for this task. Other studies using Monte Carlo simulations to assess uncertainty in climate change studies include Prudhomme et al., 2003; Tebaldi et al., 2005; Wilby and Harris, 2006 and Jung et al., 2012.

Monte Carlo simulations have been widely used in water resources and other types of analyses (e.g. New and Hulme, 2000; Prudhomme et al., 2003; Wilby and Harris, 2006; Déqué and Somot, 2010). The method involves doing random sampling of the distribution of inputs and successive model runs until a statistically significant distribution of outputs is obtained (Lee, 2002). When computational procedures are too complicated to be formulated mathematically, or when many sources of uncertainty are involved in the modeling framework (Ang and Tang, 1975), this method can be used to propagate the uncertainties through the probability distribution of model inputs.

In a Monte Carlo simulation, each input variable X_i of the system that is analyzed is given a probabilistic distribution. Values of input variables X_i are pooled from their corresponding distribution and used to calculate the corresponding system output. The process of selecting sets of X_i values and estimating the system output is repeated for a large number of times (for example, 10,000) (Modarres, 2006). Statistically significant features of the system output can then be estimated to produce the uncertainty characteristics of the output. This method is very simple and straightforward to apply.

The main disadvantage of the Monte Carlo method is that the probability distribution associated with input variables must be defined before computation can be done (Lee, 2002). In addition, the Monte Carlo method is introduced to ensure coverage of the entire probability distribution of input variables by dividing the distribution into several segments of equal probability (Modarres, 2006).

In a Monte Carlo simulation, each source of uncertainty in a model or modeling system is associated to a prescribed probability distribution function. The probability distribution for GCM structure that was adopted in this study is based on the Reliability Ensemble Averaging (REA) concept of Giorgi and Mearns (2002, 2003) and is explained in section 3.6.2.

From the envelope of all possible climate sensitivity distributions and, in line with the AR4 climate sensitivity synthesis assessment (Figure 3.7), the probability is that climate sensitivity ranges between 2.0 to 4.0°C. As the most likely value of climate sensitivity is 3.0°C (Rogejl et al., 2012), a simple symmetrical triangular distribution for the climate sensitivity parameter was adopted in this study, according to New and Hulmes (2002). In this study, the distribution is ranging from 2.0 to 4.0°C, with a central value of 3.0°C being the most likely value. Note that the IPCC AR5 (IPCC 2013) suggests a range of climate sensitivity of 1.5 to 4.5°C. This range was not adopted here as the information was not available at the time this study was conducted. Figure 3.8 presents the triangular distribution that was employed for assigning different weights to climate sensitivity. A uniform

probability distribution was also considered in order to assess the sensitivity of the simulation results to this parameter.

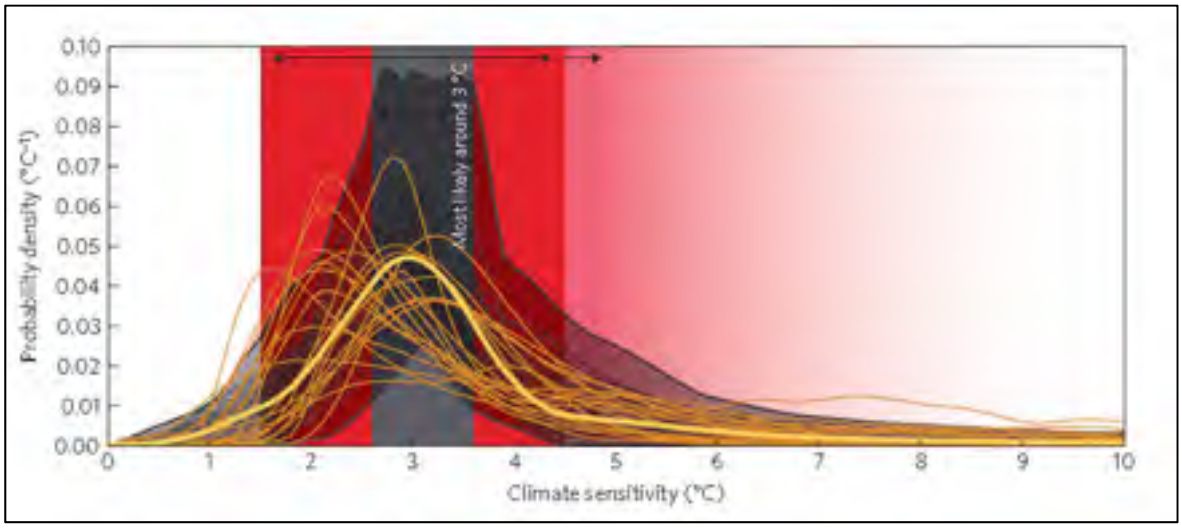

Figure 3.7 Probability density function (PDF) of climate sensitivity. The shaded grey area bounded by a thick black line on the background represents the envelope of all 10,000 randomly drawn climate sensitivity distributions (thin black lines) that are in line with the AR4 climate sensitivity statements. The grey vertical area indicates the most likely probability range around 3.0°C
Taken from Rogelj et al. (2012, p. 250)

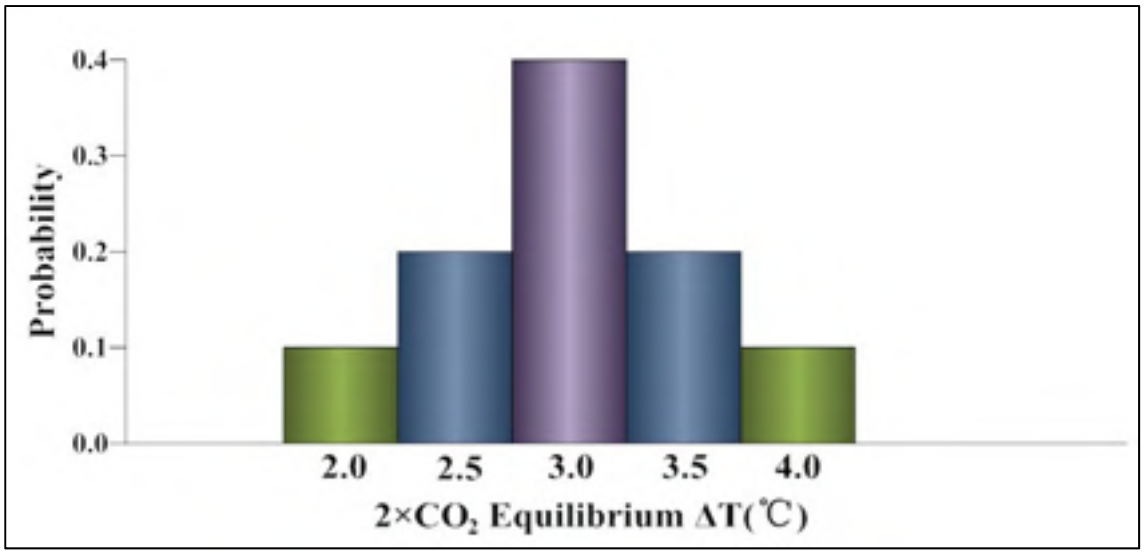

Figure 3.8 The triangular probability distribution of climate sensitivity

Uncertainty due to natural variability was assigned a uniform probability distribution. Finally, each hydrological model used in this study was assumed equally good. In other words, a uniform distribution was assumed to account for the uncertainty due to hydrological model structure.

As explained in section 3.4, 2500 time series of daily precipitation and temperature were generated to cover the uncertainty due to GCM structure, climate sensitivity and natural variability. These series were used as input into the HYDROTEL, HBV, HSAMI and HMETS models to produce a total of 4×2500 = 10,000 time series of future (2080 horizon) daily flows, from which relevant hydrological variables, in this study, annual runoff and spring peak flow, were retrieved and put into a database. The resulting database was then sampled by using the Monte Carlo approach according to the prescribed probability distributions of the sources of uncertainties. A probabilistic distribution of selected hydrological model output (e.g. annual runoff) was then obtained, from which climate change impacts on hydrological regime stemming from these sources of uncertainty were analyzed. Figure 3.9 graphically shows how the Monte-Carlo modeling process works in this study for establishing the equal-weight and unequal-weight experiments.

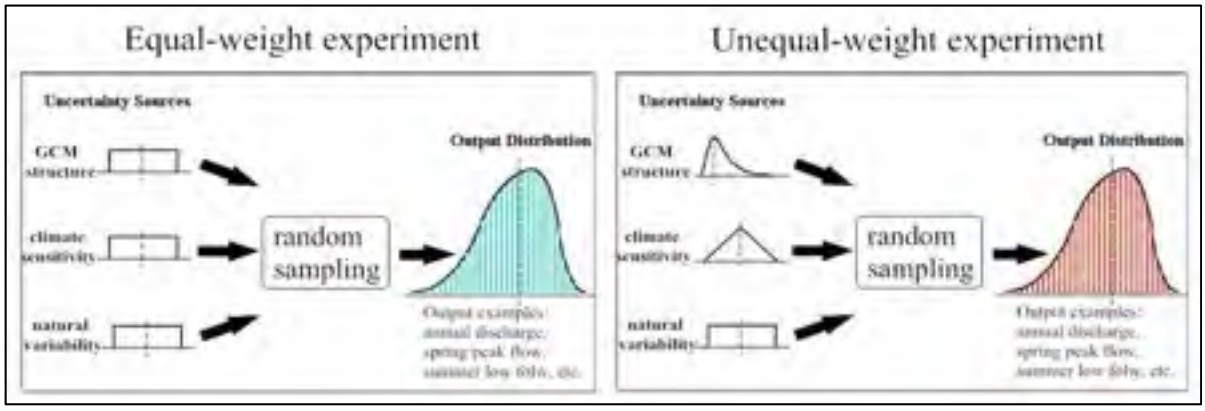

Figure 3.9 Graphical representation of Monte Carlo method

3.6.2 REA method

Attempts have been made to estimate climate model uncertainties on the basis of variables that can be retrieved easily. These include the 'impact relevant climate prediction index' presented by Wilby and Harris (2006), the maximum entropy method by Laurent and Cai (2007), the metrics used in the ENSEMBLES project (ENSEMBLES, 2009) and the Bayesian statistical method by Tebaldi et al. (2004). Such approaches have their own requirements, some of which are applicable to specific hydrological variables, such as low flows (Wilby and Harris, 2006), others are employed for RCMs (ENSEMBLES, 2009), still others need an estimation of prior probability distributions (Laurent and Cai, 2007; Tebaldi et al. 2004). In this study, the Reliability Ensemble Averaging (REA) method (Giorgi and Mearns, 2002) was chosen to estimate the relative importance of GCMs used in the uncertainty assessment. The REA method is an approach, based on individual model performance and model convergence criteria, that is used to assess climate model performance (Giorgi and Mearns, 2002; Giorgi and Mearns, 2003). To our knowledge, this is the first attempt to use the REA method to assign climate model weights in a GCM uncertainty assessment. For a given climate model i, the REA model reliability factor R_i, which can be viewed as an indicator for assigning weights to GCMs, is defined as:

$$R_i = \left[\left(R_{B,i}\right)^m \times \left(R_{D,i}\right)^n\right]^{[1/(m\times n)]} = \left\{\left[\frac{\epsilon_v}{abs(B_{v,i})}\right]^m \times \left[\frac{\epsilon_v}{abs(D_{v,i})}\right]^n\right\}^{[1/(m\times n)]} \quad (3.6)$$

The REA is usually applied at the sub-continental or continental scale (Giorgi and Mearns, 2002; Sperna Weiland, et al., 2012). Since this method was also implemented at the regional scale (Sperna Weiland et al., 2012) it is considered as a technique applicable to large watersheds, such as the MRB (see Chapter 4 for the description of the study site). $R_{B,i}$ describes the climate model performance in simulating an observed climatic variable, e.g. temperature and precipitation. $R_{D,i}$ is a factor that represents model convergence. The parameter ϵ_v is a measure of natural climate variability, which is computed as the difference between maximum and minimum value of 15-year moving averages of the series of observed

climatic data averaged in the study area. The subscript v refers to the particular variable analysed. Bias $B_{v,i}$ is defined as the difference between GCM simulations and observed historical averages of climatic variable for the control period. Distance $D_{v,i}$ is a parameter that indicates how far a given climate model is from the remaining ensemble in simulating a particular climatic variable. A high value of $D_{v,i}$ is an indication that the climate model is an "outlier" in relation to the remaining models. The parameters m and n used to weigh each criterion were assumed to be equal to 1 as suggested by Giorgi and Mearns (2002). The computed value of R_i ranges from 0 to 1. A value close to 1 indicates that the model has a good performance in simulating a given climatic variable and is not an outlier as compared to the ensemble of analyzed models. Details of the computed procedure of the REA approach can be found in Giorgi and Mearns (2002).

Once the reliability factor R_i for each climate model is calculated, the corresponding GCM weight W_i is computed as:

$$W_i = \frac{R_i}{\sum_{i=1}^{N} R_i} \tag{3.7}$$

Where W_i is the corresponding weight for model i and N is the total number of models used.

Figure 3.10 illustrates the procedure of applying the REA method to calculate the reliability factor R_i and the corresponding GCM weights. In this figure, $\bar{V}_{ob,max}$ and $\bar{V}_{ob,min}$ are respectively the maximum and minimum values of a 15-year moving average climatic variable, derived from observed data over the selected reference time period. Monthly air temperature and precipitation are the variables selected in this study. $\bar{V}_{ob,ref}$ and $\bar{V}_{i,ref}$ are the mean values of the variable for the reference time period derived from the observed data and GCM simulations respectively. $\overline{\Delta V_i}$ is the mean change of the variable derived from the simulation of GCM(i) between the future time period and the reference period, while the $\overline{\Delta V}$ is the average of the ΔV values over all GCMs.

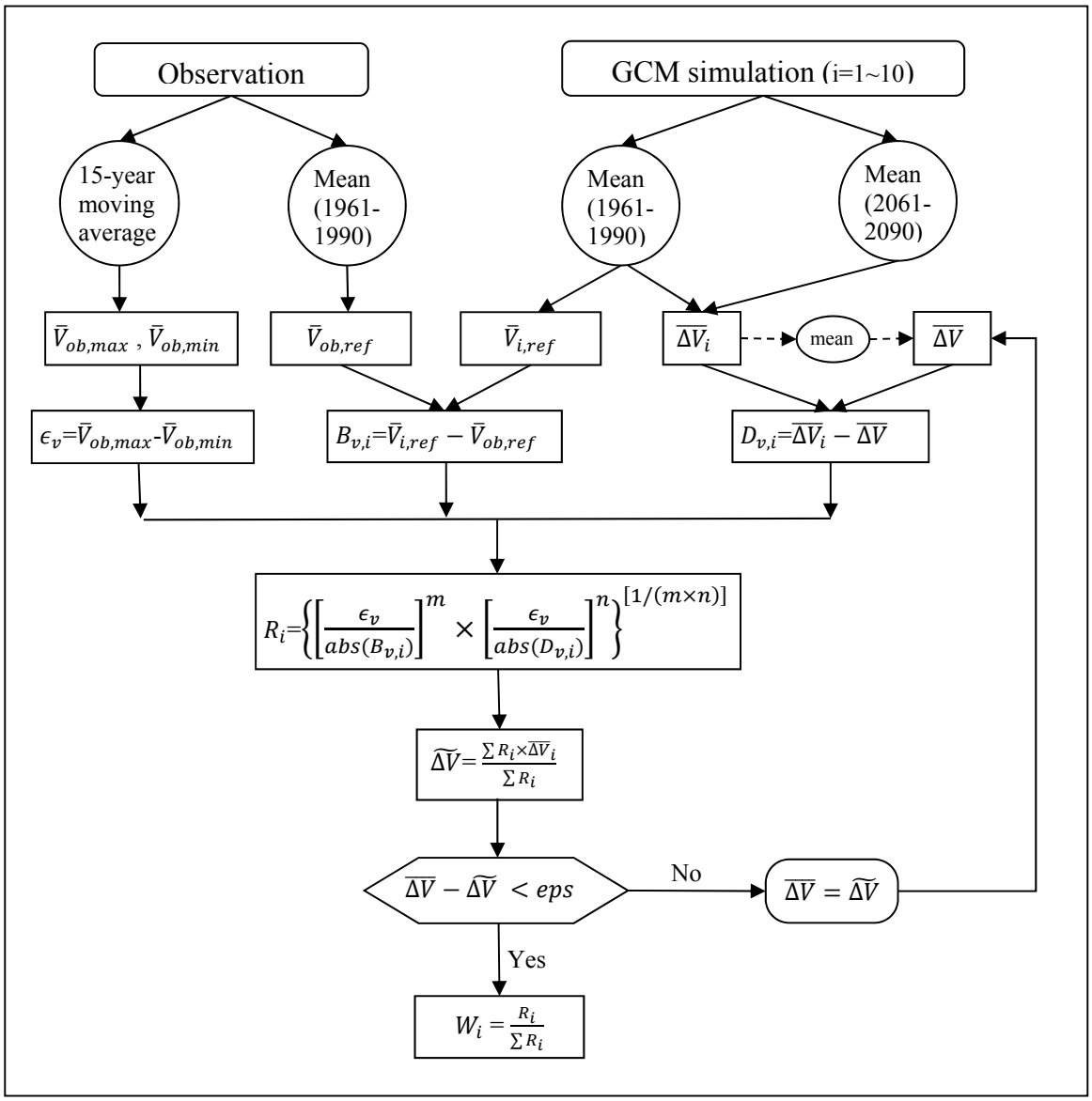

Figure 3.10 REA method implementation scheme

The procedure starts by computing $\bar{V}_{ob,max}$ and $\bar{V}_{ob,min}$. The difference between $\bar{V}_{ob,max}$ and $\bar{V}_{ob,min}$ is computed as ϵ_v. The mean values for the reference period are then calculated from meteorological observations and from each GCM(i) output as $\bar{V}_{ob,ref}$ and $\bar{V}_{i,ref}$ respectively. The difference between $\bar{V}_{ob,ref}$ and $\bar{V}_{i,ref}$ is then used to compute $B_{v,i}$, the bias between each GCM(i) and the observations. $\overline{\Delta V_i}$ is calculated for each GCM(i) as the variable between the future and the reference time period, from which $\overline{\Delta V}$ is computed, indicating the average change for all GCMs. The difference between the individual change $\overline{\Delta V_i}$ and the average

change is $D_{v,i}$, the distance between climate model i and the ensemble, which is calculated by using an iterative procedure. This is required because it is not known a priori what are the values of R_i and that the $D_{v,i}$ values are linked to R_i. A first estimate of $D_{v,i}$ is produced from GCM outputs, assuming that all GCMs share the same R_i value (or have the same weight). The dashed arrow indicates this one-time calculation. A first estimate of the reliability factor R_i for each GCM is then produced by using equation (3.6) based on the computed ϵ_v, $B_{v,i}$ and $D_{v,i}$ values. The estimated R_i factors are then used to calculate $\widetilde{\Delta V}$, which is an updated value of $\overline{\Delta V}$. The updated $\overline{\Delta V}$ is then used to recalculate R_i and the iterative procedure continues until $\widetilde{\Delta V}$ converges to $\overline{\Delta V}$ with a tolerance factor *eps*. Lastly, the relative weight of each GCM is obtained from the R_i values using equation (3.7).

The above procedure was used to rank the GCMs according to temperature and to precipitation output. The corresponding weights are W_T and W_P for temperature and precipitation, respectively. As hydrological processes can be affected by both precipitation and temperature, weights reflecting the integrated effect of both variables were also developed. To that end, empirical power functions were proposed to investigate the relative importance of each variable in the overall weight assessment. The equations are:

$$W_{(0.5P,0.5T)} = (W_P)^{0.5} \times (W_T)^{0.5} \tag{3.8}$$

$$W_{(0.25P,0.75T)} = (W_P)^{0.25} \times (W_T)^{0.75} \tag{3.9}$$

$$W_{(0.75P,0.25T)} = (W_P)^{0.75} \times (W_T)^{0.25} \tag{3.10}$$

Equation 3.8 assigns an equal importance to precipitation and temperature, while equation 3.9 (3.10) gives more (less) importance to temperature and less (more) importance to precipitation in calculating the GCMs weights.

3.6.3 Frequency analysis

Risk analyses in hydrologic engineering and in water resources management involves calculating the return periods of hydrological variables, such as spring peak flows, etc. In this study, various sources of uncertainty known or suspected to have an effect on predicted hydrological variables as a result of climate change were investigated through frequency analyses. More specifically, future climate return periods of selected hydrological variables of importance for the design and the management of hydroelectric systems were computed, taking into account the weighting schemes assigned to GCM models, climate sensitivity, natural variability and hydrological model structure. Moreover, the sensitivity of the return period to the choice of equal or unequal weights for GCM structure and climate sensitivity was evaluated. Two hydrological variables were examined: annual runoff volume and spring peak flood.

The choice of a proper probability distribution is of paramount importance in order to calculate the return periods of hydrological variables. In this study, the hydrological variables sampled with the Monte Carlo sampling procedure were fitted with a number of statistical models and the best model was used to calculate the return periods. The following statistical models were examined (using Matlab statistical toolbox): Normal, Rayleigh, extreme value, and lognormal. For the two hydrological variables investigated, the normal distribution proved to be the best model according to a Kolmogorov-Smirnov statistical test (Chakravart et al., 1967) and was used to calculate the return periods. This allowed an evaluation of how the return periods of those hydrological variables evolved with climate change and an assessment of the sensitivity of the computed future return periods, based on the choice of the weighting scheme strategy.

CHAPITRE 4

STUDY WATERSHED AND DATA

This work investigates the hydrological impact of climate change on a Canadian river basin, the Manicouagan River Basin. A description of this watershed is now presented, including its physiographic characteristics and hydrological regime. This chapter also provides a description of the meteorological and river flow data used in the study.

4.1 General watershed description

The site that is the subject of the study is the Manicouagan River Basin (MRB), which is centered at 51°23'N, 68°42'W. It is located in the Côte-Nord region in the province of Quebec, Canada. The Manicouagan River flows into the estuary of the Saint Lawrence River (Figure 4.1). The basin has a total drainage area of 44,500 km^2, with an annual mean discharge of 1,002 m^3/s at the outlet of the basin (Ministère du Développement durable, de l'Environnement et de la Lutte contre les changements climatiques: http://www.mddelcc.gouv.qc.ca/eau/bassinversant/bassins/manicouagan/). From upstream to downstream, the main sub-watersheds are: Petit lac, Manic 5, Toulnustouc, Manic 3, Manic 2 and Manic 1 (see Figure 4.1 and Table 4.1). The altitude above the sea level in the MRB varies between 37 m in the south and 1,143 m in the north, having north-south variations in temperature and precipitation fields. Its hydrological regime is typical of that of northern river watersheds and is dominated by spring snowmelt runoff. The amount of average annual rainfall in MRB is about 1,015 mm, one-third of which is in the form of snow. The MRB is characterized by cold winters and warm short summers. The accumulation of snow and lake freeze-up in the MRB starts in October and last until May, and occasionally early June. The average monthly temperature varies between -20°C in January and 21°C in July (Baie-Comeau station). Depending on which hydrological model was used, up to 29 sub-watersheds (see Figure 4.1) were included in the hydrological modeling process.

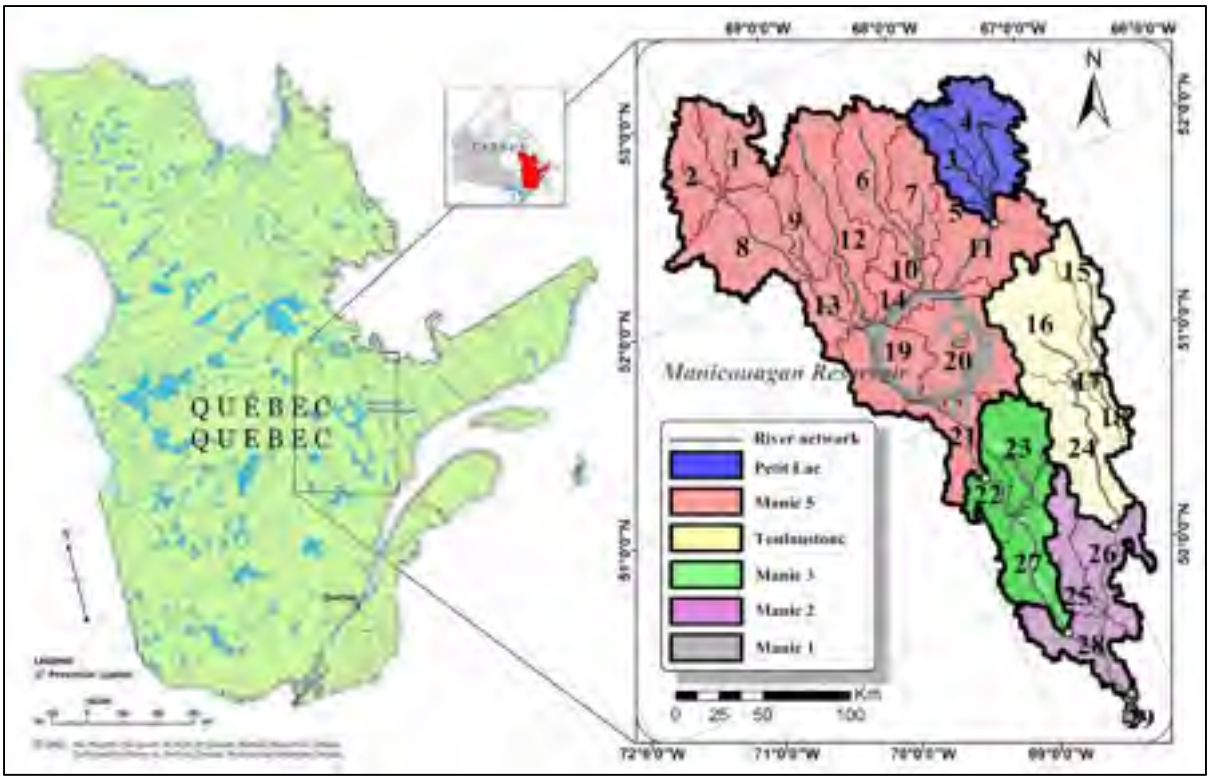

Figure 4.1 Location map of the Manicouagan basin with its river network of hydroelectric generating stations and main sub-watersheds

Table 4.1 Characteristics of the main sub-watersheds of the MRB
Derived from Haguma (2013, p. 65)

Main subwatersheds	Area (km²)	Center Latitude (°N)	Center Longitude (°W)	Average elevation (m)	Elementary subwatersheds
Petit Lac	3400	52.2	67.7	597	3
Manic 5	24700	52.0	68.9	544	14
Toulnustouc	7300	51.0	67.6	504	5
Manic 3	4500	50.5	68.5	421	3
Manic 2	4400	50.0	68.2	392	3
Manic 1	150	49.3	68.3	119	1
Manicouagan	**44500**	**51.4**	**68.4**	**546**	**29**

With its abundant water resources, the MRB is a significant hydropower source for the province of Quebec. A series of hydroelectric generating stations were built in the basin and are currently operated by Hydro-Québec, the provincial electrical utility. The Manicouagan

hydroelectric system has two major reservoirs, the Manicouagan and Toulnustouc reservoirs, as well as 7 power plants, for a total installed capacity of 5,810 MW (Haguma, 2013). Three of the hydroelectric generating stations are of the reservoir type and four are run-of-river stations. The Manicouagan reservoir, an annular lake often called the "eye of Quebec", is located in the Manic 5 sub-watershed and is the largest water body of the Manicouagan hydroelectric complex, with a surface area of 1,942 km^2 and an average depth of 73 m. The reservoir itself is the fifth largest in the world by volume, with an estimated capacity of 135,000 hm^3. It feeds two hydroelectric power plants with an installed capacity of 2,660 MW (Haguma, 2013). The presence of the Manicouagan reservoir has profoundly modified the natural hydrological regime of the river, as shown in Figure 4.2. Indeed, the power plants hold on 2,401 km^2 of water surface which is added on the water area of many lakes dispersed throughout the MRB, playing the role of a buffer pool during floods.

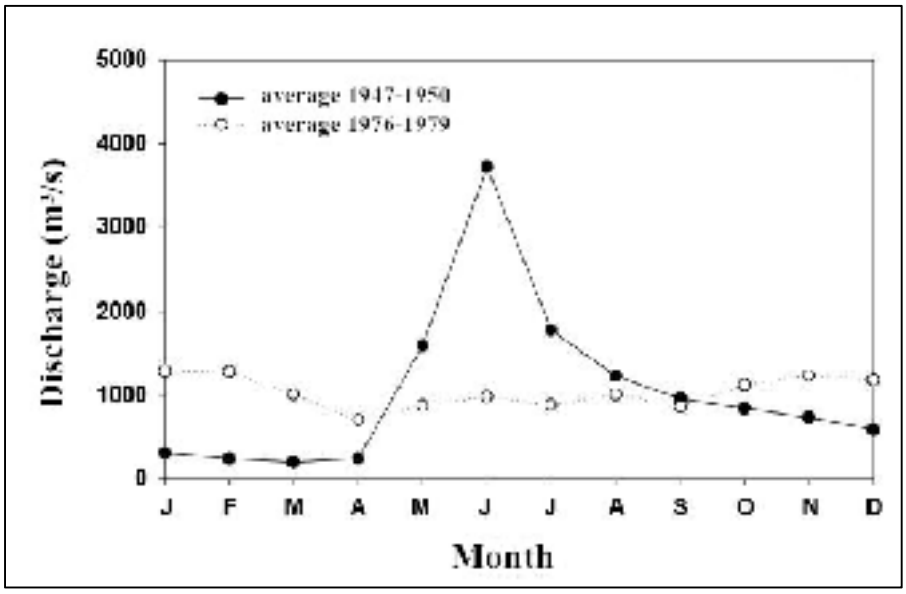

Figure 4.2 Average annual hydrograph of the Manicouagan River Basin at the McCormick station (Manic 1 power station) before (1947-1950) and after (1976-1979) building the Manicouagan Reservoir
Taken from Patoine et al. (1999, p. 14)

The MRB is characterized by a typical Laurentian topography with rounded hills reaching 1,500 m of elevation and with depressions occupied by lakes and rivers. The northern region of the MRB has steep slopes while the south region is covered with gentle slopes. According to Murtaugh (1976), the abundant molten rocks discovered in MRB, which are collectively known as “impactites”, can be grouped into four categories: shock metamorphosed country rocks, breccias, igneous rocks and contact metamorphosed rocks. The presence can be explained by the fact that this watershed was formed by a crater (Murtaugh, 1976). Adequate water resource and diversified terrain conditions result in 75% of the MRB area being covered by forest. The information on topography and land use in the MRB is presented in Figure 4.3.

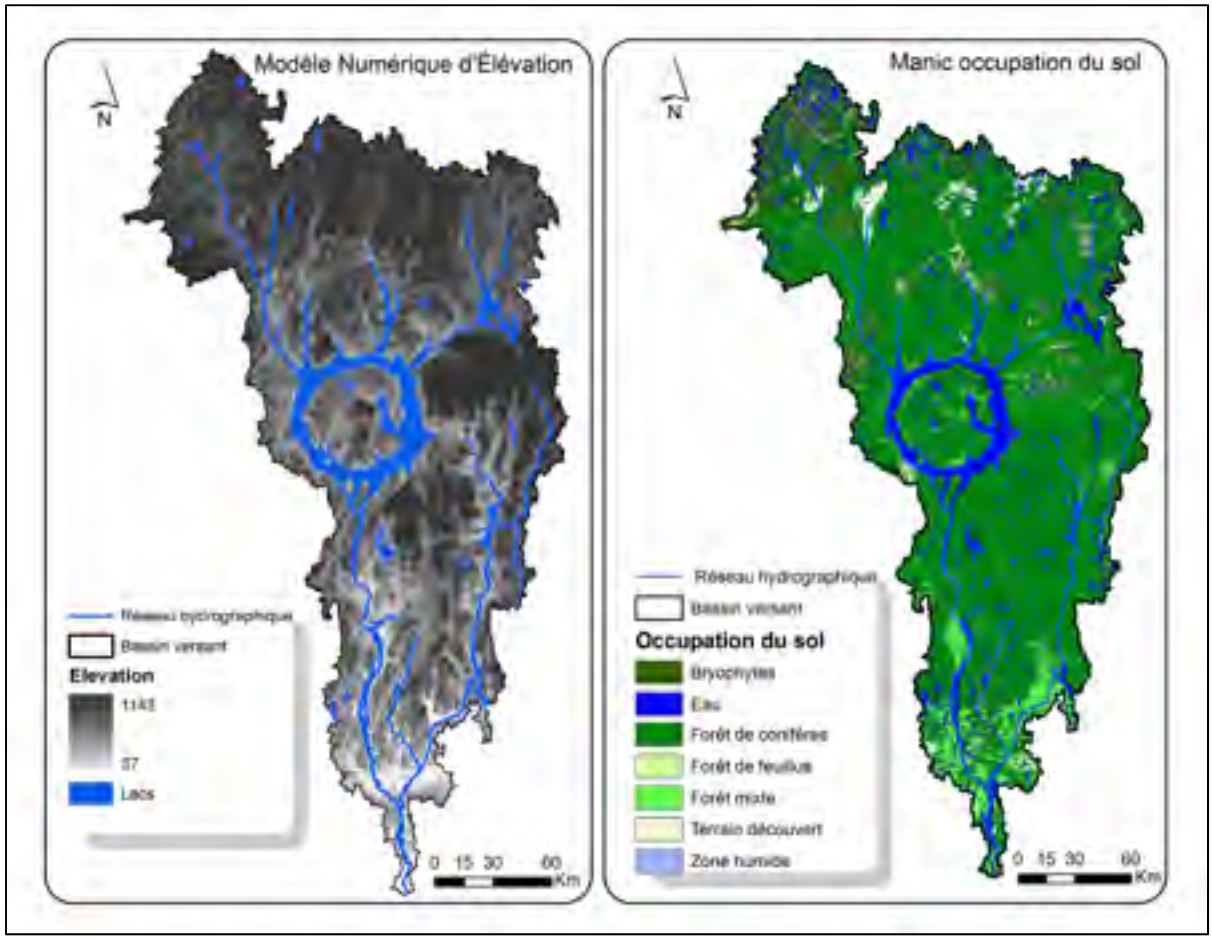

Figure 4.3 Topography and land use in the Manicouagan River Basin
Taken from: Haguma (2013, p. 36)

4.2 Climatological, physiographic, and flow data

The data used in this study are presented below, including the GCM output used to produce the climate projections and the meteorological, physiographic and hydrological data used to implement and run the hydrological models.

4.2.1 Climatological data

This study required meteorological observations describing the current climate, as well as the climate data provided by GCMs to describe future precipitation and temperature regimes. Daily precipitation and daily maximum and minimum temperatures were used. As the MRB has a vast drainage area of 44,500 km^2 and is almost uninhabited, there are currently no weather stations in it. The available weather data observed from past weather stations are short-term and incomplete. The nearest weather station is located in Baie-Comeau. The meteorological data used in this study are gridded data with a resolution of 10 × 10 km from "fictive" weather stations.

4.2.1.1 NLWIS data

As there is currently no weather station in the MRB that has been in place for a long enough duration to provide valid observations, this study used as meteorological observations the gridded weather data provided by Agriculture and Agri-Food Canada (AAFC, http://www.agr.gc.ca/eng/?id=1343071073307), which was derived from the database of the National Land and Water Information Service (NLWIS). The database contains regional daily precipitation, maximum temperature and minimum temperature data for the recent past (1975-2007) on a 10 km grid (NLWIS). A total of 440 NLWIS grids cover the study basin. Daily precipitation and temperature (Tmax, Tmin) data from the database were attributed to each sub-watershed of the MRB (up to 29, see Figure 4.1). Based on the NLWIS dataset, data of the recent past, which cover a 33-year period extending from 1975 to 2007, were used as a

base line for the generation of future climate projections and in the implementation of the REA method.

4.2.1.2 GCM data

Monthly GCM precipitation, minimum and maximum temperature data covering the entire North America region, including the study site were provided by the Ouranos Consortium on Regional Climatology and Adaptation to Climate Change. These data were taken from the "Climate of the Twentieth Century Experiment" (20C3M) (Laurent and Cai, 2007). Table 4.2 outlines the general information of the GCMs used in this study. Data from different runs (or members) of a GCM (e.g. CGCM 3.1) for a climate variable were averaged.

Table 4.2 General information on the selected GCM, including the number of grid points covering the province of Québec and climate sensitivity value

Acronym	**Agency**	**Country**	**Resolution** (lat×lon)	**Grid points** (lat×lon)	**Run**	**Estimated sensitivity (°C)**
BCCR-BCM2.0	Bjerknes Centre for Climate Research	Norway	2.8°×2.8°	6×8	Run1	3.5
CGCM 3.1	Canadian Centre for Climate Canadian Centre for Climate Modelling and Analysis	Canada	3.7°×3.7°	5×7	Run1-5	4.0
CNRM-CM3	Centre National de Recherches Météorologiques, Météo France	France	2.8°×2.8°	6×8	Run1	3.5
CSIRO-MK3.0	Commonwealth Scientific and Industrial Research Organization	Australia	1.9°×1.9°	10×12	Run1	3.5
GFDL-CM2.0	Geophysical Fluid Dynamics Laboratory	USA	2.0°×2.5°	9×9	Run1	3.0
INM-CM3.0	Institute of Numerical Mathematics, Russian Academy of Science	Russia	4°×5°	4×5	Run1	2.5
IPSL-CM4	L'institut Pierre-Simon Laplace	France	2.5°×3.75°	6×6	Run1	3.5
MIROC3.2(medres)	Center for Climate System Research	Japan	2.8°×2.8°	6×8	Run1-3	4.0
MPI-ECHAM5	Max Planck Institute for Meteorology	Germany	1.9°×1.9°	10×12	Run1-3	4.0
NCAR-PCM1	National Center for Atmospheric Research	USA	2.8°×2.8°	6×8	Run1-4	2.0

The value of climate sensitivity (last column) for each GCM was estimated, based on the temperature change between future and current climates retrieved from GCM output, which was then compared with changes produced by MAGICC/SCENGEN for a given climate

sensitivity. The region covering the province of Quebec was utilised for this comparison. The climate sensitivity parameter in MAGICC/SCENGEN was adjusted in order to minimize the difference between the original GCM output and that from MAGICC/SCENGEN.

As the uncertainty associated to GHG SRES scenarios was found to be small, compared to other sources (e.g. Prudhomme et al., 2003; Chen et al., 2011a), it was decided to select only one scenario for this work. Here the SRES A2 scenario, representing a rather "strong" increase of expected CO_2 concentration, was selected. The selected future horizon is centered around 2080 (2065-2097). This horizon corresponds to the time period for which global atmospheric CO_2 concentration has doubled compared to the present (year 2000), assuming the GHG scenario A2 (see Figure 4.4).

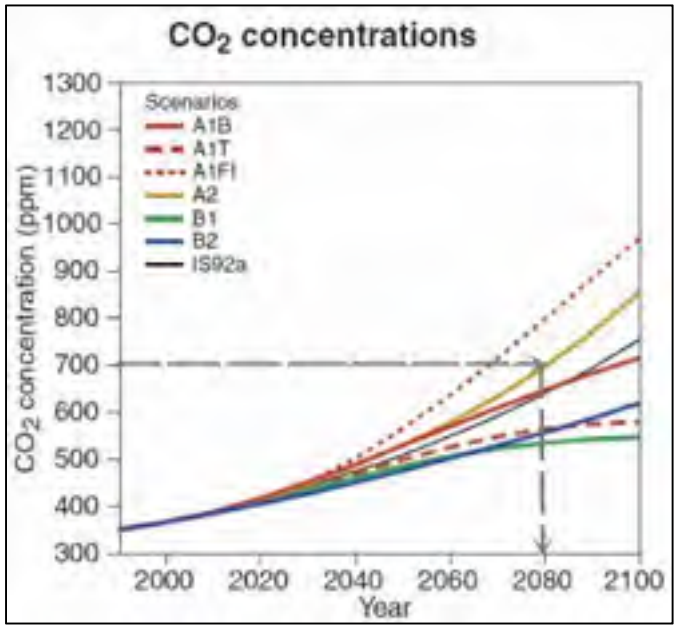

Figure 4.4 Atmospheric CO_2 concentrations projected for 6 SRES illustrative scenarios Taken from IPCC Third Assessment Report-WGI-summary for policymakers (2001, p. 14)

Figure 4.5 illustrates the expected changes in temperature and precipitation, at the 2080 horizon of the MRB, for the GCMs used in this study (solid marks in the figure). Other

GCMs are also shown in this figure, (hollowed marks) for comparison. The range of temperature and precipitation changes produced by the 10 selected GCMs were deemed adequate for the provision of a good coverage of the uncertainty due to GCM structure. One must keep in mind that each GCM displays its own climate sensitivity, therefore the changes observed in Figure 4.5 actually reflect combined uncertainties due to the GCM structure and climate sensitivity.

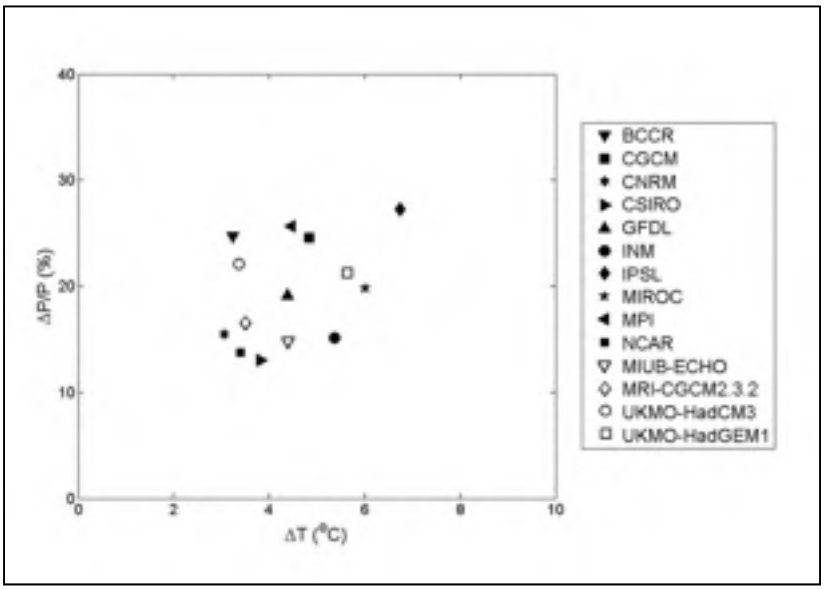

Figure 4.5 Average variation in temperature and precipitation in the Manicouagan River Basin for the 2080 time horizon

4.2.2 Physiographic data

In addition to the meteorological data, the physiographic characteristics of the sub-watersheds required to run the hydrological models, e.g. soil type, topographical information and vegetation, were retrieved from various databases. Geobase, which was developed by the Canadian Council on Geomatics, provides high-quality geospatial base information that covers the entire Canadian landmass. The Harmonized World Soil Database is a database with 30 arc-second resolution, which has over 16,000 different soil mapping units that combines existing regional and national updates of soil information worldwide. The Canadian Digital Elevation Data (CDED) produced by the Centre for Topographic

Information (CTI) consists of gridded data points of terrain elevation displayed at regularly spaced intervals and at spatial resolution scales of 30 meters (1:50,000) and 90 meters (1:250,000). The CDED is based on hypsographic and hydrographic elements of the National Topographic Data Base (NTDB) or of the Geospatial Data Base (GDB) (http://www.geobase.ca/geobase/en/data/cded/index.html). Based on this topographic and elevation information, the MRB was subdivided into 29 elementary sub-watersheds (see Figure 4.1) so that its hydrological regime could be modeled by using the HYDROTEL and the HBV models.

4.2.3 Hydrological data

The daily flow values of the six main sub-watersheds of the MRB required to calibrate the hydrological models were provided by Hydro-Québec.

It is important to note that these flows are actually 'naturalized', in other words, they were reconstructed from observed reservoir water levels and controlled flows at the hydroelectric stations by using the following mass balance equation:

$$\frac{\Delta V}{\Delta t} = I - O \tag{4.1}$$

Where V represents water volume in the reservoir, I is the inflow to the reservoir (unregulated) and O is the outflow from the reservoir (regulated). The daily inflows obtained using the above equation were filtered to avoid unrealistic streamflow values (e.g. negative flows) resulting from the reconstruction process. To determine the variation of the water volume in the reservoir, Hydro-Québec applied the empirical relationship between daily water level and reservoir storage. Note that some factors, such as wind, which could lead to inaccurate measurements of water level, were not taken into account in the mass balance calculation performed in Hydro-Québec's current work (J. Roy 2014, pers. comm., July 23).

Because Manic 1 sub-watershed is very small, compared with the others (see Table 4.1), it was decided not to consider it in the calibration effort.

CHAPTER 5

RESULTS AND DISCUSSION

This chapter presents the results and an analysis of the impacts of climate change on the hydrological regime of the MRB. Its first three sections are devoted to the following subjects: climate projections, sources of uncertainty and their impacts in the watershed's hydrological response and the Monte-Carlo analysis. Lastly, it concludes with a discussion about the uncertainty analysis and on the use of weighting schemes in climate change impact studies.

5.1 Climate projections

Future climate projections were produced as an ensemble of multiple climate models (10 models) and climate sensitivities (between 2.0°C and 4.0°C) under the A2 scenario for the 2080 time horizon (2065-2097). Scatter plots of seasonal (winter, spring, summer and autumn) and annual changes of precipitation (ratio) and mean temperature (difference) are presented in Figure 5.1.

All GCMs produce annual increases in temperature and most also produce increases in precipitation in a future climate of the MRB. Figure 5.1 shows modest increases in seasonal and annual mean temperature, associated with increasing climate sensitivity. Very little change in annual and in seasonal precipitation is observed along with increasing climate sensitivity. Going from the smallest to the largest value of climate sensitivity, the markers which represent various GCMs become increasingly dispersed along the ΔT axis, while displaying a much smaller dispersion along the $\Delta P/P$ axis. In other words, the sensitivity of $\Delta P/P$ to changes in climate sensitivity is smaller than for ΔT. One exception is the CGCM model, which shows a notable increase of $\Delta P/P$ with climate sensitivity.

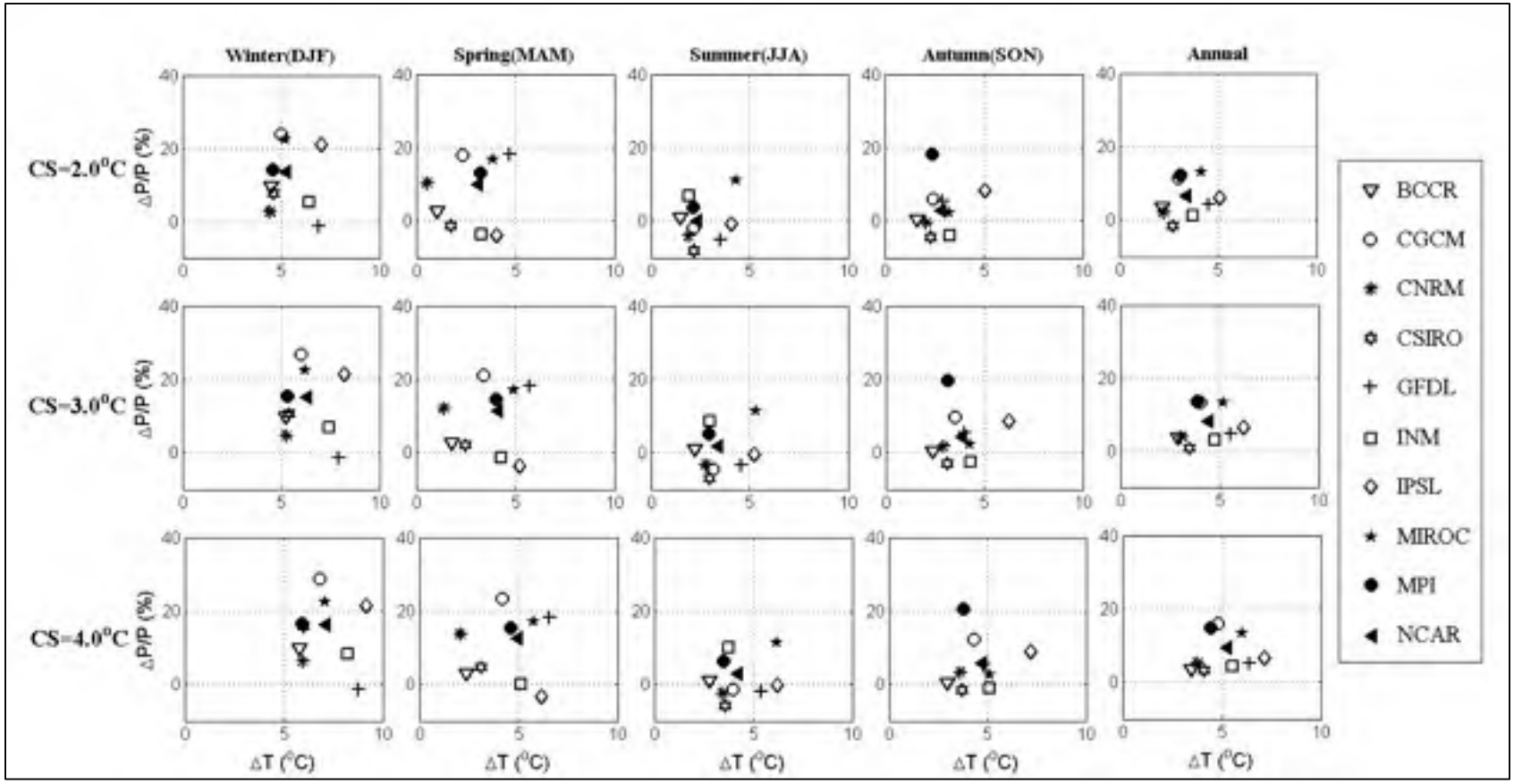

Figure 5.1 Scatter plots of seasonal and annual changes of temperature and precipitation obtained for all ten GCMs and three climate sensitivities (2.0°C, 3.0°C, 4.0°C) with scenario A2 at the 2080 time horizon (2065-2097). CS represents climate sensitivity

Generally, the range of precipitation change of the GCMs is largest in winter (DJF) and smallest in summer (JJA), and is almost not affected by climate sensitivity. For instance, in winter, the precipitation change varies from -1.4% (GFDL) to 23.9% (CGCM), when climate sensitivity is 2.0°C, while it varies from -1.4% (GFDL) to 28.9% (CGCM), when climate sensitivity is 4.0°C. In summer, the range of precipitation change varies from -8.0% (CSIRO) to 11.3% (MIROC), when climate sensitivity is 2.0°C, while it varies from -5.8% (CSIRO) to 11.5% (MIROC), when climate sensitivity is 4.0°C. On the other hand, the range of temperature change is largest in spring (MAM), varying from 0.5°C (CNRM) to 4.7°C (GFDL), when climate sensitivity is 2.0°C, and from 2.1°C (CNRM) to 6.6°C (GFDL), when climate sensitivity is 4.0°C. The spread of temperature change is smallest in summer, varying from 1.5°C (BCCR) to 4.3°C (MIROC), when climate sensitivity is 2.0°C, and from 2.8°C (BCCR) to 6.3°C (MIROC), with a climate sensitivity of 4.0°C

Table 5.1 and Table 5.2 respectively outline the precipitation change ($\Delta P/P$) and temperature change (ΔT) for three climate sensitivities (2.0°C, 3.0°C, 4.0°C) and for each GCM at the 2080 horizon. Comparing all seasonal simulated changes with climate sensitivity of 3.0°C (mid value), CSIRO shows the largest average precipitation decrease, i.e. -7.0% in summer (JJA), while CGCM shows the highest average precipitation increase with 26.8% in winter (DJF). CNRM generates the smallest mean temperature increase, with 1.4ºC in spring (MAM), while ISPL and GFDL produce the largest increase, 8.2 ºC and 7.9 ºC respectively, during the winter season (DJF). Considering mean annual changes, the smallest increases in precipitation are obtained with CSIRO and INM, while the smallest changes in temperature are produced by BCCR and CNRM. Largest annual mean changes in precipitation are obtained with CGCM, MIROC and MPI, while the largest changes in temperature are produced by IPSL, GFDL and MIROC. Therefore, it can be said that the BCCR, CNRM and CSIRO GCMs are considered as colder and dryer models, at least over the MRB, whereas CGCM, IPSL and MIROC are seen as warmer and wetter models.

In Table 5.1 and Table 5.2, the rankings (in parentheses) of climate sensitivity uncertainty (1, is the most sensitive and 10, the least sensitive) were established by computing the range of temperature or precipitation change for each GCM, i.e., the spread of the ΔT or ΔP/P values.

Table 5.1 The seasonal and annual change (in square brackets) of precipitation (ΔP/P) obtained for each GCM from three climate sensitivities (2.0°C, 3.0°C, 4.0°C) respectively with scenario A2, 2080 time horizon (2065-2097). The ranking of climate sensitivity uncertainty (1: high uncertainty; 10: low uncertainty) for each GCM is presented in parentheses, based on range

GCM	**ΔP/P (%)**				
	DJF	**MAM**	**JJA**	**SON**	**Annual**
BCCR	[9.7 9.7 9.8] (9)	[2.7 2.7 2.8] (9)	[0.9 0.9 1.0] (10)	[0.4 0.5 0.5] (9)	[3.4 3.5 3.5] (10)
CGCM	[23.9 26.8 28.9] (2)	[18.2 21.2 23.5] (2)	[-2.0 -1.7 -1.3] (7)	[6.2 9.8 12.4] (1)	[11.6 14.0 15.9] (2)
CNRM	[2.7 4.7 6.2] (3)	[10.4 12.1 13.7] (4)	[-4.0 -3.2 -2.4] (6)	[-0.4 1.7 3.4] (2)	[2.2 3.8 5.2] (4)
CSIRO	[7.5 10.5 15.7] (1)	[-1.3 2.1 4.6] (1)	[-8.0 -7.0 -5.8] (5)	[-4.5 -3.0 -1.5] (3)	[-1.6 0.6 3.2] (1)
GFDL	[-1.4 -1.4 -1.4] (10)	[18.2 18.2 18.2] (10)	[-4.9 -3.4 -1.8] (2)	[5.6 5.6 5.6] (10)	[4.4 4.7 5.1] (7)
INM	[5.1 7.0 8.4] (4)	[-3.5 -1.5 0.1] (3)	[6.8 8.6 10.0] (1)	[-3.9 -2.5 -1.0] (5)	[1.1 2.9 4.4] (3)
IPSL	[21.0 21.3 21.5 (7)	[-3.9 -3.6 -3.3] (7)	[-0.8 -0.4 -0.2] (8)	[8.3 8.6 8.9] (7)	[6.1 6.5 6.7] (8)
MIROC	[22.3 22.4 22.5] (8)	[17.0 17.1 17.1] (8)	[11.3 11.4 11.5] (9)	[2.3 2.4 2.5] (8)	[13.2 13.3 13.4] (9)
MPI	[14.0 15.4 16.4] (6)	[13.1 14.5 15.6] (6)	[3.7 5.2 6.4] (4)	[18.3 19.6 20.6] (6)	[12.3 13.7 14.8] (6)
NCAR	[13.7 15.0 16.2] (5)	[10.0 11.5 12.7] (5)	[0.1 1.7 3.1] (3)	[2.8 4.5 5.8] (4)	[6.6 8.2 9.4] (5)

Table 5.2 The seasonal and annual change (in square brackets) of temperature (ΔT) obtained for each GCM from three climate sensitivities (2.0°C, 3.0°C, 4.0°C) respectively with scenario A2, 2080 time horizon (2065-2097). The ranking of climate sensitivity uncertainty (1: high uncertainty; 10: low uncertainty) for each GCM is presented in parentheses, based on range

GCM	ΔT (ºC)				
	DJF	MAM	JJA	SON	Annual
BCCR	[4.5 5.3 5.8] (10)	[1.1 1.8 2.4] (10)	[1.5 2.2 2.8] (10)	[1.7 2.4 3.0] (10)	[2.2 2.9 3.5] (10)
CGCM	[5.0 6.0 6.8] (5)	[2.4 3.4 4.2] (5)	[2.1 3.2 4.0] (5)	[2.5 3.5 4.3] (5)	[3.0 4.0 4.8] (5)
CNRM	[4.4 5.3 6.0] (7)	[0.5 1.4 2.1] (7)	[1.9 2.8 3.5] (7)	[2.1 2.9 3.6] (7)	[2.2 3.1 3.8] (7)
CSIRO	[4.6 5.4 6.0] (8)	[1.7 2.5 3.1] (8)	[2.2 3.0 3.6] (8)	[2.4 3.1 3.7] (9)	[2.7 3.5 4.1] (8)
GFDL	[6.9 7.9 8.8] (2)	[4.7 5.7 6.6] (2)	[3.5 4.6 5.4] (4)	[2.9 4.0 4.8] (3)	[4.5 5.6 6.4] (3)
INM	[6.4 7.4 8.2] (6)	[3.3 4.3 5.1] (6)	[2.0 3.0 3.8] (6)	[3.3 4.3 5.1] (6)	[3.7 4.7 5.5] (6)
IPSL	[7.1 8.2 9.2] (1)	[4.1 5.2 6.2] (1)	[4.1 5.3 6.2] (1)	[5.1 6.3 7.2] (1)	[5.1 6.3 7.2] (1)
MIROC	[5.2 6.2 7.1] (3)	[3.9 4.9 5.7] (4)	[4.3 5.3 6.3] (2)	[3.2 4.3 5.1] (2)	[4.1 5.2 6.0] (2)
MPI	[4.6 5.3 5.9] (9)	[3.3 4.0 4.6] (9)	[2.2 2.9 3.5] (9)	[2.4 3.2 3.8] (8)	[3.1 3.9 4.5] (9)
NCAR	[5.3 6.3 7.1] (4)	[3.1 4.2 5.0] (3)	[2.3 3.4 4.2] (3)	[2.9 3.9 4.7] (4)	[3.4 4.4 5.3] (4)

As mentioned above, the uncertainty of precipitation due to climate sensitivity is overall small, represented by small range of ΔP/P change. CSIRO displays the largest uncertainty in annual precipitation change (4.8%). In contrast, BCCR displays a small range of ΔP/P change (0.1%), thus showing the smallest uncertainty among the GCMs analysed. For each climate model, the uncertainty about temperature due to climate sensitivity shows little change between the four seasons, which present almost the same range of seasonal ΔT. IPSL produces the largest uncertainty (2.1°C), while MPI and BCCR generate less uncertainty in

annual temperature change (1.4°C and 1.3°C). Note that the CSIRO model, which ranks first for precipitation uncertainty and third from last for temperature uncertainty due to climate sensitivity, is also a cold and dry model (see Figure 5.1). The IPSL model, a warm and wet model, ranks first and third from last for temperature and precipitation uncertainty, respectively.

It has been shown in Figure 5.1 that GCMs notably contribute to the dispersion on the scatter plots, which indicates that GCM structure is an important source of uncertainty. To investigate the relationship between GCM structure and climate sensitivity, the variation of annual average precipitation and temperature change, along with the increase of climate sensitivity for all ten GCMs, is presented in Figure 5.2. The 'original' climate sensitivity for each GCM is displayed by using a larger mark. In all selected GCM simulations, except INM and NCAR, the original climate sensitivity is greater than the central value of 3.0°C, which is the most likely value in the future (Rogejl et al., 2012). The slope of each line indicates the sensitivity of each GCM to the change in climate sensitivity. The steeper the line, the more sensitive the GCM is to an increase of climate sensitivity. For precipitation changes, BCCR, GFDL, IPSL and MIROC are relatively less sensitive to the increase of climate sensitivity as their lines are almost flat. In contrast, the line of CSIRO is the steepest, which indicates that CSIRO is the most sensitive model, and produces the smallest value of precipitation change compared to the other models. CGCM, IPSL and MIROC produce higher precipitation changes than the other models. On the other hand, all GCM structures show similar trends in temperature change, as they have almost identical slopes. The IPSL model is somewhat more sensitive, while the BCCR model displays a gentler slope and is therefore less sensitive to changes in climate sensitivity.

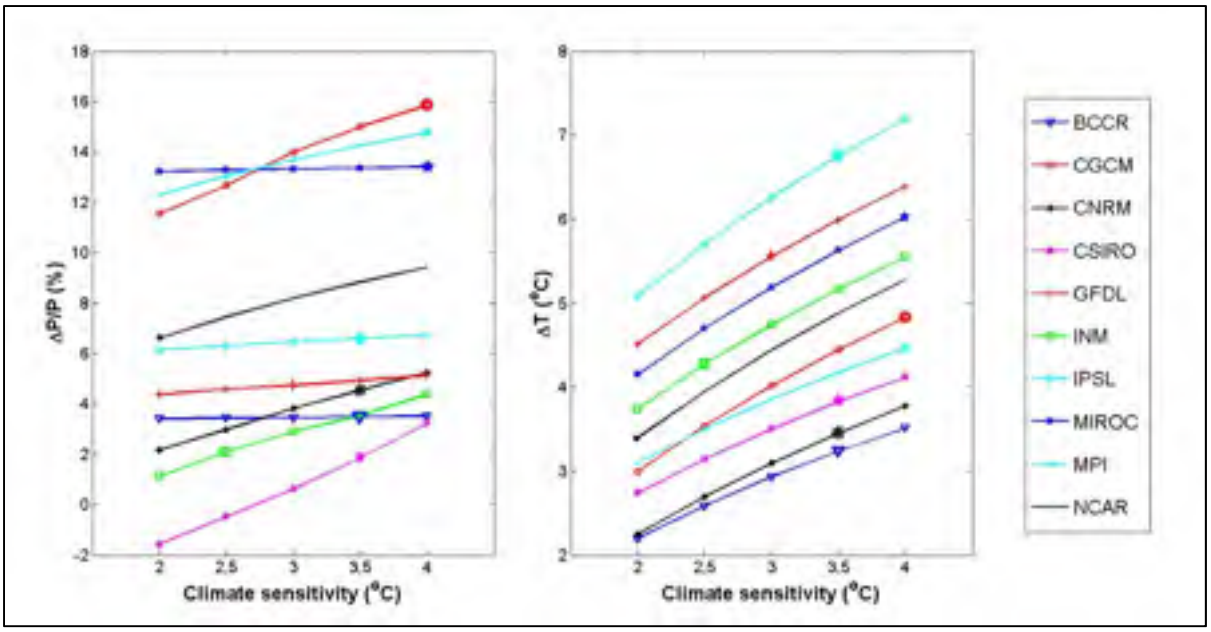

Figure 5.2 Annual average changes of precipitation (left) and temperature (right) obtained for individual GCMs with five climate sensitivities (2.0°C, 2.5°C, 3.0°C, 3.5°C, 4.0°C) by using scenario A2 at the MRB's 2080 time horizon (2065-2097)

5.2 Uncertainty in projected flows

Future flows in the MRB were generated with four hydrological models, i.e. HBV, HSAMI, HYDROTEL and HMETS, by using climate projections generated from the selected GCMs. The hydrological models were first calibrated and validated. The next section presents the calibration results, followed by an analysis of the uncertainty of GCM structure, climate sensitivity, natural variability and hydrological model structure associated to the simulated flows.

5.2.1 Hydrological model calibration

The optimal parameter sets for the hydrological models were selected through a model calibration and validation process. The Nash - Sutcliffe criterion was used to assess model performance. Results of the calibration and validation process for the four models are presented in Table 5.3. Daily precipitation and temperature values from the NLWIS data base

were used to compute the simulated flows. Both HSAMI and HMETS were automatically calibrated by using 20 years of naturalized daily flows (1975-1994) at the outlet of the MRB (See section 4.2.4). Validation was carried out by using a 13-years streamflow series (1995-2007). HSAMI obtained a better score over HMETS for both model calibration and validation. HYDROTEL was automatically calibrated for the Petit Lac, Manic 5, Toulnustouc, Manic 3 and Manic 2 main sub-watersheds. Of the 26 parameters of the model, only 12 of the most sensitive ones were calibrated automatically using the SCE-UA algorithm (Duan et al., 1992; Duan, 2003), while the others were set to the recommended values taken from Turcotte et al. (2007). In HYDROTEL's case, it is known as a computationally intensive model (for example, it took more than 100 hours, using an Intel Core i7 3.40-GHz processor, to calibrate it for a medium-sized watershed (5,000 km^2) with a 5-year flow data – Huot et al., 2014). The calibration and validation time periods for each sub-watershed were set to be no more than 11 years in HYDROTEL in order to reduce the computation time. As an automatic parameter calibration routine was not available in the HBV model, a manual calibration was performed with HBV for the Manic 5, Toulnustouc, Manic 3 and Manic 2 sub-watersheds. The different calibration and validation periods used here and shown in Table 5.3 were dictated by the availability of river flow data, the structure and complexity of the hydrological model (computational time) and the availability of an automatic calibration module in the hydrological models. Due to its relatively small size, the Petit lac sub-watershed was combined with the Manic 5 sub-watershed to simplify the manual calibration process of HBV. The time periods for both calibration and validation processes in HBV were set at 10 years on account of the manual operation. HBV generally showed a little better Nash-Sutcliffe score than HMETS, but a slightly inferior one compared to HSAMI. HYDROTEL presented the lowest Nash values among four hydrological models, with values ranging from 0.71 to 0.86 for calibration and 0.55 to 0.80 for validation.

Table 5.3 Nash-Sutcliffe coefficients obtained for four hydrological models by using flow time series at the daily time step

Subbasins			**Petit Lac**	**Manic 5**	**Toulnustouc**	**Manic 3**	**Manic 2**
HYDR-OTEL	Calibration	*Period*	*1969~1975*	*1978~1988*	*1993~2003*	*1971~1977*	*1981~1987*
		Nash	0.75	0.86	0.81	0.71	0.82
	Validation	*Period*	*1988~1998*		*1970~1980*	*1981~1991*	*1971~1981*
		Nash	0.65	0.80	0.78	0.55	0.66
HBV	Calibration *(1975~1984)*	Nash	0.88		0.81	0.88	0.90
	Validation *(1988~1997)*	Nash	0.74		0.81	0.77	0.83
HSAMI	Calibration *(1975~1994)*	Nash	0.91				
	Validation *(1995~2007)*	Nash	0.80				
HMETS	Calibration *(1975~1994)*	Nash	0.83				
	Validation *(1995~2007)*	Nash	0.72				

The average annual hydrographs produced by the four hydrological models that were analysed for both calibration and validation periods at the outlet of the MRB generally compared well against the average observed hydrograph, as shown in Figure 5.3. The standard deviations of the observed and the simulated annual discharge are presented in Figure 5.4. Both simulated and observed standard deviations show good agreement for the four analysed models. Keep in mind that HYDROTEL and HBV were calibrated and validated for distinct sub-watersheds, while HSAMI and HMETS, being global models, were calibrated using observed flows at the outlet of the MRB. Furthermore, the hydrological models had different calibration and validation periods (see Table 5.3). To facilitate the comparison, the average annual hydrograph and standard deviation of the flows simulated by HYDROTEL and HBV, and shown in Figures 5.3 and 5.4, cover the same periods of calibration and validation as HSAMI and HMETS, as indicated in Table 5.3. The flows simulated by HYDROTEL tend to be more variable than those of other models (Figure 5.4), and show increased autumn flows (SON), when compared to the observations (Figure 5.3).

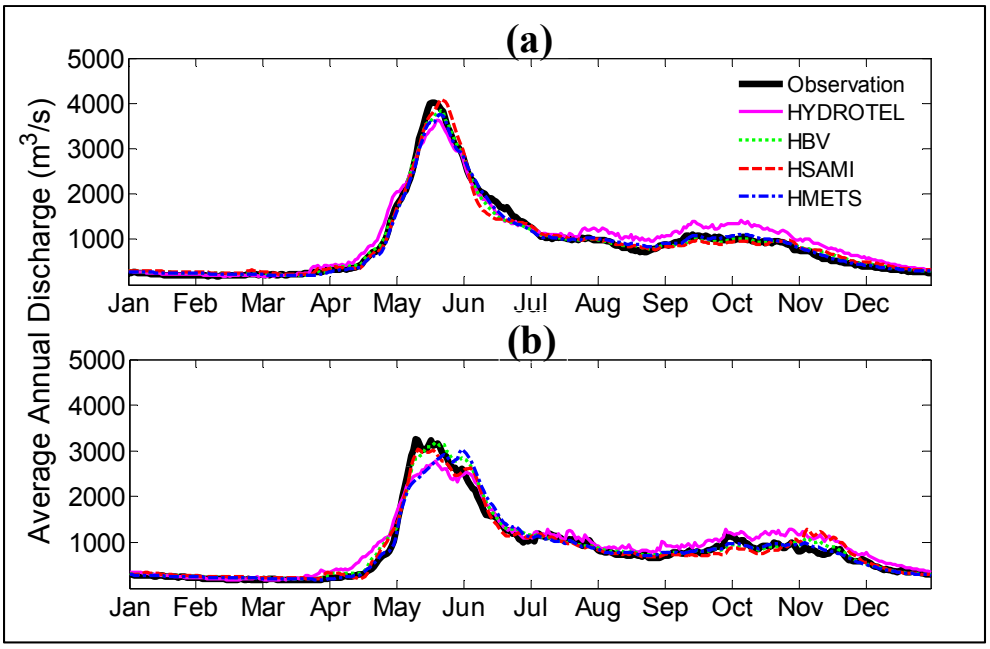

Figure 5.3 Average annual hydrographs generated by four hydrological models at the outlet of MRB under recent past climate conditions: (a) calibration period; (b) validation period. The hydrograph of observation is plotted for comparison

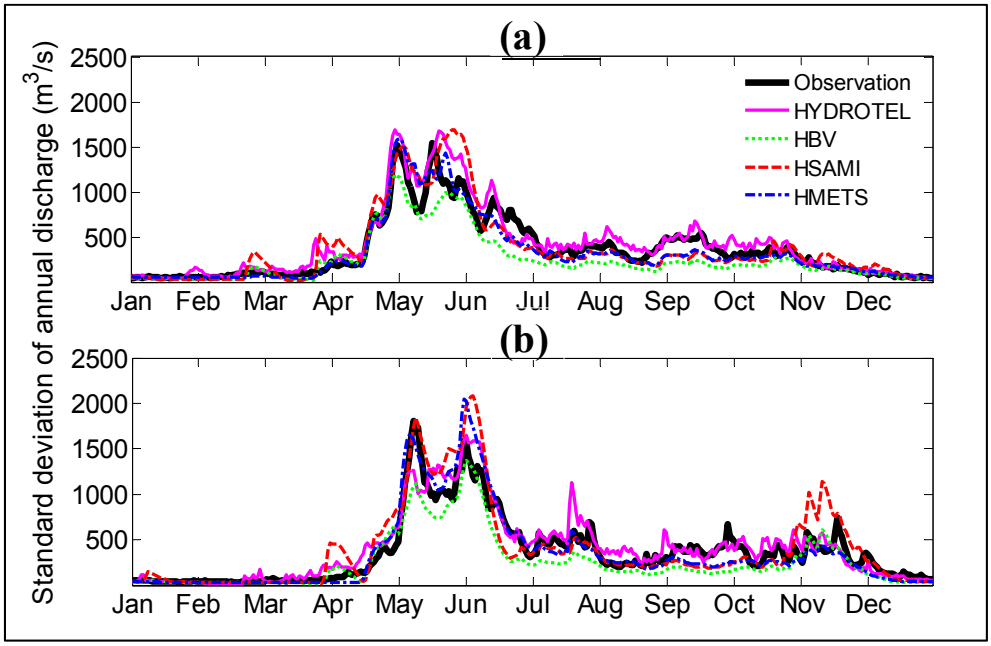

Figure 5.4 Standard deviation of annual discharge generated by four hydrological models at the outlet of MRB under recent past climate conditions: (a) calibration period; (b) validation period. The hydrograph of observation is plotted for comparison

5.2.2 Overall uncertainty

The mean hydrographs of the future annual discharge at the outlet of the MRB that were simulated by HYDROTEL, HBV, HSAMI and HMETS are displayed in Figure 5.5. The envelopes include all 2500 runs produced by using 10 GCMs, 5 climate sensitivities and 50 series of natural variability averaged over a 33-year time period centered on the 2080 horizon (2065-2097). The bold curve represents the mean annual hydrograph for the control period (1975-2007) simulated by the corresponding hydrological model. The percentage change (%) between the future period and control period is also plotted below the hydrograph. Figures 5.5(a) to (d) indicate that most simulations show a distinct trend for an early spring flood and a generally increasing peak discharge in the future. The simulated hydrographs show that the time to peak will be advanced from late May to early May and sometimes, to late April. A significant change between the future and the control period appears in April for all hydrological models. An increase in the summer (JJA) and autumn (SON) flows is also noticed for all analysed hydrological models. HYDROTEL simulated future flows during the winter season (DJF) that are larger than during the control period, while no clear trends, above or below the flows in the control period, are discerned in the HBV, HSAMI and HMETS models.

Similarly to HBV, HYDROTEL produces a larger range (larger envelope) of mean discharges in the summer and autumn season, as compared to the HSAMI and HMETS models. HYDROTEL also produces future spring peak discharges that are higher than those in the other three models. However, compared to the flows in the control period, the changes in future spring peak discharges produced by HYDROTEL are the least significant, which is mainly due to the relatively larger discharge in the month of April for the control period and the simulated future time to peak that occurs mostly in May. This is not the case with the other models, where simulated peak flows occur somewhat earlier in April and May. HMETS displays the smallest changes in discharges during the winter, summer and autumn

seasons, as compared to the flows in control period. Variability in the hydrological response is also small during these seasons.

The average annual flows and relative percentage increases for the 2080 time horizon simulated by each GCM for different climate sensitivities are calculated and shown in Table 5.4. The annual flows averaged over all GCMs and for all climate sensitivities are expected to increase by the time the 2080 time horizon is reached, ranging from 1.0% to 47.3% as compared to the current average flow. Significant increases of annual flows, which are simulated by HBV, HSAMI and HYDROTEL by using precipitation and temperature generated by the CGCM, GFDL and NCAR climate models, are obtained when compared to the other GCMs. This is particularly true with HYDROTEL, which shows increases exceeding 30% for all climate sensitivities. HMETS simulates more balanced increases for all GCMs for the 2080 time horizon, with the largest range varying from 8.1% (IPSL) to 23.1% (BCCR) when climate sensitivity is 4.0°C. It was also observed that, in general, simulated averaged flows tend to lessen when the climate sensitivity increases, with the notable exceptions of the CGCM and CSIRO models (for all hydrological models except HMETS), in which the sensitivity of $\Delta P/P$ with climate sensitivity is the largest (see Figure 5.2).

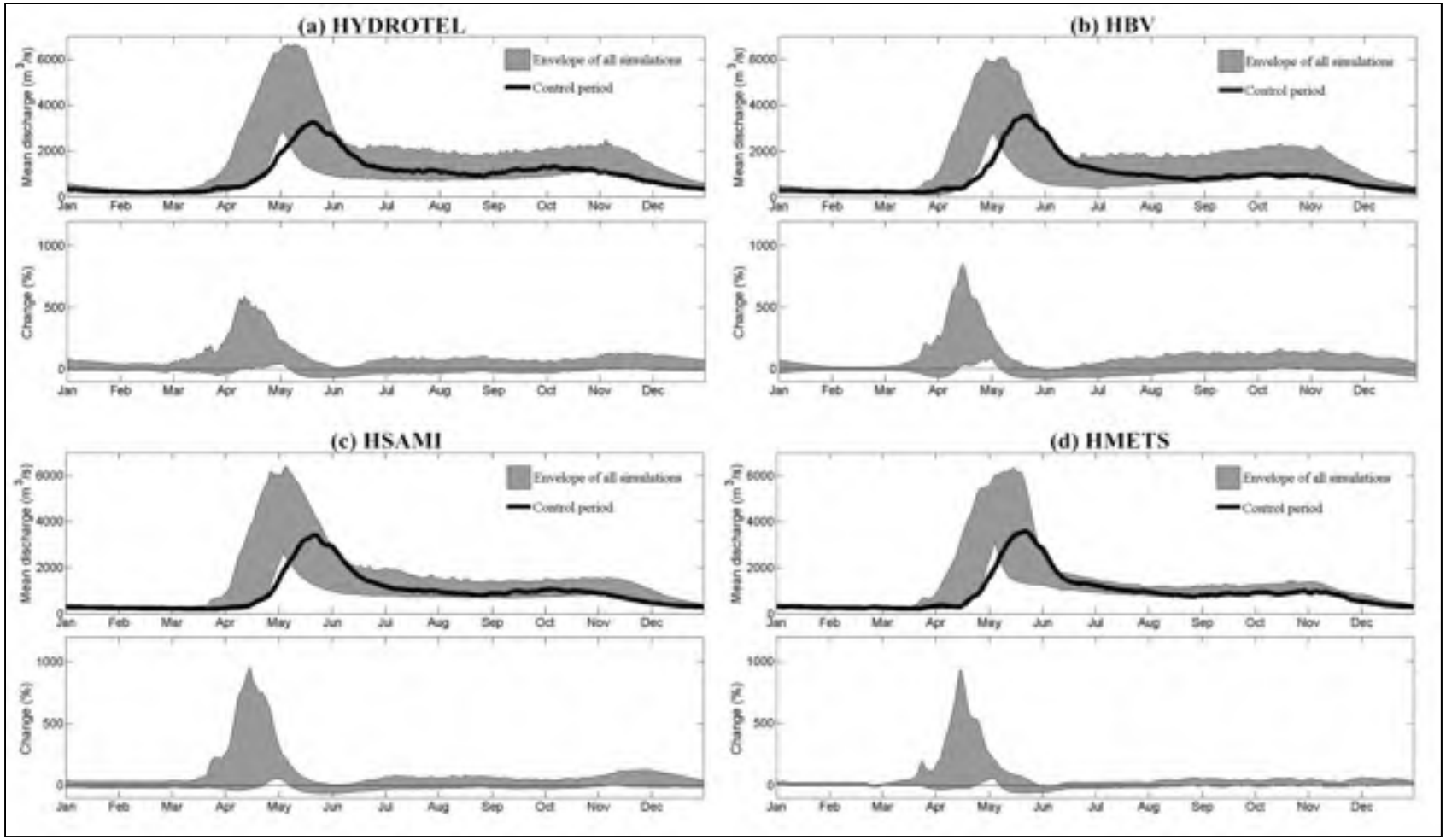

Figure 5.5 Envelopes of annual hydrographs and the corresponding changes in percentage of daily discharge that are simulated in (a) HYDROTEL, (b) HBV, (c) HSAMI and (d) HMETS by using all selected GCMs, climate sensitivities and natural variability at the outlet of MRB for the 2080 horizon (2065-2097). The hydrograph for the control period (1975-2007), which is derived from the corresponding hydrological model's simulation, is plotted for the purpose of comparison

Table 5.4 Average annual flows for 2080 time horizon (2065-2097) and relative increases (%) compared to average annual flows for control period over the MRB

Hydrological model	GCM	Control period	2080 time horizon (2065-2097)					
			Climate Sensitivity					
			2.0°C		3.0°C		4.0°C	
		Flow (m^3/s)	Flow (m^3/s)	Increase (%)	Flow (m^3/s)	Increase (%)	Flow (m^3/s)	Increase (%)
HYDROTEL	BCCR	986	1274	29.2	1252	27.0	1232	24.9
	CGCM		1322	34.0	1353	37.2	1378	39.7
	CNRM		1089	10.4	1085	10.0	1099	11.5
	CSIRO		1229	24.6	1253	27.1	1285	30.3
	GFDL		1415	43.5	1380	40.0	1348	36.7
	INM		1081	9.6	1075	9.0	1063	7.8
	IPSL		1219	23.6	1178	19.5	1146	16.2
	MIROC		1287	30.5	1259	27.7	1231	24.8
	MPI		1189	20.6	1197	21.4	1200	21.7
	NCAR		1452	47.3	1445	46.5	1443	46.3
HBV	BCCR	906	1136	25.4	1116	23.2	1099	21.3
	CGCM		1173	29.5	1204	32.9	1229	35.7
	CNRM		955	5.4	953	5.2	968	6.8
	CSIRO		1081	19.3	1103	21.7	1133	25.1
	GFDL		1241	37.0	1216	34.2	1193	31.7
	INM		951	5.0	949	4.7	943	4.1
	IPSL		1084	19.4	1056	16.6	1038	14.6
	MIROC		1133	25.1	1112	22.7	1093	20.6
	MPI		1049	15.8	1056	16.6	1062	17.2
	NCAR		1276	40.8	1275	40.7	1278	41.1
HSAMI	BCCR	888	1106	24.5	1078	21.4	1056	18.9
	CGCM		1141	28.5	1160	30.6	1173	32.1
	CNRM		943	6.2	932	4.9	940	5.9
	CSIRO		1055	18.8	1069	20.4	1091	22.9
	GFDL		1208	36.0	1169	31.6	1136	27.9
	INM		919	3.5	909	2.4	897	1.0
	IPSL		1035	16.6	993	11.8	967	8.9
	MIROC		1105	24.4	1074	20.9	1045	17.7
	MPI		1020	14.9	1020	14.9	1019	14.8
	NCAR		1246	40.3	1233	38.9	1226	38.1
HMETS	BCCR	900	1154	28.2	1128	25.3	1108	23.1
	CGCM		1122	24.7	1085	20.6	1056	17.3
	CNRM		1149	27.7	1119	24.3	1096	21.8
	CSIRO		1117	24.1	1090	21.1	1069	18.8
	GFDL		1055	17.2	1018	13.1	988	9.8
	INM		1086	20.7	1050	16.7	1022	13.6
	IPSL		1047	16.3	1005	11.7	973	8.1
	MIROC		1081	20.1	1043	15.9	1014	12.7
	MPI		1109	23.2	1082	20.2	1060	17.8
	NCAR		1102	22.4	1065	18.3	1036	15.1

5.2.3 GCM structure

The uncertainty due to the GCM structure of changes in the future hydrological regime is investigated at the seasonal level. Figures 5.6 and 5.7 show box plots of the average seasonal change in percent of simulated discharges between the future (2065-2097) and the control periods (1975-2007) that are drawn from 250 simulations that combine five climate sensitivity values and 50 natural variability runs per individual GCM, as simulated by HYDROTEL, HBV, HSAMI and HMETS. Due to the significant increase of discharge in April in a future climate, a specific analysis of monthly change in April is also described and presented in Figure 5.8. The results in these figures show that seasonal changes in river flows vary between GCMs and also between hydrological models. The following paragraphs describe in more detail how the uncertainty in GCM structure is seasonally dependent.

Winter season. In general, the warmer and wetter GCMs, such as IPSL and MIROC, tend generate more important increases in future discharge and more variability over the winter season than the colder and drier GCMs, like CNRM. However, the influence of the hydrological model is noteworthy, with distributed models such as HYDROTEL and HBV displaying an increased variability, as compared to lumped models such as HSAMI and HMETS. For example, there is an obvious increase in the winter flows with the IPSL model, compared to CNRM, as simulated by HYDROTEL and HBV. This is in contrast with the modest increases and smaller variability produced by HMETS. Table 5.5 presents the uncertainty due to GCM structure for each season when the hydrological models are investigated individually. The estimation of the uncertainty due to GCM structure is assumed here to be the largest range obtained in Figure 5.6 and 5.7, i.e., the maximum change in median flow minus the minimum change. When considering each hydrological model separately, the range in winter median flows varies from 5% with HMETS to 46% with HYDROTEL.

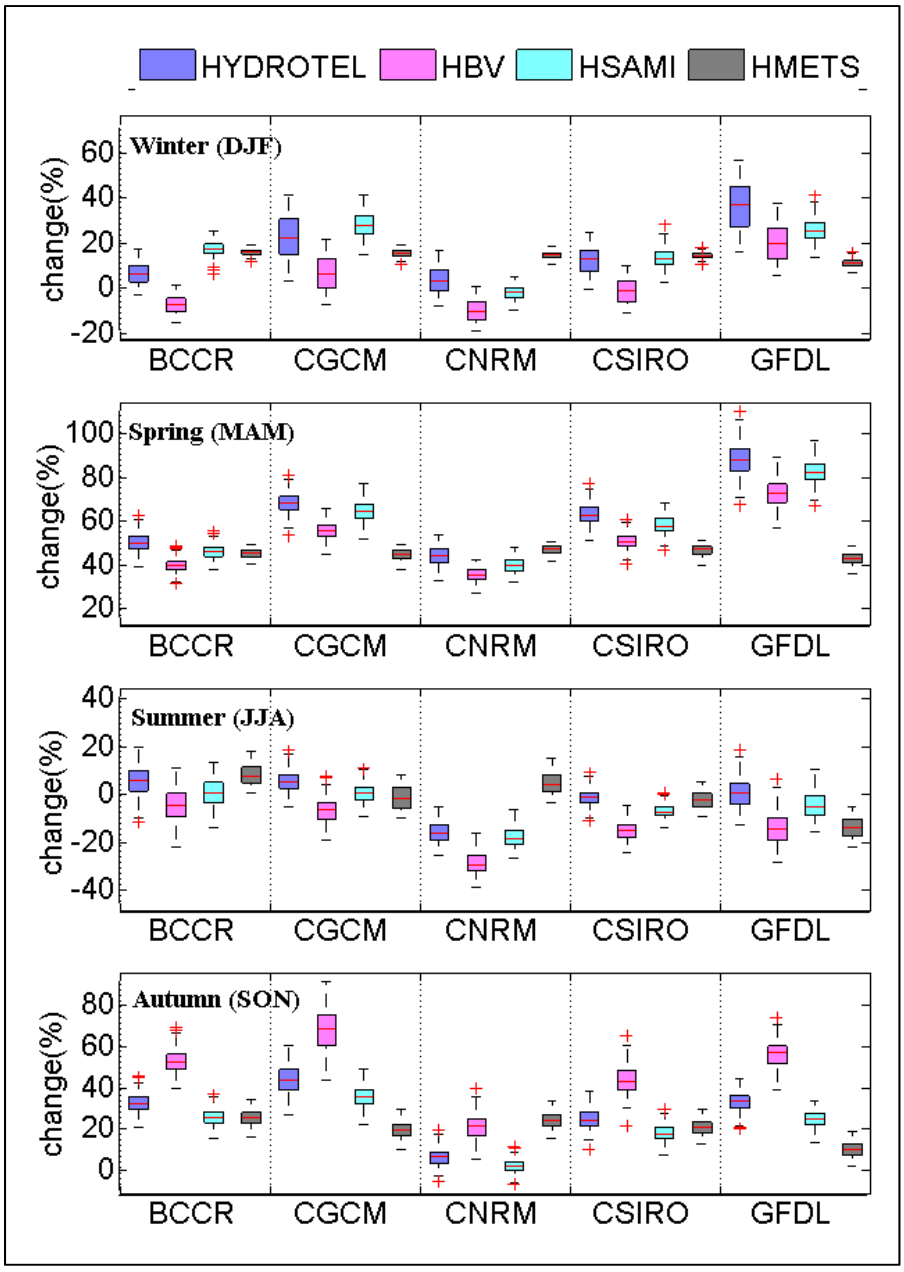

Figure 5.6 Box plots of percent of change in average seasonal discharge between the future (2065-2097) and reference (1975-2007) period simulated by four hydrological models at the outlet of MRB for five GCMs (BCCR, CGCM, CNRM, CSIRO, GFDL). All climate sensitivities and natural variability are used. On each box, the central line is the median, the top and bottom of the box are the 25th and 75th percentiles. The distance between the top and bottom is the interquartile range. The whiskers extending above and below each box indicate the 5th and 95th percentiles respectively. Outliers are displayed as red + signs

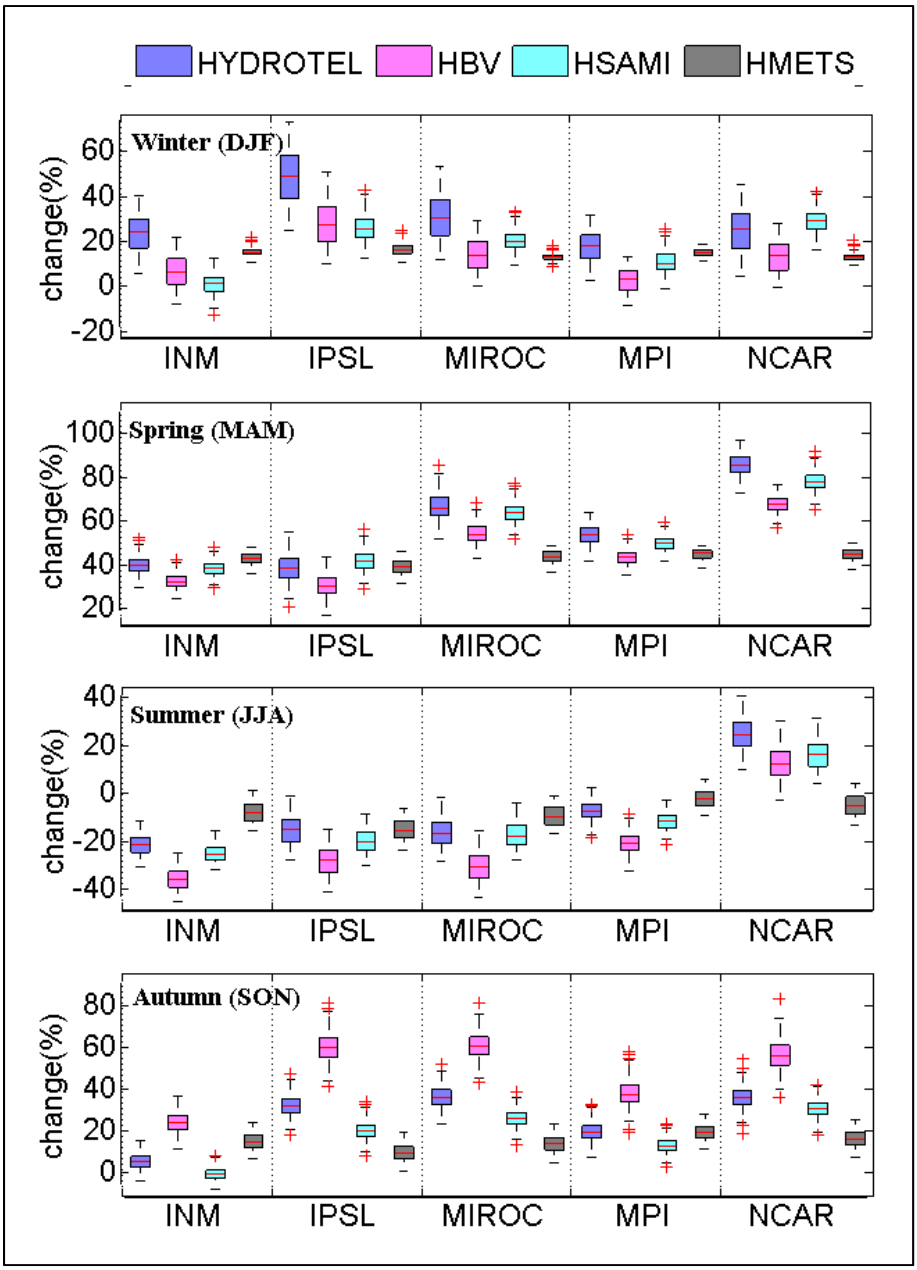

Figure 5.7 Box plot of the percent change of average seasonal discharge between the future (2065-2097) and reference (1975-2007) period simulated by four hydrological models at the outlet of MRB for five GCMs (INM, IPSL, MIROC, MPI, NCAR). All climate sensitivities and natural variability are used. See Figure 5.6 for further explanations of the box plot

Spring season. All GCMs produce significant increases of river discharge (above 20%) during the spring season and for all hydrological models. In Figures 5.6 and 5.7, the largest increases are seen in the GFDL and NCAR models (up to 80%) and this, for all the hydrological models except HMETS, which displays a more uniform increase in spring discharge (about 40%), regardless of the GCM used as an input for the model. In Table 5.5, the uncertainty that is solely due to GCM structure, when each hydrological model is investigated separately, goes from 8% with HMETS (maximum change of 48% with CSIRO, minimum change of 39% with IPSL) to 50% with HYDROTEL (maximum change of 88% with GFDL, minimum change of 38% with IPSL).

Summer season. Median changes to the summer flows tend to be mostly negative, i.e. a decrease in future flows, for a majority of GCMs investigated, regardless of the hydrological model used to simulate the flows. A few combinations of GCM and hydrological model resulted in increased future flows. A notable exception is the NCAR model, which shows increases from 10% to 20% for all hydrological models, except HMETS. Overall uncertainty when including both GCM and hydrological model structures is about 60% (increase of 24% with NCAR/HYDROTEL; decrease of 36% with INM/HBV). In Table 5.5, the uncertainty that is due solely to the GCM structure goes from 23% with HMETS to 48% with HBV.

Autumn season. The autumn season is generally characterized by increased flows in the future. The increase is seen to vary significantly according to the GCM structure. For example, increases in future flows vary from 69% with the CGCM model to 22% with CNRM when driving the HBV hydrological model. Similarly, the increase in future flows is also sensitive to the choice of the hydrological model. For example, the increase is seen to vary from 20% to more than 60% with the CGCM model depending on hydrological model structure. Therefore, the uncertainty due to GCM structure appears to be of the same order of magnitude as the one due to the choice of the hydrological model, reaching about 50% in both cases. Uncertainty due to GCM structure varies from 16% with HMETS to 47% with HBV, as shown in Table 5.5.

Table 5.5 Uncertainty of GCM structure for all four seasons produced by each hydrological model. Max (%) is the maximum change in median flow, Min (%) is the minimum change and UC is uncertainty

Models	Winter (DJF)			Spring(MAM)			Summer(JJA)			Autumn(SON)		
	Max (%)	Min (%)	UC (%)	Max (%)	Min (%)	UC (%)	Max (%)	Min (%)	UC (%)	Max (%)	Min (%)	UC (%)
HYDROTEL	49	3	46	88	38	50	24	-22	46	45	6	39
HBV	27	-10	37	72	30	42	12	-36	48	69	22	47
HSAMI	29	-2	31	82	38	44	16	-26	42	36	0	36
HMETS	16	11	5	47	39	8	7	-16	23	26	10	16

Figure 5.8 is similar to Figures 5.6 and 5.7, but focuses more specifically on the month of April, where the changes in the hydrological regime are more pronounced because of an earlier snowmelt caused by increased air temperatures. The data used to produce Figure 5.8 also combine 250 simulations covering a range of climate sensitivities and natural variability. Again, results are presented for individual GCMs and hydrological models.

Overall, Figure 5.8 confirms that the uncertainty due to GCM structure on spring flow is an important contributor to the overall uncertainty. Taking the hydrological model individually, increases in future median flows range from 120% to 530% respectively for the BCCR and the GFDL climate models when HSAMI is used to compute future flows. HYDROTEL produced the smallest range of future flow changes, with increases in median flows of 80% and 330%, again respectively for the BCCR and GFDL models. This sensitivity to the choice of the hydrological model is related to the fact that although HYDROTEL produces larger increases in average annual flows as compared to the other models (see Table 5.4), the time to peak mostly occurs in May, not in April (see Figure 5.5), which is not the case with HSAMI. A similar behaviour is observed with HMETS. Consequently, both HYDROTEL and HMETS models display a smaller variability in their changes in April flows for all

GCMs considered. The uncertainty due to hydrological model structure is more fully addressed in Section 5.2.6.

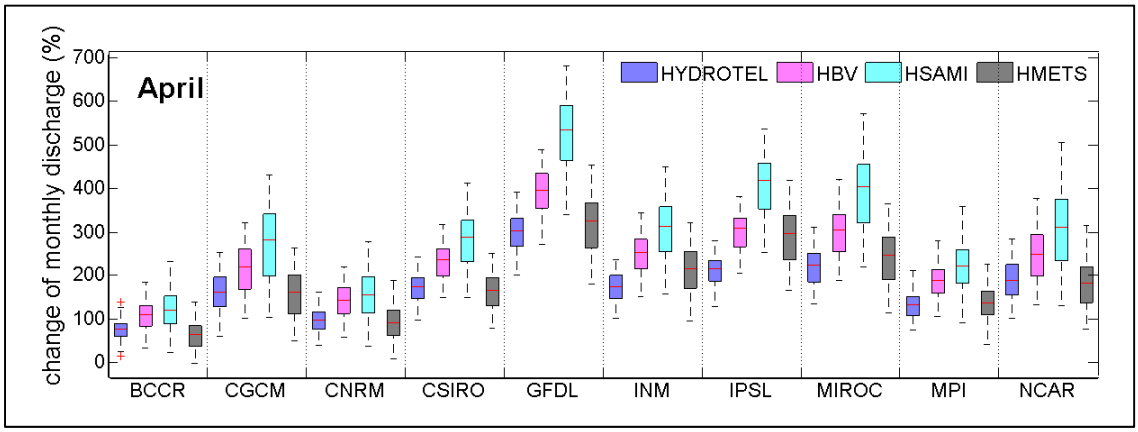

Figure 5.8 Percent change of average monthly discharge, in April only, between the future (2065-2097) and reference (1975-2007) periods simulated by four hydrological models at the outlet of MRB for ten individual GCMs. All climate sensitivities and natural variability are used. See Figure 5.6 for further explanations of the box plot

5.2.4 Climate sensitivity

The uncertainty due to climate sensitivity is presented in Figures 5.9(a) to 5.9(d) for HYDROTEL, HBV, HSAMI and HMETS, respectively. The dashed lines represent an average hydrograph at the outlet of the MRB that results from 500 simulations, using 10 GCMs and 50 series of natural variability for the future (2065-2097) period. The percent change of average daily discharge between the future and reference (1975-2007) period is also presented separately for each hydrological model. For all hydrological models, as the value of climate sensitivity increases, the time to peak occurs earlier and the peak discharge is gradually lessened. The increase of average annual flows in Table 5.4 demonstrates this impact as well. The impact of climate sensitivity is mostly significant during the spring season, followed by the autumn season, while little influence is observed during the winter and summer seasons. Finally, the uncertainty associated to climate sensitivity appears to be moderate to small depending on the season, and regardless of the hydrological models used in this study.

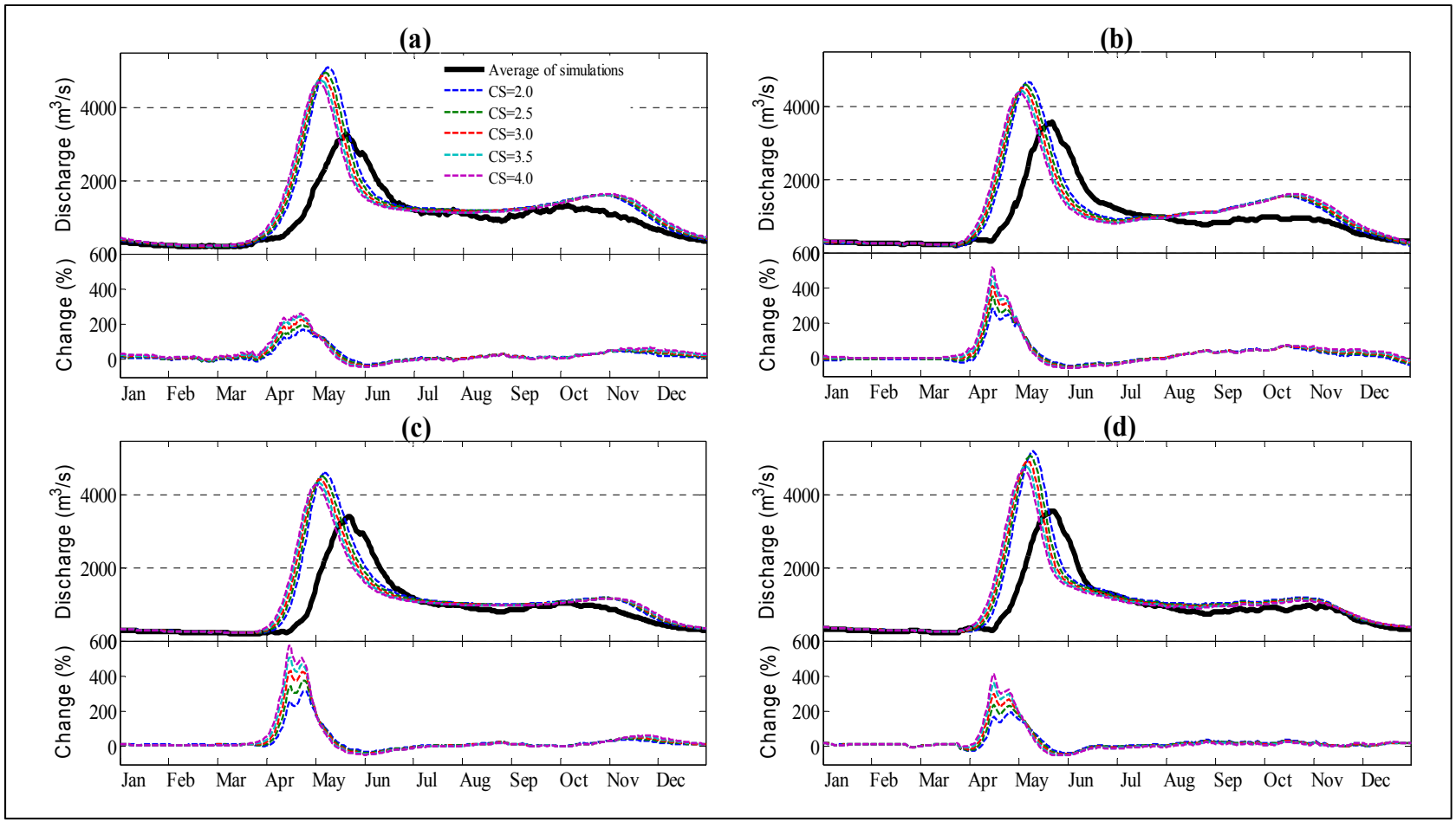

Figure 5.9 Annual mean hydrographs simulated by (a) HYDROTEL, (b) HBV, (c) HSAMI and (d) HMETS models and sorted by different values of climate sensitivity at the outlet of the MRB for the future period (2065-2097), as well as the percentage change of average daily discharge between the future (2065-2097) and reference (1975-2007) period. All GCMs and natural variability are included. Simulated hydrographs for the reference period are plotted for the purpose of comparison. CS is climate sensitivity

5.2.5 Natural variability

Figure 5.10 shows the uncertainty in flows caused by natural variability, presented as the percent change of seasonal discharge between the future (2065-2097) and control (1975-2007) time periods simulated by HYDROTEL, HBV, HSAMI and HMETS. The effect of natural variability appears here on a seasonal basis. Each box plot results from 50 series of natural variability. Each series combines all GCMs (10) and climate sensitivities (5), for a total of 10 × 5 × 33 years of daily simulated flows, from which the percent change in average seasonal flows were extracted.

As expected, the percent change in seasonal flows is significant during the spring season for all investigated hydrological models, with median increases of around 50%. Other seasons display lower seasonal changes, either positive or negative, depending on the season being considered. For example, future winter changes vary from 25% with HYDROTEL to 5% using the HBV model. A decrease in summer flows is observed, this decrease being the strongest with HBV (20%) and the smallest with HMETS (5%).

The impact of natural variability on seasonal flows is revealed through the spread of the box plots. Overall, natural variability produces notable uncertainty in all seasons and for all hydrological models investigated, with the exception of the HMETS model, which displays a very small uncertainty during the winter and spring seasons, and lower variability in the summer and autumn seasons compared with the other hydrological models.

These observations indicate that uncertainty about the season runoff caused by the natural variability is not negligible and would be affected by the choice of the hydrological models used and, to a lesser extent, by the season.

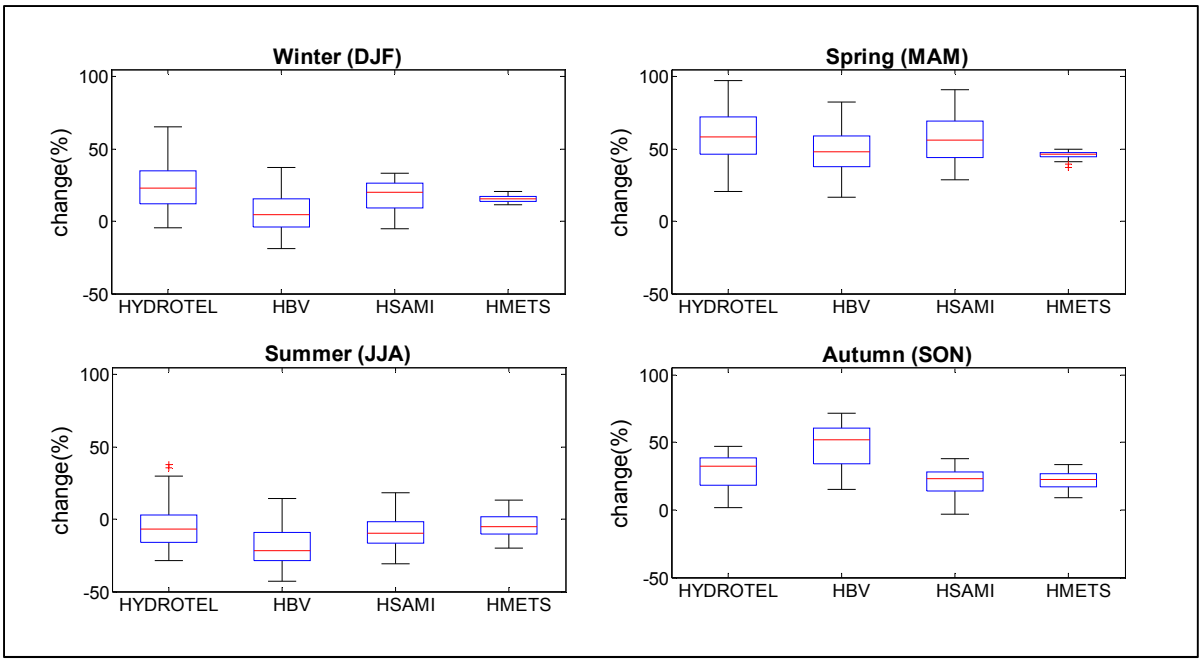

Figure 5.10 Box plots of percent change of average seasonal discharge between the future (2065-2097) and control (1975-2007) period simulated by HYDROTEL, HBV, HSAMI and HMETS simulated with all 50 series of natural variability at the outlet of MRB. See Figure 5.6 for further explanations of the boxplot

5.2.6 Hydrological model structure

Sub-sections 5.2.3 to 5.2.5 have shown that the structure of the hydrological model impacts on the estimation of future flows and can be a source of uncertainty of a magnitude comparable to other sources of uncertainty, such as GCM structure and natural variability. In this section, the uncertainty due to hydrological model structure on the spring runoff volumes is further examined. The choice of that particular hydrological variable was motivated by the fact that spring runoff is one of the most important hydrological process for effective reservoir management.

Probability density functions (PDF) of spring runoff depths (MAM) were computed using kernel density estimators and are shown in Figure 5.11 for individual GCMs over the 2065-2097 time horizon. Results are presented separately for each hydrological model. A climate

sensitivity value of 3.0°C, which is recognised as the being the most probable climate sensitivity value (Rogejl et al., 2012), was used to generate the PDFs, this to better highlight the impact of hydrological model structure on future spring flow values. Each generated PDF incorporates the simulations resulting from 50 time series of natural variability. The PDF of the annual mean spring runoff depth is averaged for the four hydrological models for the control period (1975-2007) and is plotted as a dark bold curve. Distinct curves could have been shown for each hydrological model, but it was decided to retain a single average curve because all individual PDFs were very similar, the calibrated models producing very similar results for the control period, as evidenced in Figure 5.3.

Compared to the current climate, the future spring runoff is increased, but the magnitude of the increase for each GCM varies according to the hydrological model used. For instance, the mean spring runoff and its variability in the future are largest with HYDROTEL, as compared with the other hydrological models for all GCMs. Moreover, the uncertainty of the mean spring runoff volume associated with the GCM structure, as evidenced by the spread of the PDF, depends on the hydrological model used and is largest with HYDROTEL and smallest with HMETS (see also Figures 5.6, 5.7 and 5.10). In fact, results indicate that the GCM structure has virtually no influence on the uncertainty of the mean spring runoff when HMETS is used, as evidenced by the PDF which is almost identical, no matter which GCM is used. Note that the spatially distributed HBV and lumped HSAMI models behave very similarly in simulating the spring runoff (mean and standard deviation) for all GCMs used. These results reveal that the uncertainty due to the hydrological model structure cannot be ignored. Different hydrological models may predict notable different hydrological regimes depending on the GCMs used to force the models. See, for example, the GFDL and NCAR models.

It is also noted that the spring runoff PDFs appear generally less spread in the future climate for all combinations of GCMs and hydrological models, with perhaps the exception of HYDROTEL, where runoff variability in the future climate is more significant than with the other models. As an example, the coefficient of variation (CV), i.e. the ratio of the standard

deviation to the mean value, which is derived from the average discharge in spring season (MAM), simulated by HYDROTEL for the future period is 18.5%, while it is 16.1% with HBV, 15.8% with HSAMI and 12.3% with HMETS.

Some GCMs such as CGCM, GFDL, MIROC and NCAR are characterized by a wider spread of their PDFs, i.e. they produce the largest extreme depths of spring runoff. Other GCMS, for example BCCR, CNRM and INM, produce tighter PDFs and therefore less extreme flood volumes. This is due to the warmer and wetter climate simulated by the former GCMs (e.g. GFDL and NCAR) that increase the probability to cause extreme events. Colder and dryer GCMs (e.g. BCCR, CNRM and INM) all produce future spring floods characterized by similar PDFs. Furthermore, these GCMs tend to simulate conditions that lead to extreme spring floods which are similar to today's climate conditions. Overall, Figure 5.11 reveals that future spring runoff volumes are comparatively affected by the choice of the GCM and of the hydrological model, which reinforces the need to run multiple hydrological models driven by multiple GCMs in order to better anticipate future hydrological regimes.

Generally, results presented here have repeatedly shown that the HMETS model appears to behave differently from the other hydrological models in simulating future flows, although performance of this model in simulating current hydrological regimes is comparable to the other models used in this study. This is particularly apparent in Figures 5.6, 5.7, 5.10 and 5.11 (and to a lesser extent in Figure 5.5), where the variability in winter and spring seasonal runoff produced by HMETS is much smaller than the variability produced by HYDROTEL, HBV and HSAMI models. Although no conclusions can be drawn as to the causes of this distinct behaviour, it nevertheless raises the question as to which strategy to adopt in choosing the hydrological models that will best account for hydrological model structure uncertainty in a climate change assessment study.

Finally, the median increase in April discharge, presented in Figure 5.8, is larger with HSAMI than with the other models, in addition to the variability. The median value of the

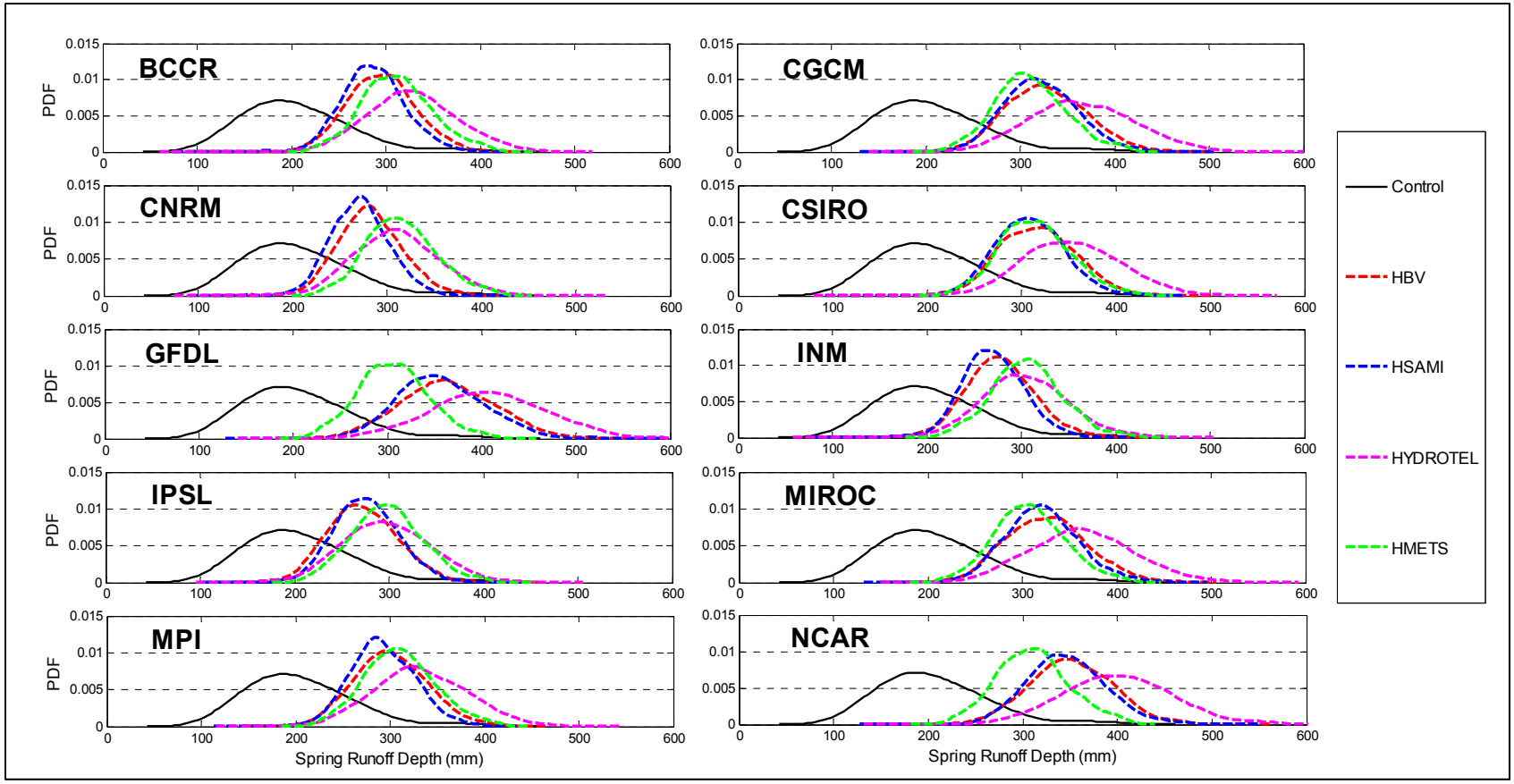

Figure 5.11 Probability density functions (PDF) of spring runoff depth simulated by HBV, HSAMI, HYDROTEL and HMETS for ten GCMs for the future (2065-2097) period at the outlet of the MRB. Each PDF curve corresponds to simulations using the central value (3.0°C) of climate sensitivity. The PDF produced with the simulated average runoff from the four hydrological models used for the control period (1975-2007) is plotted in dark solid curve for the purpose of comparison

chang in average monthly discharge varies from 120% with the BCCR model to 530% for the GFDL model, as simulated by HSAMI, with the largest range being 410%. The relative median value of change, simulated by HYDROTEL, varies from 80% for BCCR to 300% for GFDL, producing the smallest range at 220%. The overall median increase averaged over all GCMs is calculated as 305% for the HSAMI model, as compared with 241% for the HBV model, 175% for the HYDROTEL model, and 189% for the HMETS model, again highlighting the fact that the choice of the hydrological model introduces a notable uncertainty in the results.

5.3 Monte Carlo simulation

A Monte Carlo simulation was performed to sample hydrological variables using weights attributed to selected sources of uncertainty in order to analyze the distribution of uncertainty in the hydrological modeling results. An experiment in which equal and unequal weights were assigned to GCM structure and climate sensitivity was also conducted in this study.

The REA method, which is described in section 3.6.2 and is used to assign weights to climate models, typically applies to one climate variable e.g. precipitation. The reliability factors, which are based on temperature (R_T) and precipitation (R_P) as calculated by the REA method, are presented in Table 5.6. The performance factor R_B and the convergence factor R_D used to calculate the reliability factors are also listed in this table. Keep in mind that the performance factor R_B describes how well a given GCM is able to generate a current climatic variable, while the convergence factor R_D describes how far a given model is from the remaining GCMs in simulating that variable. The reliability factor varies between 0 and 1. Higher values indicate that the GCM performs well in representing the current climatic variable and is not an outlier compared to the other GCMs considered in the analysis, while lower values indicate a poor performance in simulating the current climatic variable and/or that the GCM is an outlier compared to the other GCMsOverall, the calculated R factors are consistent for the corresponding GCM regardless of the climate variable analyzed, which, in

this case, are temperature and precipitation. In other words, a GCM that scored well for T also scored well for P. The performance factor R_B appears dominant, regardless of its value, in the estimate of the reliability factor R when the convergence factor R_D is high (close to 1), in other words, when the model is not an outlier. But when R_D is low, then the GCM is seen as an outlier and it will obtain a small reliability factor R no matter how good or bad model performance (R_B) is. The relative weights (W) of each GCM, derived from the R values (see eq. 3.7), are presented in Table 5.6. The R values were rescaled so that their corresponding W values sum up to one.

Table 5.6 Reliability, performance and convergence factors R, R_B and R_D from the REA method used to generate relative weights W for each GCM, based on precipitation (P) and temperature (T)

GCM	Precipitation				Temperature			
	R_B	R_D	R_P	W_P	R_B	R_D	R_T	W_T
BCCR-BCM2.0	0.46	1.00	0.46	0.15	0.15	0.99	0.15	0.09
CGCM 3.1	0.19	1.00	0.19	0.06	0.11	0.96	0.11	0.07
CNRM-CM3	0.64	0.96	0.61	0.20	0.29	0.95	0.28	0.16
CSIRO-MK3.0	0.20	0.20	0.04	0.01	0.11	0.19	0.02	0.01
GFDL-CM2.0	0.17	0.21	0.04	0.01	0.12	0.96	0.12	0.07
INM-CM3.0	0.75	1.00	0.75	0.25	0.52	1.00	0.52	0.30
IPSL-CM4	0.20	0.30	0.06	0.02	0.14	0.22	0.03	0.02
MIROC3.2(medres)	0.20	1.00	0.20	0.07	0.27	0.67	0.18	0.10
MPI-ECHAM5	0.49	0.99	0.48	0.16	0.57	0.42	0.24	0.14
NCAR-PCM1	0.22	1.00	0.22	0.07	0.12	0.86	0.10	0.06

As river flow is influenced by temperature and precipitation, different combinations of these two variables were used in the REA approach to generate a suite of GCM weights in an attempt to rank the climate models based on their ability to properly simulate runoff at the watershed scale. The combinations proposed are as follows (see Table 5.7): (1) equal weights to all GCMs (which does not require application of the REA approach), labeled as Equal; (2) unequal weights based only on precipitation, labeled as W_P; (3) unequal weights based only on temperature, labeled as W_T; (4) unequal weights with precipitation and temperature ranked as equally important, labeled as $W_{(0.5P, 0.5T)}$; (5)-(6) unequal weights with precipitation and temperature, but with more importance given to temperature and precipitation, respectively, labeled as $W_{(0.25P, 0.75T)}$ and $W_{(0.75P, 0.25T)}$. Overall, the results of the REA

approach gave more weights to the CNRM, INM and MPI GCMs (see Table 5.7), for all considered precipitation and temperature combinations, whereas the CSIRO and IPSL GCMs obtained the smallest weights. Because the REA method provided similar weights using either precipitation or temperature as the reference variable, any combination of these two variables did not produce notably different weight schemes. These results are site specific and should not be generalized to other watersheds.

Table 5.7 Various combinations of weights calculated for each GCM

GCM	Equal	W_P	W_T	$W_{(0.5P, 0.5T)}$	$W_{(0.25P, 0.75T)}$	$W_{(0.75P, 0.25T)}$
BCCR-BCM2.0	0.10	0.15	0.09	0.11	0.13	0.10
CGCM 3.1	0.10	0.06	0.07	0.07	0.06	0.07
CNRM-CM3	0.10	0.20	0.16	0.18	0.19	0.17
CSIRO-MK3.0	0.10	0.01	0.01	0.01	0.01	0.01
GFDL-CM2.0	0.10	0.01	0.07	0.03	0.02	0.04
INM-CM3.0	0.10	0.25	0.30	0.28	0.27	0.29
IPSL-CM4	0.10	0.02	0.02	0.02	0.02	0.02
MIROC3.2(medres)	0.10	0.07	0.10	0.08	0.07	0.09
MPI-ECHAM5	0.10	0.16	0.14	0.15	0.15	0.14
NCAR-PCM1	0.10	0.07	0.06	0.06	0.07	0.06

Weights attributed to climate sensitivities are described in Section 3.6.1, which were computed by assuming a simple symmetrical triangular distribution. Equal weights were assigned to account for natural climate variability. A separate Monte Carlo analysis was conducted for each hydrological model in order to assess the relative effect of hydrological model structure on selected simulated hydrological variables. The following two hydrological variables were scrutinized in the Monte Carlo experiment: annual mean discharge and spring peak discharge. The choice was based on the fact that these variables are of importance for the total annual hydropower production (annual mean discharge) and for the proper management of hydropower facilities (spring peak discharge), although the Monte Carlo method can also be applied to other variables that characterize the hydrological regime of the MRB.

The general procedure of applying the Monte-Carlo simulation consisted in pooling the values of the simulated hydrological variables stored in a database according to prescribed weights. As described in Section 3.4, a total of 2500 hydrological simulations, reflecting a combination of GCM structure (10), climate sensitivity (5) and natural variability (50), were performed for each hydrological model, from which the database, containing the simulated results of all hydrological projections, was generated. Each simulation covered a 33-year period (2065-2097).

The results of the Monte Carlo experiments were interpreted as return periods of future hydrological events (annual runoff and spring peak runoff), these often being used for risk analysis (Ang and Tang, 1984). Prior to establishing the return periods, outputs of the Monte Carlo experiments were fitted with statistical distribution models (Normal, Rayleigh, extreme value and lognormal). The normal distribution provided the best fitting results with a 95% confidence level. This distribution was then used to compute return periods associated to given values of annual mean discharge and spring peak runoff. The assumption behind such analysis is that the variables pooled from the data base are statistically independent. The analysis was conducted for the 2065-2097 period. A comparison with current return periods (1975-2007) was performed, also by using normal distributions applied to simulated values of annual mean discharge and spring peak runoff.

5.3.1 Annual mean discharge

Tables 5.8 to 5.11 describe the return period (in years) of prescribed annual mean discharges values calculated from a Monte Carlo experiment, in which weights were assigned based on GCM structure (Table 5.7) and climate sensitivity (triangular distribution) for the distributed HYDROTEL and HBV models (Tables 5.8 and 5.9), and the lumped HSAMI and HMETS models (Tables 5.10 and 5.11) (400,000 samplings per hydrological model). Return periods were calculated for annual flow rates ranging from 1000 to 1200 m^3/s. These values correspond approximately to the smallest and largest values simulated under current climate conditions (1975-2007).

All calculated return periods are smaller for the future climate, when either equal or unequal weights are applied to climate sensitivity and to GCMs, as compared to the current climate when the HYDROTEL (Table 5.8), HBV (Table 5.9) and HSAMI (Table 5.10) models are used to simulate river discharge. This result was expected given the higher average flows in the future, as depicted in Figure 5.5 and in Table 5.4. HMETS (Table 5.11) was the only model which produced return periods larger in the future than in the present, which occurred when unequal weights were used on climate sensitivity and when average flows exceeded 1150 m^3/s. Finally, experiments with different weights on climate sensitivity produced larger return periods for the future climate, as compared to those with uniform weights on climate sensitivity for all four hydrological models.

Overall, HYDROTEL produced the smallest future return periods, between 1.0 and 1.7 years, for the range of considered mean discharges (see Table 5.8), followed by HBV, HSAMI and HMETS. HYDROTEL resulted in return periods to be univocally smaller in the future for the given exceedance flow values, especially at higher flows, as compared to the current climate, indicating that this model was more sensitive to changing climate than the other models. Therefore it appears that HYDROTEL model has a notable effect on simulating extreme flow values, which confirms the observations made above on simulating spring runoff (see Figure 5.11). However, care must be exercised in generalizing these results as the analysis was performed by using only four hydrological models.

Tables 5.8 to 5.11 also reveal that the return period for mean annual discharge is notably affected by whether a uniform or a triangular distribution for climate sensitivity is adopted. For equal weights on climate sensitivity, the average return periods of flows exceeding 1200 m^3/s for all GCM weight experiments are 1.50 years for HYDROTEL, 9.16 years for HBV, 12.9 years for HSAMI and 25.4 years for HMETS. For unequal weights on climate sensitivity, the corresponding average return periods are 1.65 years, 16.5 years, 24.5 years and 40.7 years, respectively. On the other hand, using equal or unequal weights on the GCM structure has virtually no effect on the computed return periods.

Table 5.8 Return period (in years) of annual mean discharge simulated by the HYDROTEL model for different weighting schemes on GCM and climate sensitivity (CS is climate sensitivity, = is equal weight, ≠ is unequal weight)

Q (m^3/s)	Control period	Equal GCM		Unequal GCM									
				W_T		W_P		$W_{(0.5P, 0.5T)}$		$W_{(0.25P, 0.75T)}$		$W_{(0.75P, 0.25T)}$	
		=CS	≠CS	=CS	≠CS	=CS	≠CS	=CS	≠CS	=CS	≠CS	=CS	≠CS
>1000	2.05	1.02	1.02	1.02	1.02	1.02	1.02	1.02	1.02	1.02	1.02	1.02	1.02
>1050	2.61	1.05	1.05	1.05	1.05	1.04	1.05	1.05	1.05	1.05	1.05	1.05	1.05
>1100	3.50	1.11	1.12	1.11	1.13	1.11	1.14	1.11	1.13	1.11	1.13	1.11	1.13
>1150	4.93	1.25	1.31	1.25	1.30	1.24	1.31	1.25	1.30	1.24	1.31	1.25	1.30
>1200	7.35	1.50	1.66	1.51	1.65	1.49	1.66	1.50	1.65	1.50	1.66	1.51	1.65

Table 5.9 Return period (in years) of annual mean discharge simulated by the HBV model for different weighting schemes on GCM and climate sensitivity (CS, = and ≠ are indicated in Table 5.8)

Q (m^3/s)	Control period	Equal GCM		Unequal GCM									
				W_T		W_P		$W_{(0.5P, 0.5T)}$		$W_{(0.25P, 0.75T)}$		$W_{(0.75P, 0.25T)}$	
		=CS	≠CS	=CS	≠CS	=CS	≠CS	=CS	≠CS	=CS	≠CS	=CS	≠CS
>1000	4.80	1.31	1.40	1.32	1.39	1.31	1.41	1.31	1.40	1.31	1.41	1.31	1.40
>1050	9.43	1.71	1.97	1.72	1.95	1.70	1.98	1.71	1.97	1.70	1.98	1.71	1.96
>1100	19.0	2.57	3.32	2.59	3.30	2.56	3.34	2.58	3.33	2.57	3.33	2.58	3.31
>1150	50.1	4.29	6.38	4.33	6.36	4.31	6.39	4.32	6.41	4.31	6.38	4.33	6.39
>1200	153	9.04	16.4	9.17	16.5	9.19	16.3	9.19	16.6	9.17	16.4	9.19	16.6

Table 5.10 Return period (in years) of annual mean discharge simulated by the HSAMI model for different weighting schemes on GCM and climate sensitivity (CS, = and ≠ are indicated in Table 5.8)

Q (m^3/s)	Control period	Equal GCM		Unequal GCM									
				W_T		W_P		$W_{(0.5P, 0.5T)}$		$W_{(0.25P, 0.75T)}$		$W_{(0.75P, 0.25T)}$	
		=CS	≠CS	=CS	≠CS	=CS	≠CS	=CS	≠CS	=CS	≠CS	=CS	≠CS
>1000	4.11	1.36	1.43	1.37	1.42	1.35	1.44	1.36	1.43	1.35	1.43	1.36	1.43
>1050	7.06	1.81	2.06	1.82	2.05	1.80	2.08	1.82	2.06	1.81	2.07	1.82	2.06
>1100	12.3	2.83	3.65	2.85	3.63	2.82	3.67	2.84	3.64	2.83	3.66	2.85	3.66
>1150	23.4	5.35	8.23	5.38	8.20	5.37	8.25	5.38	8.21	5.36	8.24	5.39	8.28
>1200	48.8	12.8	24.5	12.8	24.5	13.0	24.4	12.9	24.5	12.9	24.5	12.9	24.8

Table 5.11 Return period (in years) of annual mean discharge simulated by the HMETS model for different weighting schemes on GCM and climate sensitivity (CS, = and ≠ are indicated in Table 5.8)

Q (m^3/s)	Control period	Equal GCM		Unequal GCM									
				W_T		W_P		$W_{(0.5P, 0.5T)}$		$W_{(0.25P, 0.75T)}$		$W_{(0.75P, 0.25T)}$	
		=CS	≠CS	=CS	≠CS	=CS	≠CS	=CS	≠CS	=CS	≠CS	=CS	≠CS
>1000	3.44	1.06	1.15	1.07	1.16	1.07	1.16	1.07	1.16	1.07	1.16	1.07	1.16
>1050	4.92	1.49	1.53	1.56	1.61	1.50	1.64	1.54	1.68	1.52	1.66	1.55	1.60
>1100	8.20	4.33	5.95	4.91	5.52	4.34	5.95	4.65	5.25	4.49	5.10	4.81	5.42
>1150	13.4	11.1	18.5	11.2	18.4	11.1	18.6	11.6	18.3	11.3	18.1	11.2	18.6
>1200	26.5	25.9	41.7	25.2	40.7	24.9	40.5	25.4	40.0	25.5	40.9	25.3	40.1

5.3.2 Spring peak discharge

Extreme events such as peak flow values are important hydrological variables for the design of water resources systems components, such as dams and spillways. Similar to Tables 5.8 to 5.11, Tables 5.12 to 5.15 express the return period (in years) of selected spring peak discharge amounts retrieved from a 400,000-run Monte Carlo simulation. High peak flow values for the current spring period, varying from 6600m^3/s to 7000m^3/s with an interval of 100m^3/s, were used to estimate the corresponding return periods for the future climate. The standard normal distribution was applied to compute return periods for the future (2065-2097) and current climates (1975-2007).

Overall, the remarks pertaining to the annual mean discharge also apply for the spring peak flow. For instance, return periods increase when unequal weights on climate sensitivity are employed, as compared to a uniform weighting scheme, for all combinations of GCM weighting strategies (including equal weights) and for all selected peak flow discharges. The difference in return periods, between equal and unequal weights for climate sensitivity, increases as peak flow increases. Significant differences are again observed in return periods depending on which hydrological model was used to simulate future flows. For example, the average return periods of all equal weighted experiments of climate sensitivity for a peak discharge event exceeding 7000 m^3/s are 6.10 years for HYDROTEL (compared to 25.0 years for the current climate), 32.9 years for HBV (current climate = 56.3years), 12.9 years

for HSAMI (current climate = 22.5 years) and 12.4 years for HMETS (current climate = 10.9 years). For unequal weights on climate sensitivity, the corresponding average future return periods are 9.18 years, 72.9 years, 22.6 years and 14.3 years. However, no conclusions could be drawn regarding the magnitude of the future return periods in relation to the spatial structure of the hydrological models (distributed versus lumped) used to compute the peak flows.

Finally, the selection of the GCM weighting strategy does not seem to be critical, as the return periods are not significantly affected by using equal or unequal weights, irrespective of the hydrological model selected for the analysis. For example, the return period for a peak flow event exceeding 6900 m^3/s is 20.8 years with the HBV model (Table 5.13) when equal weights are used for both GCM structure and climate sensitivity, compared to an average of 20.2 years when unequal weights are applied to the GCMs.

Table 5.12 Return period (in years) of annual spring peak discharge simulated by the HYDROTEL model for different weighting schemes on GCM and climate sensitivity (CS, = and ≠ are indicated in Table 5.8)

Q_{peak} (m^3/s)	Control period	Equal GCM		Unequal GCM									
				W_T		W_P		$W_{(0.5P, 0.5T)}$		$W_{(0.25P, 0.75T)}$		$W_{(0.75P, 0.25T)}$	
		=CS	≠CS	=CS	≠CS	=CS	≠CS	=CS	≠CS	=CS	≠CS	=CS	≠CS
>6600	14.7	2.69	3.26	2.69	3.19	2.64	3.21	2.67	3.19	2.66	3.20	2.68	3.20
>6700	16.3	3.34	4.30	3.32	4.17	3.27	4.21	3.30	4.18	3.29	4.19	3.31	4.18
>6800	20.1	4.27	5.88	4.22	5.66	4.18	5.75	4.20	5.67	4.20	5.71	4.21	5.67
>6900	22.4	5.11	7.41	5.04	7.09	5.01	7.24	5.02	7.11	5.02	7.17	5.03	7.10
>7000	25.0	6.21	9.50	6.09	9.03	6.08	9.28	6.08	9.06	6.09	9.16	6.08	9.05

Table 5.13 Return period (in years) of annual spring peak discharge simulated by the HBV model for different weighting schemes on GCM and climate sensitivity (CS, = and ≠ are indicated in Table 5.8)

Q_{peak} (m^3/s)	Control period	Equal GCM		Unequal GCM									
				W_T		W_P		$W_{(0.5P, 0.5T)}$		$W_{(0.25P, 0.75T)}$		$W_{(0.75P, 0.25T)}$	
		=CS	≠CS	=CS	≠CS	=CS	≠CS	=CS	≠CS	=CS	≠CS	=CS	≠CS
>6600	22.2	7.80	12.1	7.64	11.6	7.59	11.8	7.62	11.6	7.61	11.7	7.60	11.6
>6700	29.1	11.5	19.8	11.2	18.7	11.2	19.3	11.2	18.8	11.2	18.9	11.2	18.7
>6800	35.1	15.4	28.3	14.8	26.5	14.9	27.6	14.8	26.7	14.9	26.9	14.7	26.6
>6900	46.5	20.8	41.5	20.0	38.5	21.2	40.3	20.0	38.9	20.1	39.3	19.9	38.7
>7000	56.3	34.2	77.3	32.5	70.5	33.0	74.8	32.5	71.4	32.8	72.4	32.2	70.9

Table 5.14 Return period (in years) of annual spring peak discharge simulated by the HSAMI model for different weighting schemes on GCM and climate sensitivity (CS, = and ≠ are indicated in Table 5.8)

Q_{peak} (m^3/s)	Control period	Equal GCM		Unequal GCM									
				W_T		W_P		$W_{(0.5P, 0.5T)}$		$W_{(0.25P, 0.75T)}$		$W_{(0.75P, 0.25T)}$	
		=CS	≠CS	=CS	≠CS	=CS	≠CS	=CS	≠CS	=CS	≠CS	=CS	≠CS
>6600	12.1	4.96	6.90	4.86	6.58	4.92	6.81	4.88	6.64	4.89	6.69	4.90	6.61
>6700	13.4	6.18	9.08	6.01	8.58	6.12	8.95	6.05	8.68	6.06	8.76	6.07	8.63
>6800	16.3	7.83	12.2	7.56	11.4	7.77	12.0	7.64	11.6	7.67	11.7	7.66	11.5
>6900	18.2	10.1	16.9	9.68	15.6	10.0	16.6	9.83	15.9	9.88	16.1	9.83	15.7
>7000	22.5	13.3	23.8	12.6	21.8	13.2	23.4	12.9	22.2	12.9	22.6	12.8	22.0

Table 5.15 Return period (in years) of annual spring peak discharge simulated by the HMETS model for different weighting schemes on GCM and climate sensitivity (CS, = and ≠ are indicated in Table 5.8)

Q_{peak} (m^3/s)	Control period	Equal GCM		Unequal GCM									
				W_T		W_P		$W_{(0.5P, 0.5T)}$		$W_{(0.25P, 0.75T)}$		$W_{(0.75P, 0.25T)}$	
		=CS	≠CS	=CS	≠CS	=CS	≠CS	=CS	≠CS	=CS	≠CS	=CS	≠CS
>6600	6.18	2.22	2.34	2.38	2.49	2.25	2.38	2.33	2.44	2.29	2.41	2.36	2.47
>6700	7.20	3.02	3.24	3.27	3.48	3.07	3.30	3.19	3.41	3.13	3.36	3.24	3.46
>6800	8.45	4.40	4.81	4.81	5.23	4.48	4.92	4.68	5.12	4.58	5.04	4.76	5.20
>6900	9.19	6.92	7.74	7.62	8.49	7.05	7.94	7.40	8.29	7.23	8.16	7.54	8.44
>7000	10.9	11.8	13.5	13.0	14.9	12.0	13.9	12.6	14.5	12.3	14.3	12.9	14.8

5.4 Discussion

The impacts of climate change on future hydrological regimes were assessed in the MRB watershed area for the 2065-2097 time period. Climate projections from 10 GCMs, reflecting a range of ΔT and of $\Delta P/P$ values, were downscaled using the change factor method described in section 3.3. An approach based on the MAGICC-SCENGEN climate model was developed to generate GCM projections for different climate sensitivities. A weather generator was used to account for natural climate variability. The resulting daily P and T scenarios were used for input into four hydrological models to produce future hydrological scenarios. These in turn were analysed for both overall uncertainty and specific sources of uncertainty. Finally, a Monte-Carlo simulation was executed in order to perform a frequency analysis of simulated hydrological variables under equal-weighted and unequal-weighted schemes strategies. The following paragraphs further examine the results obtained.

The future change in temperature and precipitation that was produced by all the studied GCMs was presented in Figure 5.1. It was found that precipitation and temperature over the MRB will increase in the future (2065-2097 horizon) for all GCMs projections. With an increase of climate sensitivity, temperature changes are increasing while precipitation changes are almost invariant. Based on the magnitude of increase in future temperature and precipitation, some GCMs can be classified as warmer and wetter models, such as CGCM, IPSL and MIROC, while others are seen as colder and dryer models like BCCR, CNRM and CSIRO. To evaluate the climate change due to GCM structure, Figure 5.2 displays the increase of precipitation and temperature which is accompanied by an increase in climate sensitivity. The 'original' climate sensitivity for each GCM computed for the study site is also shown in Figure 5.2. Average climate sensitivity of the 10 GCMs selected in this study is 3.4°C. Although the number of GCMs used in this study is limited (more GCMs could have been added), this result is coherent with Loehle (2014), who states that climate model projections generated by GCMs are very likely to reflect a high climate sensitivity, as the commonly accepted average climate sensitivity is 3.0°C (Rogejl et al., 2012). This raises the point that conducting climate change studies by incorporating a suite of GCM precipitation and temperature outputs that reflect high climate sensitivity may induce an overall bias on future hydrological regimes because the simulated flows are affected by these climate variables. Clearly, there is a need to select GCMs with care so that their average climate sensitivity corresponds to the average climate sensitivity accepted by the scientific community. An alternative approach could be to adjust precipitation and temperature output of the selected GCMs, using models such as MAGICC-SCENGEN, in order that their average climate sensitivity equals the commonly accepted average value.

5.4.1 Uncertainty study

Results presented in the preceding sections have shown that predicted flows in a future climate are affected by a number of sources of uncertainty such as GCM structure, hydrological model structure, natural variability and climate sensitivity.

For example, future average annual hydrographs (Figure 5.5) predict a higher discharge in the summer and autumn for all hydrological models, lower winter discharge using HYDROTEL and HBV, a general increase in winter flows with the HSAMI model, and an almost unvarying winter discharge with HMETS. Such contrasting behavior displayed by the models for the winter regime is a potential issue, given, for example, the current difficulties to predict the compounding effect of river ice on flooding by river hydraulic models which use flows predicted by hydrological models as input, especially during mid-winter thaw events. These results suggest the hydrological model structure to be a non-negligible source of uncertainty in assessing the magnitude of the impacts of climate change on the hydrological regime of a watershed. Similar findings were obtained by Coulibaly et al. (2009), Chen et al. (2011a) and Poulin et al. (2011).

The contribution of each source of uncertainty investigated in this study (GCM structure, climate sensitivity and natural variability) to the overall uncertainty of the average annual future streamflow hydrograph was analysed by comparing the difference between the envelope areas of overall uncertainty to that of all sources of uncertainty, less the individual source of uncertainty under scrutiny. This was accomplished by reducing a given source of uncertainty to a single value and establishing the resulting uncertainty envelope area. For example, the contribution of climate sensitivity to the overall uncertainty of future hydrographs was estimated as being the difference between the envelope of overall uncertainty and the envelope produced by the combined contribution of GCM structure and natural variability with a prescribed, single value of climate sensitivity, here 3.0°C. The relative contribution of each source of uncertainty, defined as a percentage (%) of overall uncertainty, is presented in Table 5.16 for each hydrological model used in this study.

Table 5.16 Relative contributions (in percent) of each source of uncertainty (GCM structure, climate sensitivity and natural variability) to the overall uncertainty of future annual streamflow hydrographs.

Contribution	GCM structure	Climate sensitivity	Natural variability
HYDROTEL	50.5%	20.5%	29.0%
HBV	49.7%	20.5%	29.8%
HSAMI	50.3%	20.5%	29.2%
HMETS	48.3%	24.0%	27.7%

As expected, GCM structure is the most significant source of uncertainty and accounts for approximately 50% of the overall uncertainty, irrespective of the hydrological model used in the study. The second most important source of uncertainty is natural variability, which generates a contribution ranging from 28 to 30% of the overall uncertainty. Climate sensitivity comes last, with a contribution ranging from 20 to 24% of overall uncertainty. Generally, it was found that the choice of the hydrological model has a marginal influence on the relative contributions of each source of uncertainty. Such a result was somewhat expected if one assumes that each hydrological model performs equally well in simulating future hydrological regimes. Note that the HMETS model produced slightly different relative contributions of GCM, climate sensitivity and natural variability to the overall uncertainty. The fact that the HMETS model behaved differently, i.e. produced uncertainty envelopes that were different from the envelopes produced by the other hydrological models (see for instance Figures 5.6, 5.7 and 5.10) explains perhaps the results presented in Table 5.16. Whether these differences are statistically significant, or are merely caused by ‘chance’, remains to be ascertained.

The seasonal changes in percent of simulated discharges between the future period (2065-2097) and the control period (1975-2007) for individual GCMs, displayed in Figures 5.6 to 5.7, show that the changes in seasonal discharge vary according to GCM structure. Furthermore, these changes are different among the four hydrological models used in this

study. As an example, cold and dry GCMs (such as BCCR, CNRM and CSIRO) induce a significant reduction in winter flows with the HBV model, but produce an increase with HYDROTEL, HSAMI and HMETS. Furthermore, an increase in the winter and spring discharge is more notable with HYDROTEL than with the other models. HBV also produces more increase in the autumn discharge compared to the other hydrological models. The HMETS model, in particular, presents slight variations of change for all GCMs and seasons.

This distinction in observed behaviour between hydrological models displaying different spatial structure and complexity (e.g. snow accumulation and melt module) may be attributed, at least partly, to the way each model handles the climatic input data (distributed or lumped). The explicit representation of the land cover of each sub-watershed by spatially-distributed models like HYDROTEL, as compared to the general geographic descriptions in lumped conceptual models like HMETS, may also explain part of the discrepancies observed.

Results presented in this study therefore highlight the fact that choosing a single hydrological model in climate change studies may result in neglecting a non-negligible source uncertainty in climate change studies. With the selection of a single hydrological model, there is therefore the possibility of introducing a bias on resulting flows, with possible impacts on devising proper adaptation strategies. Also, the difference observed between the simulations from the four hydrological models with regard to the uncertainty of natural variability (see Figure 5.10), highlights differences which may be attributed to the models structure. In other words, explicitly considering the spatial heterogeneity of the watershed and of meteorological variables in a distributed hydrological model may be responsible for introducing a wider spread of changes in the simulated flows due to natural variability and this, for all seasonal flows. Therefore, selecting a single hydrological model may have implications for the design of hydraulic structures that are able to cope with climate change impacts.

In Figure 5.11, the PDFs of future spring runoff depths are shifted to the right for all GCMs. Also, the PDFs generally appear less spread in a future climate, compared to current climate for all hydrological models, except HYDROTEL. This is generally due to increasing spring temperatures and accumulated winter snow under the future climate conditions created by an increase in winter precipitation (see Figure 5.1) and will cause intense snowmelt and higher spring runoff. The coefficient of variation (CV) of average spring discharge (from March to May) for the future period was calculated for each PDF and average values produced by the hydrological model. The CV is a metric used to standardize the dispersion of PDFs and allows comparing distributions with different means. Average CV values obtained are 18.5%, 16.1%, 15.8% and 12.3%, respectively for HYDROTEL, HBV, HSAMI and HMETS. Although no statistical tests were conducted, CV values are higher for the distributed hydrological models than for the lumped models. This highlights the fact that explicitly recognizing the distributed properties of climate input and watershed physiographic characteristics may be responsible for creating more variability in the spring runoff volumes. Finally, extreme spring runoff events are similar for four of ten GCMs (i.e. BCCR, CNRM, INM and MPI) when comparing the control and simulated PDF curves. This indicates that the cold and dry GCMs (except MPI which is cold and wet models) tend to simulate conditions that lead to extreme spring floods which are similar to today's climate.

Regarding the relative contributions of each source of uncertainty to the overall uncertainty presented in Table 5.16, as the climate sensitivity was produced using MAGICC/SCENGEN and the natural variability was conducted using WeaGETS, the values of estimated contributions would consequently be effected by the methods used.

5.4.2 Analysis using a Monte-Carlo simulation

The distribution of uncertainty of future runoff volumes and spring peak flows was analyzed by using Monte-Carlo simulations. Equal and unequal weights were attributed to sources of uncertainty in the numerical experiments. The REA method was used to generate the relative weights of GCMs, based on model performance and model convergence. Table 5.6 presents

the reliability factors produced by the REA method that was applied to GCM simulated the precipitation and temperature from which the GCM weights were computed. Three GCMs (INM, CNRM and MPI) obtained the highest weights, in comparison to the other GCMs, for both precipitation and temperature.

As anticipated, return periods for given mean discharge values are expected to decrease in the future, for all the investigated hydrological models (see Tables 5.8 to 5.11). Furthermore, these tables indicate that applying unequal weights on climate sensitivity, instead of equal weights, will induce significant impact in the return period of future mean discharge, especially at higher flows. Overall, an increase in return periods is seen when unequal weights on climate sensitivity are applied, as compared to using equal weights. For the range of mean discharge values considered in the analysis, corresponding increases in return periods range between 0-11%, 7-81%, 5-91% and 8-61% respectively for HYDROTEL, HBV, HSAMI and HMETS, with unequal weights on climate sensitivity. HYDROTEL produced the smallest increase, but HBV produced increases of comparable magnitude to those of HSAMI and HMETS. Therefore, no conclusion could be drawn in regards to hydrological model structure. On the other hand, using equal or unequal weights on the GCM structure has virtually no effect on the return period. This seems at first glance counter intuitive, given that GCM structure is a major source of uncertainty for seasonal discharge (see Figure 5.6, 5.7, Table 5.16) and spring runoff volume (see Figure 5.11), while climate sensitivity's influence is more modest (see Table 5.16).

Note that, in Table 5.7, three GCMs, namely CNRM, INM and MPI, have by far the largest weights among the 10 analyzed GCMs. A closer look at the PDF distributions of annual runoff produced by the GCMs (see Figure 5.11) reveals that the PDFs of these three GCMs are very similar and also representative of the 10 GCMs, i.e. they sit in the 'middle portion' of the PDF range of all analyzed GCMs. Consequently, it may perhaps explain, in this respect, why using equal or unequal weights on GCM structure marginally affected the results.

The results obtained on climate sensitivity are perhaps best explained by the fact that 'warmer' models produce more evapotranspiration and therefore potentially reduce the mean annual runoff, providing that the increase in evapotranspiration outweighs any increase in annual precipitation. Adopting a triangular PDF distribution for climate sensitivity puts less weight for the warmer (and also the colder) models, as compared with a uniform distribution, which brings a decrease in the frequency of extreme events. In this study, the unequal weighing scheme caused an overall decrease in the annual runoff, compared with an equal weighting scheme, and this resulted in a corresponding increase in the return periods. This behavior can be observed in all four hydrological models.

Finally, Tables 5.8 to 5.15 again show a distinct increase of the return periods when unequal weights are applied to climate sensitivity. The return period is observed as being different depending on the hydrological model used for simulations, and this reflects on the different probability calculated for a specific stream flow. Among the four hydrological models, regardless of the simulated hydrological variables, HYDROTEL always produces the smallest future return period for both annual mean discharges or annual spring peak discharges and for all experiments, especially when it uses an unequal weighting scheme on climate sensitivity, which indicates that this hydrological model could generate more occurrence of high flow events in the future. This can also be observed in Figure 5.5 and Table 5.4.

Based on the above analysis, the decision to select equal and unequal weighted schemes for climate sensitivities should be given due attention in the uncertainty assessment of climate change impacts studies. However, the impact of using equal or unequal weights on the GCM structure appears to be marginal. The choice of the hydrological model also seems to bear a significant effect on flow design values.

CONCLUSION

In recent scientific literature, a significant amount of attention has been given to the uncertainty of climate change impacts on hydrology with respect to GCM, GGES, downscaling method, and hydrological model (New and Hulme, 2000; Katz, 2002; Prudhomme, et al., 2003; Wilby, 2005; Wilby and Harris, 2006; Kay, et al., 2009; Prudhomme and Davies, 2009b; Christensen, et al., 2010; Chen, et al., 2011a; Nichols, et al., 2011, Poulin, et al., 2011; Jung, et al., 2012). Until recently, most investigations focussed on the uncertainty of GCM and GGES. Other sources of uncertainty, such as climate sensitivity and natural variability, have not been given as much attention. There is also an ongoing scientific debate about whether climate models that perform 'best' should be assigned larger weights in uncertainty analyses. Reflecting this debate, some studies investigated approaches in which weighting schemes were used to combine various sources of uncertainty in climate change studies (New and Hulme, 2000; Wilby and Harris, 2006; Christensen et al., 2010), while others criticized such approaches (Stainforth et al., 2007; Weigel et al., 2010).

In this study, a framework was developed to analyze the uncertainty of GCM structure, climate sensitivity, natural variability and, to a lesser extent, hydrological model structure for the purpose of investigating the impact of climate change on the hydrological response of the Manicouagan River Basin (MRB), a northern river basin in the province of Quebec, Canada. More specifically, future climate series with various climate sensitivities were generated from GCM output, using MAGICC/SCENGEN to vary the climate sensitivity values. These climate series were then downscaled at the watershed scale by using a change factor method. To assess the impact of natural variability, the climate projections were inputted into a stochastic weather generator, in this case WeaGETS, to generate statistically similar projections of the original time series. Finally, future flows were simulated by several hydrological models using these time series. Ten GCMs, five climate sensitivities, fifty series of natural variability and four hydrological models were used in the uncertainty assessment. Furthermore, the Monte Carlo method was used, as a probabilistic approach, to distribute the range of uncertainty by sampling the simulated hydrological outputs, based on various

weighting schemes being assigned to the GCM structure and climate sensitivity. Unequal weights for GCMs were obtained from the REA method by using temperature and precipitation as climate variables to rank the GCMs. Unequal weights for climate sensitivity were retrieved from a triangular probability distribution, proposed by New and Hulme (2000).

Climate sensitivity is always considered an inherent factor in climate models. Thus, uncertainty due to climate sensitivity has not been widely investigated up to the present. Moreover, the effect of assigning different weights to the various sources of uncertainty is a question that has been up until now marginally addressed in climate change impact studies on watershed hydrological regimes. Such questions are important and they represent the main novelty of the present study.

Overall, the combined use of all GCMs, climate sensitivities, natural variability and hydrological models produced a large spectrum of future hydrological response due to climate change (Figure 5.5). The spring peak flow will rise significantly and set in early because of an advanced snow melting trend. Spring runoff and average annual runoff will augment. An increase in the summer-autumn (June to November) flows is also expected. The projected hydrological response during the winter season (December to February) slightly increases with all hydrological models. The way each hydrological model considers heterogeneity in both climatic variables and watershed physiographic properties needs to be more fully analyzed.

The uncertainty of GCM structure was shown to be significant throughout the modeling cascade process (Figures 5.6 and 5.7). The average discharges predicted by different GCM structures vary seasonally. Cold and dry climate models, such as BCCR and CNRM, present a decrease in winter discharge at the 2065-2097 time horizon, compared to the reference period (1975-2007). On the other hand, warm and wet climate models, like IPSL and MIROC, generally display a significant increase of their future discharge in winter. During the month of April when the spring peak flow occurs (Figure 5.8), a range of monthly

discharge changes was observed among the GCMs, with BCCR producing the smallest change and GFDL, the largest. Future spring runoff is also significantly influenced by GCM structure (Figure 5.11). In general, there will be an appreciable increase in the volume of spring runoff caused by an increase in winter snow accumulation, as higher winter precipitation is predicted. The peak flow will occur earlier by 3 weeks on average because of a temperature increase throughout the winter-spring season. The cold and dry climate models, e.g. BCCR, will generate smaller extreme spring runoff events than the warm and wet models, such as GFDL. In other words, the probability that the spring runoff volume exceeds a given threshold will be smaller, or the associated return period will be larger, for the cold and dry models, as compared with the warm and wet models. This study further confirms the findings of other researchers (Wilby and Harris, 2006; Prudhomme and Davies, 2009a; Chen, et al., 2011a) that the GCM structure remains one of the most important sources of uncertainty in the climate change impacts on hydrological regimes.

The variations in climate sensitivity introduced small (summer and winter seasons) to moderate (autumn season) to important (spring season) changes in the hydrological regime of the MRB, when compared with the uncertainty linked to GCM structure (Table 5.4 and Figure 5.9). A range of values from 2.0 to 4.0 Celsius of climate sensitivity was selected for this study. Increasing the climate sensitivity resulted in an earlier and lower spring peak runoff. The uncertainty due to climate sensitivity on the hydrological regime of the MRB is not significantly affected by the choice of the hydrological model. The contribution of climate sensitivity to the overall uncertainty of the future hydrological regime of the study watershed is notable, but ranked third, behind that of GCM structure and natural variability (Table 5.16).

The effect of natural variability on the hydrological regime of the MRB, which was expressed by doing an analysis of percent changes in seasonal river flows, revealed that natural variability generated variable uncertainty with the season, with more uncertainty for the spring flows. This is explained by the fact that the natural variability in precipitation and

temperature creates variability in both the timing and the volume of the spring runoff. The uncertainty of the future hydrological regime of the MRB caused by natural variability ranked second, behind GCM structure (Table 5.16).

Four hydrological models, i.e. HYDROTEL, HBV, HSAMI and HMETS, differing in their conceptual representation of a watershed, were used in this study as a first step in assessing the effect of hydrological model structure on the hydrological response of the MRB. HYDROTEL and HBV are spatially distributed models, while HSAMI and HMETS are classified as lumped conceptual models. It was shown in this study that the way the hydrological models represent the spatial heterogeneity of both climatic and physiographic data has a significant effect on the simulated future flows. For example, HYDROTEL and HBV generated higher discharge in future summer-autumn flows for all modeling runs, while the opposite was observed with HSAMI and HMETS. It was also noted that the variability of the hydrological response of HYDROTEL, represented by the envelope of all runs, is similar to that of HBV. This is in contrast with the lower variability found with the HSAMI and HMETS models, both lumped models and which use simplified algorithms for representing the main hydrological processes occurring in a watershed (e.g. degree-day approach for snow melt). Although it is not possible to separate the effect of the spatial structure from that of the algorithms used in the models, it is surmised that the explicit representation of the spatial variability in the temperature and precipitation fields in HYDROTEL and in HBV accounts for some of the observed variability. In fact, hydrological processes, such as snow accumulation, snow melt and evapotranspiration amongst others, are affected by temperature and precipitation fields, and their non-linear behavior and spatial distribution will translate into more variability in the overall hydrological response, given that the MRB displays strong north-south variations in its temperature and precipitation fields. Probability density functions (PDF) of spring runoff depth (Figure 5.11) reveal that this hydrological variable is affected by both GCM structure and hydrological model structure. The HYDROTEL model generated more variability in the annual range of percent change as compared to the other models. Again, a combination of the spatial structure of the models, along with the equations used to describe processes sensitive to meteorological variables, is probably responsible for

the observed differences. The variability of HMETS, compared to that of HSAMI, was found to be smaller (except in spring) (Figure 5.5) and it also showed less variations of change for each GCM (Figure 5.6 and 5.7).

A Monte Carlo experiment was performed to assess whether assigning equal of different weights to GCM models and climate sensitivity would affect the probability of occurrence of hydrological events. To that end, two hydrological variables of the MRB were investigated: the mean annual discharge and the spring peak runoff. The REA approach was used to assign weights to each GCM, while a triangular probability density function was assumed to calculate weights for the given climate sensitivities. Results have shown that assigning equal or unequal weights to the GCM structure had a marginal effect on the return periods that were calculated for the preselected values of annual runoff and spring peak flow. However, assigning equal or unequal weights to climate sensitivity notably influenced the probability of the occurrence of both annual runoff and spring peak flow. This is commensurate with the fact that the uncertainty of the future hydrological regime of the MRB due to climate sensitivity, although smaller than to GCM structure, is still notable (see Table 5.16). In studying the spring peak discharge, the HBV model showed the greatest increase in return period while HYDROTEL presented the smallest return periods among four hydrological models used. Thus, care should be taken in selecting hydrological models and in assigning weighting schemes to climate sensitivities in order to assess the uncertainty associated with impact studies on the effects of climate change on future hydrological regimes.

In summary, the framework developed in this study could be adopted in the analysis of the magnitude of uncertainty due to various sources. This framework is modulable and flexible. The structure of the database in which the results of the hydrological model simulations are stored makes it easy to insert/replace other sources of uncertainty, so that additional Monte Carlo analysis can be easily conducted. These sources of uncertainty include downscaling techniques, GGES, GCM initial conditions, etc.

RECOMMENDATIONS

All research work should be improved through analysis and self-reflection. This section outlines the limitations of this study and presents recommendations for further research.

1) Sources of uncertainty

This study focused on the uncertainty linked to GCM structure, climate sensitivity, natural variability and hydrological model structure. Other sources of uncertainty, for example, GGES, the downscaling method and hydrological model parameters were not addressed in this work. The downscaling method was revealed to be a noticeable source of uncertainty in the watershed's hydrological response (Prudhomme and Davies, 2009a; Chen, et al., 2011a). The uncertainty of GGES and of GCM initial conditions were also found to have lesser impact, as compared to GCM structure and the downscaling method in producing climate projections (Chen, et al., 2011a). For the purpose of a more comprehensive investigation and to further develop the present framework, these latter sources of uncertainty should be taken into consideration.

2) GCM structure

A major issue in quantifying the uncertainty in GCM structure is related to the number of GCMs to be included in the analysis. Ten different GCMs were selected in this research and were individually assigned various weights in Monte Carlo simulations. As more and more GCMs output are becoming available, an approach must be developed so that the proposed framework is implementable with current computing capabilities. This may require, for example, aggregating GCMs in order to form 'families' of models that produce similar hydrological responses. The number of GCMs used for constructing an effective multi-ensemble may also be efficiently reduced by removing those which will have small weights in Monte Carlo analyses. Some GCMs used in this study, e.g. CSIRO and IPSL, which were assigned small weights, had the slightest impacts on the generated hydrological projections. Murphy et al. (2004) and Laurent and Cai (2007) made similar attempts in their researches.

In future studies, a robust and scientifically sound methodology for the selection of GCMs should be developed.

3) Downscaling method

The change factor method technique employed in this work is a relatively straightforward and popular downscaling technique. Although it is very easy to apply and allows one to directly establish the scenarios in line, by adding the changes predicted by GCMs to the baseline climatology, it has some drawbacks. Its key disadvantage is in the supposition that the spatial pattern of the current climate remains unchanged in the future. As only this downscaling technique was used in this research, other approaches, such as statistical downscaling methods, should be employed in future studies to investigate their impact. A study by Chen et al, (2011a) confirmed that uncertainty due to the downscaling method can be an important contributor to the overall uncertainty of future hydrological regimes. The possibility of assigning different weights to the various downscaling techniques should also be investigated, as the few analyses conducted so far found all downscaling methods to be performing equally well.

4) Natural variability

A simple weather generator, WeaGETS, was implemented to generate long-term series, which were statistically similar to the input data, for the purpose of establishing the natural variability. The version of WeaGETS used here did not take into account interannual variability. Recently, WeaGETS was improved to correct the underestimation of interannual variability found in standard weather generators (Chen et al., 2012). Future studies should be performed with improved weather generators to assess how interannual climate variability could affect future hydrological regimes and associated uncertainty. Other developed approaches for assessing the magnitude of natural variability, such as block resampling and other types of weather generators, may also be employed.

5) Hydrological variables

This work examined the impact of various sources of uncertainty on simulated annual mean discharge, monthly mean discharge, as well as spring runoff volume and peak flow. In future related studies, other variables of interest to water resources managers, such as seasonal flows, low flows, time to peak, etc., should also be investigated to provide a more comprehensive evaluation of future hydrological regimes.

6) Weighting experiments

Weighting experiments were done in this study to evaluate the impacts on the watershed response to the use of equal-weight and unequal-weight schemes on two sources of uncertainty, namely GCM structure and climate sensitivity. Other sources of uncertainty, such as the hydrological model structure, that are known to have a noticeable impact on the simulated hydrological variables, should be taken into consideration. For example, Chiang et al. (2007) introduced a methodology for assigning relative weights to hydrological models according to their performance in simulating the hydrological response under selected rainfall events. It is therefore recommended to explicitly incorporate hydrological model structure as a source of uncertainty in Monte-Carlo simulations by assigning weights to hydrological models based on their performance.

7) Hydrological models

Four hydrological models including two lumped conceptual models (HSAMI and HMETS), one physically-based distributed model (HYDROTEL) and one semi-distributed conceptual (HBV) were used in this work. Using models with these two different structures resulted in some notable distinctions in the resulting hydrological response. In particular, it was shown that distributed and semi-distributed models were more sensitive to changing climate than lumped conceptual models. It is difficult to draw general conclusions about the uncertainty related to hydrological model structure since only four hydrological models were used while the literature abounds with models displaying contrasting structures. Either other hydrological models should be involved in future investigations or an approach should be

devised to group models according to their similarities in simulating hydrological regimes and using representative models in the uncertainty study.

Overall, even though this work has produced several innovations, avenues for future research are numerous. It is hoped that the contributions presented in this thesis will serve as a solid foundation to build upon.

LIST OF BIBLIOGRAPHICAL REFERENCES

Alekseev, G.V., A. I. Danilov, V. M. Kattsov, S. I. Kuz'mina and N. E. Ivanov. 2009. Changes in the climate and sea ice of the Northern Hemisphere in the 20th and 21st centuries from data of observations and modeling. Izvestiya Atmospheric and Oceanic Physics, vol. 45, n° 6, p. 675-686.

Ang, A.H-S. and W. H. Tang. 1975. Probability concepts in engineering planning and design: Volume I: Basic Principles. John Wiley and sons, Inc., New York, 409p.

Ang, A.H-S. and W. H. Tang. 1984. Probability concepts in engineering planning and design: Volume II: Decision, Risk and Reliability. John Wiley and sons, Inc., New York, 562p.

Arora, V. K. and G. J. Boer. 2001. Effects of simulated climate change on the hydrology of major river basins. Journal of Geophysical Research, vol. 106, n° D4, p. 3335-3348.

Arsenault, R., A. Poulin, P. Côté and F. Brissette. 2013. A comparison of stochastic optimization algorithms in hydrological model calibration. Journal of Hydrologic Engineering, doi:10.1061/(ASCE)HE.1943-5584.0000938.

Baguis P., O. Boukhris, V. Ntegeka, E. Roulin, P. Willems and G. Demarée. 2008. Climate change impact on hydrological extremes along rivers and urban drainage systems. I. Literature review. Belgian Science Policy – SSD Research Programme, Technical report CCI-HYDR project by K.U. Leuven – Hydraulics Section and Royal Meteorological Institute of Belgium, May 2008, 57p.

Bardossy, A. and S.K. Singh. 2008. Robust estimation of hydrological model parameters. Hydrology and Earth System Sciences, vol. 12, n° 3, p. 1273-1283.

Bedford, T. and R. Cooke. 2001. Probabilistic Risk Assessment: Foundations and Methods. Cambridge University Press.

Benke, K. K., K. E. Lowell and A. J. Hamilton. 2008. Parameter uncertainty, sensitivity analysis and prediction error in a water-balance hydrological model. Mathematical and Computer Modelling, vol. 47, n° 11-12, p. 1134-1149.

Bergström, S., J. Harlin and G. Lindström. 1992. Spillway design floods in Sweden: I. New guidelines. Hydrological Sciences Journal, vol. 37, n° 5, p. 505-519.

Bergström, S., G. Lindström and A. Pettersson. 2002. Multi-variable parameter estimation to increase confidence in hydrological modelling. Hydrological Processes. vol. 16, n° 2, p. 413-421.

Bergström, S. 1995. The HBV model. In: V.P. Singh (Ed.), Computer Models of Watershed Hydrology. Water Resources Publications. Highlands Ranch, CO., p. 443-476.

Beven, K., 2006. A manifesto for the equifinality thesis. Journal of Hydrology, vol. 320, n° 1, p. 18-36.

Beven, K.J. and A.M. Binley. 1992. The future of distributed models: model calibration and uncertainty prediction. Hydrological Processes, vol. 6, n° 3, p. 279-298.

Blenkinsop, S. and H. J. Fowler. 2007. Changes in drought frequency, severity and duration for the British Isles projected by the PRUDENCE regional climate models. Journal of Hydrology, vol. 342, n° 1, p. 50-71.

Bradley, B. A. 2010. Assessing ecosystem threats from global and regional change: hierarchical modeling of risk to sagebrush ecosystems from climate change, land use and invasive species in Nevada, USA. Ecography, vol. 33, n° 1, p. 198-208.

Brekke, L. D., M. D. Dettinger, E. P. Maurer and M. Anderson. 2008. Significance of model credibility in estimating climate projection distributions for regional hydroclimatological risk assessments. Climatic Change, vol. 89, n° 3, p. 371-394.

Brissette, F., 2010. Hydrology model École de Technologie Supérieure – HMETS. User Manual, 10 p.

Butts, M. B., J. T. Payne, M. Kristensen and H. Madsen. 2004. An evaluation of the impact of model structure on hydrological modelling uncertainty for streamflow simulation. Journal of Hydrology, vol. 298, n° 1, p. 242-266.

Caldeira, K., A. K. Jain and M. I. Hoffert. 2003. Climate sensitivity uncertainty and the need for energy without CO_2 emission. Science, vol. 299, n° 5615, p. 2052-2054.

Canadian Energy Overview 2010 - Energy Briefing Note.National Energy Board. 2011. 20 p.

Caron, A., R. Leconte and F. Brissette. 2008. An improved stochastic weather generator for hydrological impact studies. Canadian Water Resources Journal, vol. 33, n° 3, p. 233-256.

Chakravarti, I. M., R. G. Laha and J. Roy. 1967. Handbook of Methods of Applied Statistics, Volume I, John Wiley and Sons, pp. 392-394.

Chen, J., F. Brissette and R. Leconte. 2010. A daily stochastic weather generator for preserving low-frequency of climate variability. Journal of Hydrology, vol. 388, n° 3-4, p. 480-490.

Chen, J., F. Brissette, A. Poulin and R. Leconte. 2011a. Overall uncertainty study of the hydrological impacts of climate change for a Canadian watershed. Water Resources Research, vol. 47, n° 12, 16p.

Chen, J., F. Brissette and R. Leconte. 2011b. Uncertainty of downscaling method in quantifying the impact of climate change on hydrology. Journal of Hydrology, vol. 401, n° 3, p. 190-202.

Chen, J., F. Brissette, R. Leconte and A. Caron. 2012. A versatile weather generator for daily precipitation and temperature. American Society of Agricultural and Biological Engineers, vol. 55, n° 3, p. 895-906.

Chen, J., X.-C. Zhang, W.-Z. Liu and Z. Li. 2009. Evaluating and extending cligen precipation generation for the loess plateau of China. Journal of the American Water Resources Association, vol. 45, n°2, p. 378-396.

Chiang, S., Y. Tachikawa and K. Takara. 2007. Hydrological model performance comparison through uncertainty recognition and quantification. Hydrological Processes, vol. 21, n° 9, p. 1179-1195.

Christensen, H. J., E. Kjellström, F. Giorigi, G. Lenderink and M. Rummukainen. 2010. Weight assignment in regional climate models. Climate Research, vol. 44, n° 3-4, p. 179-194.

Cont, R. 2006. Model uncertainty and its impact on the pricing of derivative instruments. Mathematical Finance, vol. 16, n° 3, p. 519-547.

Coulibaly, P. 2009. Multi-model approach to hydrologic impact of climate change. From Headwater to the Ocean: Hydrological Change and Water Management, p. 249-255.

Coulibaly P, Y. B. Dibike and F. Anctil. 2005. Downscaling precipitation and temperature with temporal neural networks. Journal of Hydrometeorology, vol. 6, n° 4, p. 483–496.

Cvetko, R., K. W. Chase and S. P. Magleby. 1998. New Metrics for Evaluating Monte Carlo Tolerance Analysis of Assemblies. ASME-PUBLICATIONS-MED, Assembly modeling and systems Symposium, p. 379-386.

De Rocquigny, E., N. Devictor and S. Tarantola. 2008. Uncertainty in Industrial Practice: A Guide to Quantitative Uncertainty Management. Wiley, ISBN: 978-0-470-99447-4.

Déqué, M., D.P. Rowell, D. Lüthi, F. Giorgi, J.H. Christensen, B. Rockel, D. Jacob, E. Kjellström, M. de Castro and B. van den Hurk. 2007. An intercomparison of regional

climate simulations for Europe: Assessing uncertainties in model projections. Climatic Change, vol. 81, n° S1, p. 53–70.

Déqué, M. and S. Somot. 2010. Weighted frequency distributions express modelling uncertainties in the ENSEMBLES regional climate experiments. Climate Research, vol. 44, n° 2, p. 195–209.

Diaz-Nieto, J., and R. L. Wilby. 2005. A comparison of statistical downscaling and climate change factor methods: Impacts on low flows in the River Thames, UK, Climate Change, vol. 69, n° 2, p. 245–268.

Duan, Q. 2003. Calibration of watershed models, vol. 6. Eds. By Duan, Qingyun and H. Gupta, A.N. Sprooshian, Water science and application, Washington D.C., 345 p.

Duan, Q., S. Sorooshian and V. K. Gupta. 1992. Optimal use of the SCE-UA global optimazation method for calibrating watershed models. Journal of Hydrology, vol. 158, n° 3-4, p. 265-284.

Edwards, P. N. 2010. A Vast Machine: Computer Models, Climate Data, and the Politics of Global Warming. The MIT Press, Cambridge, MA.

ENSEMBLE, D3.2.2. RCM-specific weights based on their ability to simulate the present climate, 2009. European FP6 project: ENSEMBLE-based predictions of climate changes and their impact, calibrated for the ERA40-based simulations, available at www.ensembleseu.org. Organization: ICTP (International Centre for Theoretical Physics) and DMI (Danish Meteorological Institute).

Farhangmehr, F. and I. Y. Tumer. 2009. Optimal Risk-Based Integrated Design (ORBID) for multidisciplinary systems. DS 58-4: Proceedings of ICED 09, the 17th International Conference on Engineering Design. vol. 4, p. 287-298.

Ferrari, M. R. 2008. Mid and high latitude hydroclimatology: a modeling study of the observations and future temperature trends in the Fraser and Lena river basins. Ph.D. thesis. Rutgers, the state university of New Jersey.

Fordham, D. A., T. M. L. Wigley, M. J. Watts and B. W. Brook. 2012. Strengthening forecasts of climate change impacts with multi-model ensemble averaged projections using MAGICC/SCENGEN 5.3. Ecography, vol. 35, n° 1, p. 4-8.

Fortin, J.-P., R. Moussa, C. Bocquillon and J.-P. Villeneuve. 1995. Hydrotel, un modèle hydrologique distribué pouvant bénéficier des données fournies par la télédétection et les systèmes d'information géographique. Revue des sciences de l'eau, vol. 8, n° 1, p. 97-124.

Fortin, J.-P., S. Duchesne, M. Bernier, K. H. Huang and J.-P. Villeneuve, 2007. HYDROTEL, un modèle hydrologique distribué pouvant générer des informations spatialisées détaillées très utiles pour la gestion de bassins versants de tailles diverses. Actes des Journées Scientifiques Inter-Réseaux de l'Agence Universitaire de la Francophonie, Hanoi, Viet Nam, November 6-7.

Fortin, Vincent. 2000. Le modèle météo-apport HSAMI: historique, théorie et application. Varennes: Institut de Recherched'Hydro-Québec, p. 68.

Fortin, J.-P., R. Turcotte, S. Massicotte, R. Moussa, J. Fitzback and J.-P. Villeneuve. 2001. Distributed watershed model compatible with remote sensing and GIS data. I: Description of the model. Journal of hydrologic engineering, vol. 6, n° 2, p. 91-99.

Fowler , H. J. and M. Ekström. 2009. Multi-model ensemble estimates of climate change impacts on UK seasonal precipitation extremes. International Journal of Climatology. vol. 29, n° 3, p. 385-416.

Fowler, H. J., S. Blenkinsop and C. Tebaldi. 2007. Linking climate change modelling to impacts studies: recent advances in downscaling technique for hydrological modelling. International Journal of Climatology. vol. 27, n° 12, p. 1547-1578.

Fowler, H. J. and C. G. Kilsby. 2007. Using regional climate model data to simulate historical and future river flows in northwest England. Climatic Change, vol. 80, n° 3, p. 337-367.

Gates, W. L., J.F.B. Mitchell, G. J. Boer, U. Cubasch, and V. P. Meleshko. 1992. Climate modeling, climate prediction and model validation. In: Houghton, J.T., Callander, B.A. and Varney, S.K. (eds) Climate Change 1992: The Supplementary Report to the IPCC Scientific Assessment. Cambridge University Press, Cambridge, UK, p. 97-134.

Ghosh, S. and S. Katkar. 2012. Modeling uncertainty resulting from multiple downscaling methods in assessing hydrological impacts of climate change. Water Resources Management, vol. 26, n° 12, p. 3559-3579.

Giorgi, F. and L. O. Mearns. 2002. Calculation of average, uncertainty range, and reliability of regional climate changes from AOGCM simulations via the "reliability ensemble averaging" (REA) method. Journal of Climate, vol. 15, n° 10, p. 1141-1158.

Giorgi, F. and L. O. Mearns. 2003. Probability of regional climate change based on the Reliability Ensemble Averaging (REA) method. Geophysical Research Letters, vol. 30, n°12, p. 31-1- 31-4.

Giorgi, F., L. O. Mearns. C. Shields and L. Mayer. 1988. A regional model study of the importance of local versus remote controls of the drought and the 1993 flood over the central United States. Journal of Climate, vol. 9, n°5, p. 1150–1161.

Gitau, W. M. and I. Chaubey. 2010. Regionalization of SWAT model parameters for use in ungauged watersheds. Water, vol. 2, p. 849-871, doi:10.3390/w2040849.

Goegebeur, M. and V. Pauwels. 2007. Improvement of the pest parameter estimation algorithm through extended kalman filtering. Journal of Hydrology, vol. 337, n° 3, p. 436-451.

Gottlieb, S. 1997. What is science? The lecture at the Harbinger symposium on April 3.

Hansen, J., G. Russell, D. Rind, P. Stone, A. Lacis, S. Lebedeff, R. Ruedy and L. Travis. 1983. Efficient three-dimensional models for global climate studies: Models I and II. Monthly Weather Review, vol. 111, n° 4, p. 609-662.

Haguma, D. 2013. Gestion des ressources hydriques adaptée aux changements climatiques pour la production optimale d'hydroélectricité, étude de cas : bassin versant de la rivière manicouagan. Ph.D. thesis. University of Sherbrooke.

Hasting, W. K. 1970. Monte Carlo sampling methods using Markov chains and their applications. Biometrika, vol. 57, n° 1, p. 97-109.

Hatton, L. 1997. The T Experiments: Errors in Scientific Software. IEEE Computational Science and Engineering, vol. 4, n° 2, p. 27-38.

Hay, L. E., and M. P. Clark. 2003. Use of statistically and dynamically downscaled atmospheric model output for hydrologic simulations in three mountain basins in the western United States. Journal of Hydrology, vol. 282, n° 10, p. 56-75.

Hay, L. E., R. L. Wilby and G. H. Leavesly. 2000. A comparison of delta change and downscaled GCM scenarios for three mountainous basins in the United States. Journal of the American Water Resources Association, vol. 36, n°2, p. 387–397.

Henson, R. 2008. The rough guide to climate change. Rough Guide Ltd, London, 374 p.

Hernández-Henríquez, M. A., T. J. Mlynowski and S. J. Déry. 2010. Reconstructing the natural streamflow of a regulated river: A case study of la granderivière, Québec, Canada. Canadian Water Resources Journal, vol. 35, n° 3, p. 301-316.

Horton, P., B. Schaefli, A. Mezghani, B. Hingray and A. Musy. 2006. Assessment of climate-change impacts on alpine discharge regimes with climate model uncertainty. Hydrological Processes, vol. 20, n° 10, p. 2091-2109.

Hubbard, D. W. 2010. How to Measure Anything: Finding the Value of Intangibles in Business. John Wiley & Sons, ISBN: 978-0-470-53939-2.

Huisman, J.A., L. Breuer, H. Bormann, A. Bronstert, B.F.W. Croke, H.-G. Frede, T. Gräff, L. Hubrechts, A.J. Jakeman, G. Kite, J. Lanini, G. Leavesley, D.P. Lettenmaier, G. Lindström, J. Seibert, M. Sivapalan, N.R. Viney and P. Willems. 2009. Assessing the impact of land use change on hydrology by ensemble modeling (LUCHEM) III: Scenario analysis. Advances in Water Resources, vol. 32, n° 2, p. 159-170.

Huot, P.L, A. Poulin and S. Alarie. 2014. Assessment of blackbox optimization methods for efficient calibration of computationally intensive hydrological models. HIC, 11th International Conference on Hydroinformatics.

Hydro-Quebec. 2006. Plan stratégique 2006-2010, Hydro-Quebec, 54 p.

Hydro-Quebec. 2010. Annual Report 2010. Montreal. 118 p.

IPCC, 2001. Climate Change 2001: Synthesis Report. A Contribution of Working Groups I, II, and III to the Third Assessment Report of the Integovernmental Panel on Climate Change [Watson, R.T. and the Core Writing Team (eds.)]. Cambridge University Press, Cambridge, United Kingdom, and New York, NY, USA, 398 pp.

IPCC, 2007. Summary for Policy smakers. In: Climate Change 2007: The Physical Science Basis. Contribution of Working Group I to the Fourth Assessment Report of the Intergovernmental Panel on Climate Change [Solomon, S., D. Qin, M. Manning,Z. Chen, M. Marquis, K.B. Averyt, M.Tignor and H.L. Miller (eds.)]. Cambridge University Press, Cambridge, United Kingdom and New York, NY, USA, 996 pp.

IPCC, 2013. Climate Change 2013: The Physical Science Basis. Contribution of Working Group I to the Fifth Assessment Report of the Intergovernmental Panel on Climate Change. http://www.climatechange2013.org/ [Stocker, T. F., D. Qin, G.-K. Plattner, M. Tignor, S. K. Allen, J. Boschung, A. Nauels, Y. Xia, V. Bex and P. M. Midgley (eds.)]. Cambridge University Press, Cambridge, United Kingdom and New York, NY, USA, 1535 pp.

ISO (International Organization for Standardization). 1993. International Vocabulary of basic and general terms in Metrology, Geneva, Switzerland, ISBN 92-67-10175-1.

Isukapalli, S. S. 1999. Uncertainty analysis of transport-transformation models. Ph.D. thesis. The State University of New Jersey.

Johnson, T. E. and C. P. Weaver, 2009. A framework for assessing climate change impacts on water and watershed systems. Environmental Management, vol. 43, n° 1, p. 118-134.

Jones, R. N., F. H. S. Chiew, W. C. Boughton and L. Zhang, 2006. Estimating the sensitivity of mean annual runoff to climate change using selected hydrological models. Advances in Water Resources, vol. 29, n° 10, p. 1419-1429.

Jung, Il-Won, H. Moradkhani and H. Chang. 2012. Uncertainty assessment of climate change impacts for hydrologically district river basins. Journal of Hydrology, vol. 466-467, p. 73-87.

Kay, A. L. and H.N. Davies. 2008. Calculating potential evaporation from climate model data: A source of uncertainty for hydrological climate change impacts. Journal of Hydrology, vol. 358, n° 3, p. 221-239.

Kay, A.L., H.N. Davies, V.A. Bell and R.G. Jones. 2009. Comparison of uncertainty sources for climate change impacts: flood frequency in England. Climate Change, vol. 92, n° 1, p. 41-63.

Katz, R. W. 2002. Techniques for estimating uncertainty in climate change scenarios and impact studies. Climate Research, vol. 20, n° 2, p. 167-185.

Khan, M. S., P. Coulibaly and Y. Dibike. 2006. Uncertainty analysis of statistical downscaling methods. Journal of Hydrology, vol. 319, n° 1, p. 357-382.

Kiureghian, A. D. and O. Ditlevsen. 2009. Aleatory or epistemic? Does it matter? Structural safety, vol. 31, n° 2, p. 105-112.

Knutti, R. and G.C. Hegerl. 2008. The equilibrium sensitivity of the Earth's temperature to radiation changes. Nature Geoscience, vol. 1, n° 11, p. 735-743.

Knutti, R., R. Furrer, C. Tebaldi, J. Cermak and G. A. Meehl. 2010. Challenges in combining projections from multiple climate models. Journal of Climate, vol. 23, n° 10, p. 2739-2758.

Laurent, R. and X. Cai. 2007. A maximum entropy method for combining AOGCMs for regional intra-year climate change assessment. Climate Change, vol. 82, n° 3-4, p. 411-435.

Lee, J. S. 2002. Uncertainty analysis in dam safety risk assessment. Ph.D thesis, Chapter 2, 6-19. Utah State University.

Lindström, G., B. Johansson, M. Persson, M. Gardelin and S. Bergström. 1997. Development and test of the distributed HBV-96 hydrological model. Journal of Hydrology, vol. 201, n° 1-4, p. 272-288.

Liu, Y. and H.V. Gupta. 2007. Uncertainty in hydrologic modeling: Toward an integrated data assimilation framework. Water Resources Research, vol. 43, n° 7, W07401, doi:10.1029/2006WR005756.

Loehle, C. 2014. A minimal model for estimating climate sensitivity. Ecological Modelling, vol. 276, p. 80-84.

Ludwig, R., I. May, R. Turcotte, L. Vescovi, M. Braun, J.-F. Cyr, L.-G. Fortin, D. Chaumont, S. Biner, I. Chartier, D. Caya and W. Mauser. 2009. The role of hydrological model complexity and uncertainty in climate change impact assessment. Adcances in Geosciences, vol. 21, p. 63-71.

Maurer, E. P. 2007. Uncertainty in hydrologic impacts of climate change in the Sierra Nevada, California, under two emission scenarios. Climatic Change, vol. 82, n° 3, p. 309-325.

Masters, Troy. 2013. Observational estimates of climate sensitivity from changes inthe rate of ocean heat uptake and comparison to CMIP5 models. Climate Dynamics, http://dx.doi.org/10.1007/s00382-013-1770-4.

Meehl, G. A., T. F. Stocker, W. Collins, P. Friedlingstein, A. Gaye, J. M. Gregory, A. Kitoh, R. Knutti, J. Murphy, A. Noda, S. C. B. Raper, I. Watterson, A. Weaver and Z.-C. Zhao. 2007. Chapter 10: Global Climate Projections, in: IPCC Fourth Assessment Report, edited by Solomon, S., D. Qin, M. Manning, Z. Chen, M. Marquis, K. B. Averyt, M. Tignor and H. L. Miller. Cambridge University Press, Cambridge, p. 747–845.

Meinshausen, M., S.C.B. Raper and T.M.L. Wigley. 2011a. Emulating coupled atmosphere-ocean and carbon cycle models with a simpler model, MAGICC6 – part 1: model description and calibration. Atmospheric Chemistry and Physics, vol. 11, p. 1417-1456.

Meinshausen, M., T.M.L. Wigley and S.C.B. Raper. 2011b. Emulating coupled atmosphere-ocean and carbon cycle models with a simpler model, MAGICC6 – part 2: applications. Atmospheric Chemistry and Physics, vol. 11, p. 1457-1471.

Merz, B. and A. H. Thieken. 2005. Separating natural and epistemic uncertainty in flood frequency analysis. Journal of Hydrology, vol. 309, n° 1, p. 114-132.

Minville, M., F. Brissette and R. Leconte. 2008. Uncertainty of the impact of climate change on the hydrology of a nordic watershed. Journal of Hydrology, vol. 358, n° 1, p. 70-83.

Modarres, M. 2006. Risk analysis in engineering. Techniques, tools and trends. Chapter 5. CRC Press. Taylor and Francis group.

Montanari, A. 2011. Chapter 2.17 Uncertainty of hydrological predictions. Treatise on water science, p. 459-478.

Moore, R.J. 2007. The PDM rainfall-runoff model. Hydrology and Earth System Sciences, vol. 11, n° 1, p. 483-499.

Moradkhani, H. and S. Sorooshian 2009. General review of rainfall-runoff modeling: model calibration, data assimilation and uncertainty analysis. Hydrological Modelling and the Water Cycle: coupling the atmospheric and hydrological models. Water Science and Technology Library, vol. 63, p. 1-24.

Morgan, M. G. and M. Henrion. 1990. Uncertainty: a guide to dealing with uncertainty in quantitative risk and policy analysis. Cambridge University Press. Cambridge.

Murphy, J. M., D.M.H. Sexton, D. N. Barnett, G. S. Jones, M. J. Webb, M. Collins and D. A. Stainforth. 2004. Quantification of modelling uncertainties in a large ensemble of climate change simulations. Nature Publishing Group, vol. 430, n° 7001, p. 768-772.

Murtaugh, J. G. 1976. Stream sediment geochemistry, Manicouagan area, Saguenay County. Quebec Dept. Nat. Resources. DP 443, 9 p.

Muttil, N. and A. W. Jayawardena. 2008. Shuffled complex evolution model calibrating algorithm: enhancing its robustness and efficiency. Hydrological Processes, vol. 22, n° 23, p. 4628-4638.

Nash, J. E., and J. V. Sutcliffe. 1970. River flow forecasting through conceptual models part I - A discussion of principles. Journal of Hydrology, vol. 10, n° 3, p. 282-290.

New, M., and M. Hulme. 2000. Representing uncertainty in climate change scenarios: a Monte-Carlo approach. Integrated Assessment, vol. 1, n° 3, p. 203-213.

Nichols, J. D., M. D. Koneff, P. J. Knutson, M. E. Seamans, J. E. Lyons, J. M. Morton, M. T. Jones, G. S. Boomer and B. K. Williams. 2011. Climate change, uncertainty, and natural resource management. Journal of Wildlife Management, vol. 75, n° 1, p. 6-18.

Oberkampf, W. L., J. C. Helton, C. A. Joslyn, S. F. Wojtkiewicz and S. Ferson. 2004. Challenge problems: uncertainty in system response given uncertain parameters. Reliability Engineering and System, vol. 85, n° 1, p. 11-19.

Ouranos. Learning to Adapt to Climate Change, editors: C. DesJarlais, M. Allard, D. Bélanger, A. Blondlot, A. Bouffard, A. Bourque, D. Chaumont, P. Gosselin, D. Houle, C. Larrivée, N. Lease, A.T. Pham, R. Roy, J.-P. Savard, R. Turcotte and C. Villeneuve, Montreal, 2010, 128p.

Patoine, A., A.-M. Blais, M.H. Forget, S. Lamontagne and J. Marty. 1999. Respecter la variabilité naturelle pour une gestion durable des ressources aquatiques. Mémoire remis au BAPE dans le cadre des audiences publiques sur la gestion de l'eau au Québec, 16 p.

Poulin, A., F. Brissette, R. Leconte, R. Arsenault and J.-S. Malo. 2011. Uncertainty of hydrological modelling in climate change impact studies in a Canadian, snow-dominated river basin. Journal of Hydrology, vol. 409, n° 3, p. 626-636.

Prudhomme, C., D. Jakob and C. Svensson. 2003. Uncertainty and climate change impact on the flood regime of small UK catchments. Journal of Hydrology, vol. 277, n° 1, p. 1-23.

Prudhomme, C. and H. Davies. 2007. Comparison of different sources of uncertainty on climate change impact studies in Great Britain. Climatic and anthropogenic impacts on the variability of water resources – UNESCO, Paris, p. 183-190.

Prudhomme, C. and H. Davies. 2009a. Assessing uncertainties in climate change impact analyses on the river flow regimes in the UK, Part 1: baseline climate. Climate Change, vol. 93, n° 1, p. 177-195.

Prudhomme, C. and H. Davies. 2009b. Assessing uncertainties in climate change impact analyses on the river flow regimes in the UK, Part 2: future climate. Climate Change, vol. 93, n° 1, p. 197-222.

Prudhomme, C., N. Reynard and S. Crook. 2002. Downscaling of global climate models for flood frequency analysis: where are we now? Hydrological Processes, vol. 16, n° 6, p. 1137–1150.

Randall, D. A., R. A. Wood, et al. 2007: Chapter 8 Climate Models and Their Evaluation. In: Climate Change 2007: The Physical Science Basis. Contribution of Working Group I to the Fourth Assessment Report of the Intergovernmental Panel on Climate Change [Solomon, S., et al. (eds)]. Cambridge University Press, Cambridge, UK and New York, NY.

Rogelj J., M. Meinshausen and R. Knutti. 2012. Global warming under old and new scenarios using IPCC climate sensitivity range estimates. Nature Climate Change, vol. 2, p. 248-253.

Roy, J. 2014. Personal communication. Hydrometeorology advisor at Hydro-Québec, Montreal, QC, Canada.

Salathé Jr. E. P. 2003. Comparison of various precipitation downscaling methods for the simulation of streamflow in a rain shadow river basin. International Journal of Climatology, vol. 23, n° 8, p. 887-901.

Sansom P.G., D.B. Stephenson, C. A. T. Ferro, G. Zappa and L. Shaffrey. 2013. Simple uncertainty frameworks for selecting weighting schemes and interpreting multimodel ensemble climate change experiments. Journal of Climate, vol. 26, p. 4017-4037.

Santer B.D., T.M.L. Wigley, M.E. Schlesinger and J.B.F. Mitchell. 1990. Developing climate scenarios from equilibrium GCM results. Hamburg, Germany: Max-Planck-institute für Meteorologie, Report No. 47.

Semenov M. A. and E. M. Barrow. 1997. Use of stochastic weather generator in the development of climate change scenarios. Climate Change, vol. 35, n° 4, p. 397–414.

Semenov M. A. and E. M. Barrow. 2002. LARS-WG: A Stochastic Weather generator for Use in Climate Impact Studies, Version 3.0, User Manual. Rothamsted Research, Harpenden, Hertfordshire, UK.

Schmidli, J., C.M. Goodess, C. Frei, M.R. Haylock, Y. Hundecha, J. Ribalaygua, T. Schmith. 2007. Statistical and dynamical downscaling of precipitation: An evaluation and comparison of scenarios for the European Alps. Journal of Geophysical Research, vol. 112, n° D4.

Scholze, M., W. Knorr, N. W. Arnell and I. C. Prentice. 2006. A climate-change risk analysis for world ecosystems. PNAS, vol. 103, n° 35, p. 13116-13120.

Schwartz, S. E. 2008. Uncertainty in climate sensitivity: Causes, consequences, challenges. Energy and Environmental Science, vol. 1, n° 4, p. 430-453.

Serrat-Capdevila, A., J. B. Valdés, J. G. Pérez, K. Baird, L. J. Mata, T. Maddock III. 2007. Modeling climate change impacts – and uncertainty – on the hydrology of a riparian system: Te San pedro Basin (Arizona/Sonora). Journal of Hydrology, vol. 347, n° 1, p. 48-66.

Shannon C. 1948. A mathematical theory of communications, I-IV. Bell Systems Technical Journal, vol. 27, p. 379-443 and 623-656.

Singh S. K., J. Liang and A. Bardossy. 2012. Improving the calibration strategy of the physically-based model WaSiM-ETH using critical events. Hydrological Sciences Journal, vol. 57, n° 84, p. 1487-1505.

Singh V. P. and D. A. Woolhiser. 2002. Mathematical modeling of watershed hydrology, Journal of Hydrologic Engineering, vol. 7, n° 4, p. 270-292.

Solman, S. and M. Nunez. 1999. Local estimates of global climate change: a statistical downscaling approach. International Journal of Climatology, vol. 19, n° 8, p. 835-861.

Sperna Weiland, F.C., L.P.H. van Beek, A.H. Weerts and M.F.P. Bierkens. 2012. Extracting information from an ensemble of GCMs to reliably assess future global runoff change. Journal of Hydrology, vol. 412-413, p. 66-75.

Stainforth, D. A., M. R. Allen, E. R. Tredger and L. A. Smith. 2007. Confidence, uncertainty and decision-support relevance in climate predictions. Philosophical Transactions of The Royal Society A: Mathematical, Physical and Engineering Sciences , vol. 365, n° 1857, p. 2145-2161.

Staudinger, M., K. Stahl, J. Seibert, M.P. Clark and L. M. Tallaksen. 2011. Comparison of hydrological model structures based on recession and low flow simulations. Hydrology and Earth System Sciences Discussions, vol. 15, p. 3447-3459.

Stump, G. M., M. Yukish, T. W. Simpson and J. J. O'Hara. 2004. Trade space exploration of satellite datasets using a design by shopping paradigm. Aerospace conference, vol. 6, p. 3885-3895.

Stute, M., A. Clement and G. Lohmann. 2001. Global climate models: Past, present and future. Proceedings National Academy of Sciences, vol. 98, n° 19, p. 10529-10530.

Sun, Q., C. Miao and Q. Duan. 2014. Projected changes in temperature and precipitation in ten river basins over China in 21st century. International Journal of Climatology, DOI: 10.1002/joc.4043.

Tang, J. and Q. Zhuang. 2008. Equifinality in parameterization of process-based biogeochemistry models: a significant uncertainty source of the estimation of regional carbon dynamics. Journal of Geophysical Research, vol. 113, n° G4.

Taylor, K. E., R. J. Stouffer, G. A. Meehl. 2012. An overview of CMIP5 and the experiment design. Bull. American Meteorological Society, vol. 93, n° 4, p. 485-498, doi:10.1175/BAMS-D-11-00094.1.

Tebaldi, C., L. O. Mearns, D. Nychka, and R. L. Smith. 2004. Regional probabilities of precipitation change: a Bayesian analysis of multimodel simulations. Geophysical Research Letters, vol. 31, n° 24, L24 213.

Tebaldi, C., R. L. Smith, D. Nychka and L. O. Mearns. 2005. Quantifying uncertainty in projections of regional climate change: a Bayesian approach to the analysis of multimodel ensembles. Journal of Climate, vol. 18, n° 10, p. 1524-1540.

Thunnissen, D. P. 2003. Uncertainty classification for the design and development of complex systems. 3rd Annual Predictive Methods Conference.

Torres R. R. and J. A. Marengo. 2013. Uncertainty assessments of climate change projections over South America. Theoretical and Applied Climatology, vol. 112, n° 1-2, p. 253-272.

Turcotte, R., L.-G. Fortin, V. Fortin and J.-P. Villeneuve. 2007. Operational analysis of the spatial distribution and the temporal evolution of the snowpack water equivalent in southern Quebec, Canada. Nordic Hydrology, vol. 38, n° 3, p. 211-234.

Ullman, D. G. 2006. Trade studies with uncertainty information. Sixteenth annual international symposium of the International Council On Systems Engineering (INCOSE).

Vensteenkiste, T., M. Tavakoli, N.V. Steenbergen, F. De Smedt, O. Batelaan, F. Pereira and P. Willems. 2014. Intercomparison of five lumped and distributed models for catchment runoff and extreme flow simulation. Journal of Hydrology, vol. 551, p. 335-349.

Vicuna, S., E. P. Maurer, B. Joyce, J. A. Dracup and D. Purkey. 2007. The sensitivity of California Water Resources to climate change scenarios. Journal of The American Water Resources Association, vol. 43, n° 2, p. 482-498.

WEC. 2010. Survey of energy resources 2010. World Energy Council.

Weigel, A. P., R. Knutti, M. A. Liniger and C. Appenzeller. 2010. Risk of model weighting in multimodel climate projections. Journal of climate, vol. 23, n°15, p 4175-4191.

Whitfield, P. H. and A. J. Cannon. 2000. Recent variation in climate and hydrology in Canada.Canada water Resources Journal, vol. 25, n° 1, p. 19-65.

Wigley, T.M.L., et al. 2000. MAGICC: Model for the assessment of greenhouse-gas induced climate change – version 2.4. Climatic research unit, Norwich.

Wilby, R. L., H. Hany and K. Hanaki. 1998. Statistical downscaling of hydrometeorological variables using general circulation model output. Journal of Hydrology, vol. 205, n° 1, p. 1–19.

Wilby, R. L. and I. Harris. 2006. A framework for assessing uncertainties in climate change impacts: Low-flow scenarios for the River Thames, UK. Water Resources Research, vol. 42, n° 2, W02419, doi:10.1029/2005WR004065.

Wilby, R. L. 2005. Uncertainty in water resource model parameters used for climate change assessment. Hydrological Processes, vol. 19, n° 16, p. 3201-3219.

Wilby, R. L., C. W. Dawson and E. M. Barrow. 2002. SDSM - a decision support tool for the assessment of regional climate change impacts. Environmental Modelling and Software, vol. 17, n° 2, p. 145-157.

Willows, R., N. Reynard, I. Meadowcroft and R. Connell. 2003. Climate adaptation: Risk, uncertainty and decision-making. UKCIP Technical Report. Oxford, UK Climate Impacts Programme, 166pp.